

# Ku-band patch antenna design

Martin Johansen

Master Thesis, Satellite Engineering  
Faculty of Engineering Science and Technology  
Department of Electrical Engineering  
UiT The Arctic University of Norway,  
Narvik,  
Norway,  
[mnjohansen11@gmail.com](mailto:mnjohansen11@gmail.com)

June 28, 2016

Master thesis project 2015-2016  
for  
Stud. Techn. Martin Johansen

## Ku-band patch antenna design

At UiT The Arctic University of Norway, former Narvik University College, there is an ongoing project in which an array antenna for satellite ground terminals is under development. An increasingly valuable market area for satellite communication is for on-the-move applications. Antennas must not only have high gain and large bandwidth, they must also be highly portable, rugged, lightweight, and have a low power consumption. For on-the-move applications an array antenna possess several advantages over traditional parabolic antennas where the option for electronic steering being a particular advantage. Satellite communication usually uses the Ku-band for up and downlink, in Europe, Ku-band downlink is used from 10.7 to 12.75 GHz while Ku-band uplink is used from 14.0 to 14.5 GHz.

### **Main task**

The main task of this project is to synthesise different patch antenna designs in Ku-band and evaluate them through simulations in Microwave Office.

### **Subtask**

1. Perform a literature survey on existing methods of vertical feeds of patch antennas and design strategies. Relevant parameters for evaluation are electromagnetic performance and complexity of manufacturing.
2. Present mathematical models of the patch element and its feed for the different designs to be evaluated. Hereby describing the antenna performance through electromagnetic principles.
3. Develop a design and tuning procedure for a wide band patch- or dual-band patch antenna element feed allowing for future frequency band migration.
4. If possible implement alternatives for different polarizations and means for dynamically switch in between them.

Supervisor: Arne Bjørk

Advisor: Tor-Aleksander Johansen

# Abstract

The market for on-the-move satellite communication is increasing, and phased array antennas have characteristics that makes them suited for this. In this thesis design and tuning of a wide-band microstrip patch antenna element for a Ku-band antenna array is presented. The SSFIP structure with a resonating aperture is used for the antenna element, and double resonance allows for operation at both uplink and downlink frequencies. The antenna element is simulated with a metal plane reflector, and a patch reflector. A qualitative design and tuning procedure for wide/dual-band microstrip patch antennas is provided. Simulations are carried out with the electromagnetic 3D analyser AXIEM from NI AWR, and the results from the simulations are presented.

# Preface

This thesis is part of a project aiming at making an antenna array for satellite communication. The research and development of the project is run by associate professor Arne Bjørk and researcher Tor-Aleksander Johansen, at the Department of Electrical Engineering, at UiT campus Narvik. The main goal with the work in the thesis has been to synthesise and evaluate wide-band microstrip patch antenna element designs for the Ku-band, and to make a design and tuning procedure for wide/dual-band antenna elements.

I owe special thanks to my advisor, Tor-Aleksander Johansen, for training and guiding in use of the software for design and simulations, and for support through the whole working process. I want to thank my supervisor Arne Bjørk for his help answering questions I have had during my work. I also want to thank them for giving me the opportunity to work with this very interesting topic in a free and creative way.

I want to express my thanks to Stig Espen Kristiansen for his company, and for being a good classmate through our studies. I'm grateful to Tom Stian Andersen for his help and tips regarding LaTeX.

University of Tromsø campus Narvik, June 28, 2016

---

Martin Johansen

# Contents

<b>Abstract</b>	<b>ii</b>
<b>Preface</b>	<b>iii</b>
<b>1 Introduction</b>	<b>1</b>
1.1 Background and purpose . . . . .	1
1.1.1 Historical background . . . . .	1
1.1.2 Background of project . . . . .	2
1.1.3 Purpose of project . . . . .	3
1.2 Previous work . . . . .	4
1.2.1 Early development . . . . .	4
1.2.2 Basic characteristics . . . . .	4
1.2.3 Feeding techniques . . . . .	4
1.2.4 Increase of bandwidth and multiple frequency operation . . . . .	9
1.2.5 SSFIP principle . . . . .	11
1.2.6 Polarization . . . . .	13
1.2.7 MPA Arrays . . . . .	15
1.2.8 Computer tools . . . . .	16
1.2.9 Applications . . . . .	16
1.3 Contribution . . . . .	17
1.4 Outline . . . . .	17
<b>2 Preliminaries</b>	<b>19</b>
2.1 Theoretical preliminaries . . . . .	19
2.1.1 Electromagnetism . . . . .	19
2.1.2 Antennas . . . . .	21
2.1.3 Antenna measurements . . . . .	24
2.1.4 Materials in microstrip structures . . . . .	26
2.1.5 Microstrip circuits . . . . .	27
2.1.6 Methods and models . . . . .	29
2.1.7 Design of MPAs . . . . .	32
2.2 Technologic preliminaries . . . . .	36
2.2.1 Antenna configuration and requirements . . . . .	36
2.2.2 Program for design and simulation . . . . .	36

<b>3</b>	<b>Antenna design</b>	<b>39</b>
3.1	Initial design of the antenna . . . . .	39
3.1.1	Choice of feeding technique and structure . . . . .	39
3.1.2	Substrates . . . . .	40
3.1.3	Patch . . . . .	41
3.1.4	Stub and feed-line . . . . .	41
3.1.5	Aperture and reflector . . . . .	42
3.1.6	Superstrate . . . . .	47
3.1.7	The initial design . . . . .	50
3.2	Tuning . . . . .	50
3.3	Tuned antenna design . . . . .	51
3.3.1	Simulation results . . . . .	54
3.4	Antenna with patch reflector . . . . .	60
3.4.1	Simulation results . . . . .	64
3.5	Comments on results . . . . .	69
3.6	Other design considerations . . . . .	69
3.6.1	Different shaped aperture and patch . . . . .	69
3.6.2	Alternatives for polarization . . . . .	70
<b>4</b>	<b>Design and tuning procedure</b>	<b>73</b>
4.1	Effects of parts . . . . .	73
4.1.1	Patch . . . . .	73
4.1.2	Aperture . . . . .	73
4.1.3	Stub . . . . .	74
4.1.4	Feed-line . . . . .	74
4.1.5	Substrates . . . . .	76
4.1.6	Superstrate . . . . .	76
4.1.7	Reflector . . . . .	76
4.1.8	Simulation of different parts . . . . .	77
4.2	Design procedure . . . . .	85
4.3	Tuning procedure . . . . .	87
<b>5</b>	<b>Concluding remarks</b>	<b>89</b>
5.1	Discussion . . . . .	89
5.2	Conclusions . . . . .	90
5.3	Recommendations for future work . . . . .	90
	<b>Bibliography</b>	<b>91</b>
	<b>Appendices</b>	<b>94</b>
<b>A</b>	<b>CD index</b>	<b>95</b>

# Chapter 1

## Introduction

In this chapter, a short historical background of electronic communication is given, before the background and purpose of this thesis and project is presented. Previous work, development and examples of application of microstrip antennas are covered. It is discussed what new this thesis contributes with compared to other work. In the end a brief outline of the thesis is given.

### 1.1 Background and purpose

#### 1.1.1 Historical background

An important characteristic of the modern society is how people can express intentions and emotions, transfer knowledge or provide entertainment to other people all over the world in an instant. When we want to reach people who is far away in short time, we need help from technology. Up through the history, humans have solved this problem in many different ways, and many early techniques are covered in Chakravarthi (1992). For example, messages could be sent with pigeons, runners or horsemen, covering long distances. Even faster was the use of drums, horns or whistles, which can carry much longer than human voice and stay clearer, or the famous example of smoke signals used by the American Indians. Fire beacons and lighthouses has also been used to send messages fast over long distances. To increase the distance a message could be sent, networks of the different communication methods could be used. However, these early methods didn't reach very big audiences, and it would take long time to send much information. This changed when people started to use electricity for communication.

The use of electrical signals in communication is covered in Consonni and Silva (2010). Electrical signals were first used for communication in telegraphs in 1837, and since the early 1840s, the Morse code was the international standard for communication. After 1876, when Bell developed the telephone, voice could also be transmitted with analog signals. Both the telegraph and the telephone used wires to transfer signals, and in big cities there were wires hanging everywhere, and it was a wish to reduce the amount of wires, and find some form of wireless way to communicate.

In 1865, Maxwell had published his theory, which demonstrated that electric and magnetic

fields are electromagnetic waves that propagate through space with the speed of light, and that accelerated electric charges will send out electromagnetic waves. Hertz proved this in 1888, when he made a dipole transmitter, which generated sparks that were reproduced on the ends of a copper ring placed at a distance from the transmitter. In 1897, Marconi patented his telegraph transmitter, which was based on ideas and devices developed by others, and which used the same kind of sparks that Hertz had made in his work to send Morse messages. Later, Fessenden realized that it was not necessary with a spark to generate radio waves, but instead he used a high frequency continuous-wave. This could be used to send voice and music, not only Morse code, and had much less dispersion in the frequency spectra than the transmitters that used sparks. In 1906, amplitude modulation was made possible with the invention of the triode vacuum tube, and in 1933, Armstrong demonstrated the benefits of frequency modulation. These inventions made the foundation of communication technology, and the modern society.

According to Evans et al. (2011), Sir Arthur C. Clarke's paper "Wireless World" was published in 1945, just after World War II. In this paper, Clarke proposed a vision of a worldwide communication system which would consist of three communication stations in 24-hour orbits around the Earth. The first satellite, Sputnik 1, was launched in 1957, and in the years after, many more satellites were launched, and we started to gain knowledge about operating in space. According to IEEE (2012), satellite communication became possible after World War II because of developments in microwave electronics made after the development of radar technology, such as waveguides and cavity resonators that could operate up to 100 GHz. In the late 1950s, theories and concepts of microwave transmission and reception was well established. The first communication satellite, Echo I, was launched in 1960, and it proved that transatlantic communication was possible. The first active satellite, a satellite that can receive and retransmit, was Telstar I in 1962. The use of satellites has grown since then, and still today, satellites are providing us TV and radio. Satellites enables communication with remote areas, whether it is on land, on ocean or in the air. Now, we also use satellites to see and predict our climate and environment, and to do positioning and navigation more accurately than ever before.

### 1.1.2 Background of project

In an ongoing project at UiT The Arctic University of Norway, an array antenna for satellite ground terminals is under development. The antenna shall be used for so-called on-the-move satellite communication, which means that the equipment needed for the communication should be easy to transport on a vehicle and simultaneously utilized for transmission of data via satellite in any place at any time while the vehicle moves. It can be used for satellite communications over private, commercial or military networks, or for communication in accident sites. Lately, several big companies have announced that they want to use networks of satellites to give global internet connection, and in the recent years many *High Throughput Satellites* (HTS), satellites that can deliver higher throughput in bits per second, have been launched. As said by John Finney, founder of Isotropic Systems Ltd., a company developing low profile, multi-band, electronically steered antenna

for satellite operators; *"To fully enable HTS the industry needs very innovative antennas with varying price and performance, able to track from mobile platforms, or track moving satellites whether fixed or on the move, efficiently and at costs that create accretive returns for operators through an attractive end-user business case."*(SpaceNews, May 23, 2016). Antennas for on-the-move satellite applications will provide satellite communications in various environments, especially in remote locations with no telecom network coverage, or in complicated topographic surroundings.

To accomplish on-the-move satellite communication, a flat-panel/phased array antenna will be suitable. An array antenna is an antenna made up of a number of radiating elements, and it can be made electronically controllable, meaning it doesn't need to be moved physically to change its pointing direction. This will allow rapid tracking of satellite position, such that communication can be maintained while both the vehicle and the satellite moves. For the antenna, this means that it has to be highly portable, rugged, lightweight, and have a low power consumption. To meet these requirements a microstrip patch antenna array is a good alternative. A microstrip patch antenna array is an array antenna where the radiating elements are microstrip patch antennas. Microstrip patch antennas (MPA) are a category of planar antennas, which consists of a metal patch printed on a dielectric substrate with a ground plane on the bottom. This kind of antenna gives an advantage for on-the-move applications, since patch antennas have low profile, light weight and can be made rugged. MPAs are used on aircrafts, missiles, satellites, ships and other vehicles in for example radar, communication and navigation systems.

### 1.1.3 Purpose of project

The main task of this thesis is to synthesise different patch antenna designs in Ku-band (Kurtz-under-band), and evaluate them through simulations in Microwave Office. Some factors that will be important in the process of making an MPA array for satellite communication are the patch element design, feeding technique, wide-band or multiple frequency operation, and which polarization to use, and these factors will be worked with or covered in this thesis.

The patch element must be designed to operate in the right frequency band, which is the Ku-band for this project. The feeding shall be vertical, since this will give more space for the layout of the feeding network, which can be a problem for antenna arrays. The feeding technique is also affecting the bandwidth, and it has to be decided if the antenna shall work on a wide band or with multiple frequencies. If the antenna shall be able to transmit and receive, it must be able to operate on downlink frequencies for the Ku-band (10.7 to 12.75 GHz), and for uplink in the Ku-band (14 to 14.5 GHz). It can also be looked at if the antenna shall have any special type of polarization, and if it is possible to make switching between different polarizations. In addition to the electromagnetic properties of the antenna, the complexity of manufacturing should be considered.

A mathematical model of the patch element and its feed shall be presented for the patch antenna design to be evaluated. Based on this, an electromagnetic description of the antenna can be given. To make any future frequency band migrations possible, it is of interest to make a design and tuning procedure for wide-band or dual-band patch antenna element

feed. Then antennas operating at other frequencies can be made based on the experiences from design and tuning of the Ku-band MPA.

## 1.2 Previous work

### 1.2.1 Early development

According to Kevin (2007), the concept of microstrip antennas were first proposed in 1953 by Deschamps, not long after the microstrip transmission line was introduced. In 1955, Gutton and Baissinot patented the first microstrip antenna. Some years later, in 1969, Denlinger showed how rectangular and circular microstrip resonators (patches) could work as efficient radiators. The increasing need for thin and conformal antennas that could be fitted onto the surfaces of missiles and spacecrafts, was pushing the development of the microstrip antennas, and the first MPAs were made in the early 1970s. These early and simple MPAs had a narrow bandwidth, and low efficiency. Through the years, researchers have developed different methods for overcoming these drawbacks, and improving the functions of the MPA.

### 1.2.2 Basic characteristics

An MPA is built up by a patch of some conducting material on top of a grounded substrate. The shape of the patch can be rectangular, circular, elliptic, annular, triangular or other variations. Choice of shape is dependent on different factors such as bandwidth, polarization, side lobes and gain. The more complicated the shape is, the harder it will be to analyze its characteristics. In Zürcher and Gardiol (1995), it is stated that the amplitude of the surface currents of the patch becomes larger when the signal frequency is close to resonance, which will occur when the conductor size is approximately one half of the wavelength. This means that when for example the length of a squared MPA is close to half of a wavelength, it will resonate and radiate at the frequency of this wavelength. Due to fringing electric fields at the open ends of the patch, the electric field doesn't stop at the end of the patch, so the patch will behave like if it is slightly larger.

According to Chen and Chia (2006), the main advantages of MPAs are their low profile, low weight, low cost, conformability and versatility, and the ease of production and integration with circuits. These features make the MPA suitable for many modern wireless communication systems. The main drawbacks of basic MPAs are narrow bandwidth, poor polarization purity and low radiation efficiency.

### 1.2.3 Feeding techniques

The feeding technique is important for an effective transmission of the signal to the antenna. Many factors must be considered when choosing a feed method. There are three common techniques for feeding a patch antenna, which are transmission line feed/microstrip edge feed, coaxial probe feed, and electromagnetically coupled feed. In this thesis, vertical feeding techniques will be emphasized, since this is desired when making an MPA array.

### Microstrip edge feed

Microstrip edge feed means that the patch is fed directly with a microstrip line connected to it, as seen in Figure 1.1 (b). It is a simple feeding method, and is easily fabricated. A benefit of the method is that both feeding network and patch is on the same plane. The major drawback with microstrip feeding is the difficulty with impedance matching, since the input resistance at the edge of the patch is relatively high. Two different techniques for better impedance matching are commonly used. The first is to use a quarter wave transformer between the feed line and the patch, the other is to make an inset depth where the patch is fed. However, spurious and unwanted radiations will generally lower the performance of this method. Microstrip edge feed is not a vertical feeding technique.

### Coaxial probe feed

Coaxial probe feed means that the patch is fed through a coaxial probe, which is connected to the patch from below, through the ground plane and the substrate. This is shown in Figure 1.1 (a). The input impedance depends on the location of the feed on the patch. With this method the feed line and the patch are separated by the ground plane, and therefore shielded from each other. There is a number of different ways to design this feed in order to get larger bandwidth and less spurious radiation. In practice the construction with the coaxial probe is not very suitable for arrays, as said in Chen and Chia (2006), due to the great number of soldering points and coaxial lines. The feeding method with probe can also increase spurious radiation and surface waves.

Thick substrates can be used to obtain greater bandwidth for patch antennas. With the coaxial probe feeding technique, the input inductance will increase for antennas with thick substrate, and this is unwanted. In Kevin (2007), different ways to overcome the increased input inductance are presented. For example etching slots in the patch, or using different shapes of the feeding probe reduce the inductance. The feeding probe can be bent into an L-shape, which will form a capacitive reactance. The probe will then not be in direct contact with the patch, but excite it through electromagnetic coupling. Instead of a probe, a strip can be used for this method. The L-shaped feeding probe will cause high cross-polarization level in the magnetic plane and co-polarized polarization pattern in the electric plane, which are unwanted effects. The cross-polarization can be suppressed by use of two L-shaped feeding probes, which are separated by a half wavelength, placed either face-to-face as seen in Figure 1.2, or parallel. Another method is to use a meandered probe feed, where the feeding probe are bent such that it has two horizontal and three vertical portions. This will suppress unwanted radiation from vertical arms, and remove the co-polarization. However, these feeding techniques with different shaped probes are complicated to fabricate. In Kevin (2007), a new feeding mechanism is proposed. It is called vertical plate feeding, and it consists of a vertical standing plate, which is transferring the signal from the feeding probe to the patch. The vertical plate is physically coupled to both the feeding probe and the patch. This method allows the use of thick substrates, and a bandwidth over 65% is seen in the simulations.

Another type of probe fed MPA is called *Suspended Plate Antenna*(SPA). It consists of a ground plane, a thick substrate with low permittivity, a feed, and the patch. The SPA is

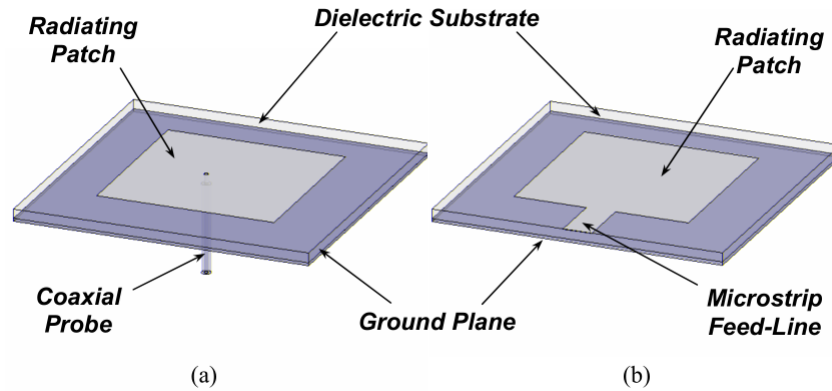


Figure 1.1: Different feeding techniques: (a) coaxial probe, (b) microstrip edge. Kevin (2007)

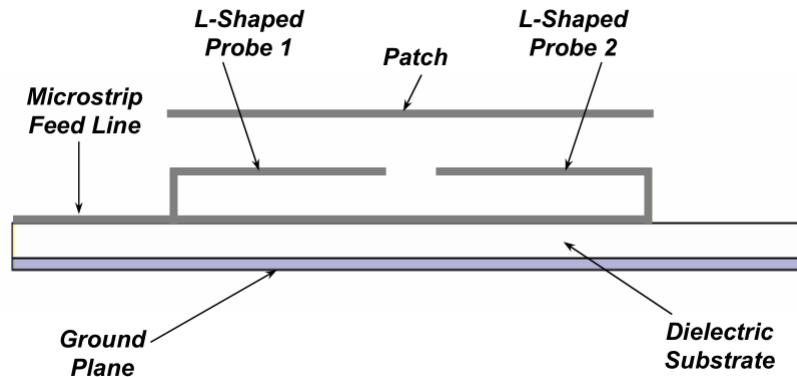


Figure 1.2: Two L-shaped probes. Kevin (2007)

presented in Chen and Chia (2006), and different techniques to broaden bandwidth, enhance radiation performance, and implement SPAs in arrays are introduced there.

### Electromagnetically coupled feed

Electromagnetically coupled feed means that the feed and the patch is not physically touching each other, but the energy of the signal is transferred to the patch through electromagnetic coupling with the feed. In Sharma (2012) it is stated that this kind of feed avoids cross-polarization which is produced with microstrip and coaxial feed, and there is no need for soldering of conductors. Only the electromagnetic coupled feeding techniques that are vertical will be presented here.

#### Proximity coupled feed

When using proximity coupled feed, the patch is fed by a stripline, which is placed

below the patch with a dielectric layer between them. Under the feeding strip is a grounded substrate. The double layer of dielectrics can increase the bandwidth if the feed and the patch are placed properly. The structure of more layers is more complex to analyze, and will increase fabrication costs. Also surface wave losses will increase with this technique according to Sharma (2012). In Kumar et al. (2013), a comparison of different feeding techniques is done, and the proximity coupled feed had the best radiation performance.

#### Aperture coupled feed

The aperture coupled feed was invented by D. M. Pozar in 1985, and has become an important and popular feeding technique, also for making patch antenna arrays, according to Sharma (2012). The structure of the aperture coupled feed is shown in Figure 1.3. An aperture coupled MPA consists of a microstrip feed line on the bottom of a dielectric called the feed substrate. It is really a feed *superstrate*, since it is above the feed line, but it is called substrate in the literature, and it will be called that here too. Above the feed substrate, there is a ground plane with an aperture/slot cut in it, and above this ground plane is another layer of dielectric, the antenna/patch substrate, with the radiating patch on top of that. The patch is fed by electromagnetic coupling with the feeding strip through the aperture. The ground layer between the feed line and the patch works as shielding of radiation from the feed line to the patch. Aperture coupled feed will increase the bandwidth of an antenna, and bandwidths over 50% has been achieved with stacked patches according to Kevin (2007). In the comparison done in Kumar et al. (2013), aperture coupling had the best bandwidth of the different feeding techniques.

When designing an aperture coupled MPA, there are many parameters that can be adjusted to get the desired performance. Because of the many possibilities for adjustments, there are many variations and possibilities with aperture coupled MPAs. The shape and size of the aperture decides how good the coupling will be. According to Pozar and Targonski (1991), rectangular shaped aperture gives approximately 10 times better coupling than a circular aperture, and other types of apertures, for example dogbone and H-shaped apertures can increase the coupling further. The aperture should not resonate on the operating frequency, since it would make radiation toward the back of the antenna. A centered aperture will give a symmetric feeding of the patch, which will result in good cross-polarization levels compared to probe or microstrip edge feed. The two-layered structure of the aperture coupled antennas make them suited for antenna arrays, since it gives more space for the layout of the feeding network because it is placed on another substrate layer. A drawback of the aperture coupled feed is the back-lobe radiation, but this can be reduced by another ground layer placed beneath the feeding network, working as a reflector, as suggested in Pozar (1996). Other drawbacks with aperture coupled feed are higher complexity of manufacturing compared to single layer structures, and the increased height due to many layers.

In Pavuluri et al. (2008) an aperture coupled patch antenna is made for frequencies in the Ku-band. This antenna has air as patch substrate and is therefore supported by a polymer ring. The measured bandwidth is 19%, and the peak gain is 8.3dBi.

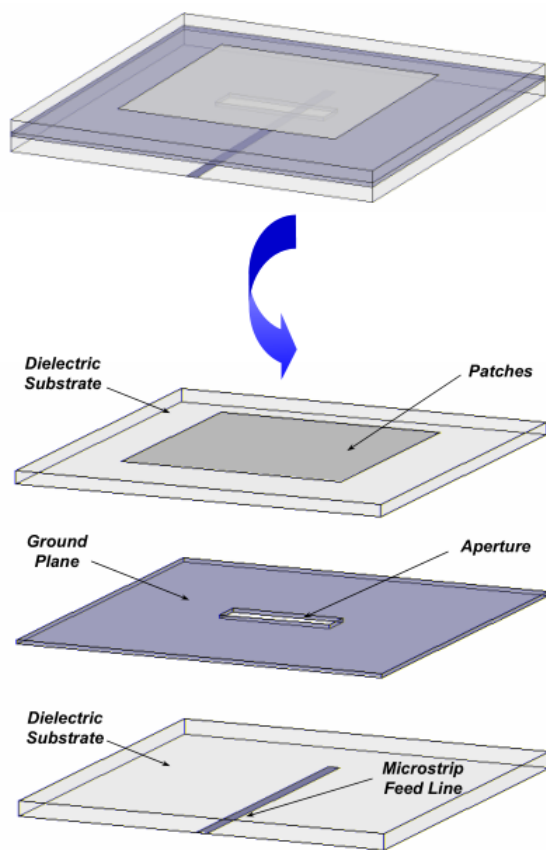


Figure 1.3: Aperture coupled MPA. Kevin (2007)

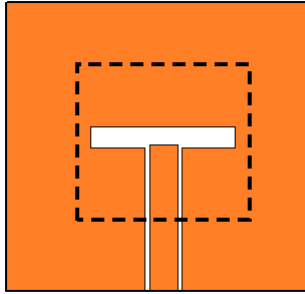


Figure 1.4: A CPW feed with a slot at the end.

#### Coplanar waveguide feed

A coplanar waveguide (CPW) consists of a transmission line for microwave signals with ground plane on each side of the line, separated by a small gap. The CPW feeding method uses electromagnetic coupling for transferring the signal between the feed and the patch. The waveguide is cut in the ground plane, and a slot is etched at the end of the CPW to achieve impedance matching. An illustration of a CPW with a slot is given in Figure 1.4. According to Chen and Chia (2006), slots in the ground plane causes back radiation, so to suppress this, a loop can be made at the end of the CPW. It is easy to integrate electronic components on the same layer as the CPW, since the distance between transmission line and ground is short, so CPW is often used when electronics shall be integrated. CPW structures are suitable for arrays, since it is the TM modes that are dominant in the coupled slot line. This means that the magnetic currents in closely located slots are out of phase, and the radiation from the feeding structure is small. Compared to the aperture coupled feed, the coplanar waveguide feed requires less layers, and thus can be made thinner. This can be seen in Hettak et al. (2001), where CPW feed with a crossed slot is used to obtain dual frequency operation. The drawback of this method is that it is harder to obtain the same bandwidth as with aperture coupling, since there are less parameters to adjust.

#### 1.2.4 Increase of bandwidth and multiple frequency operation

The bandwidth considered in this section is the impedance bandwidth, which is the range of frequencies for which the antenna is well matched to the feed, such that more energy of a signal is transmitted from the feed to the antenna, or from antenna to receiver load. The bandwidth of an antenna is the part of the frequency band that the antenna will transmit effectively in. The bandwidth can be quantized as the frequency range for which the antenna has a input reflection coefficient (S parameter  $S_{11}$ ) that is less than -10 dB, or a voltage standing wave ratio (VSWR) less than 2. If the bandwidth is narrow, the antenna may be unable of receiving if there is small changes in the frequency transmitted. With changes in temperature, the materials used in the antenna will change its properties, and the center frequency can be drifting, which will be a problem if the antenna has a narrow bandwidth. Basic MPAs have narrow bandwidth, so methods for increasing the bandwidth have been

Table 1.1: Properties of different substrates

Relative permittivity $\epsilon_r$	Substrate thickness	
	Thin	Thick
Small	-	Antenna
Large	Lines and circuits	Surface waves

developed and investigated. The methods can be divided into three different approaches; lowering the Q (Quality factor), impedance matching network, and multiple resonances.

### Lowering the Q

Since basic MPAs has a low bandwidth, they also have a high Q, since Q is inverse proportional to the bandwidth. So lowering the Q can increase the bandwidth. The Q represents losses in the antenna. The shape of the patch can affect the Q according to Chen and Chia (2006), though not much, and since the shape is important for the radiation performance, changing the patch shape is not always a practical way to lower the Q.

Another way to lower the Q, is by using a thicker substrate with low relative permittivity. Table 1.1 shows the properties of different combinations of relative permittivity and thickness of substrate, and the combination of a thick substrate with low permittivity is good for antennas. A drawback of thicker substrates is that it will increase surface waves and thus give a lower radiation efficiency, but the efficiency will increase with a lower relative permittivity. In general the Q is inverse proportional to the volume of the antenna, so increasing the width of the MPA will also increase the bandwidth. For the coaxial probe feeding, a thicker substrate means a longer feeding probe, which will increase the inductance of the probe. This extra inductance will limit the increase of bandwidth which is possible to obtain. There are methods that can reduce the extra inductance, these were reviewed in the section on coaxial probe feed. For example the L-shaped probe has proved to give a broad bandwidth, according to Kevin (2007). For aperture coupling, more substrates are used, and this improves the bandwidth because of the overall thicker substrate. The tuning stub of the aperture coupled structure can be adjusted to offset the inductive change in impedance caused by the thick substrates.

### Impedance matching network

An impedance matching network can be introduced to improve the bandwidth. There are different ways of making this, it can be a separate network with tuning stub or quarter wave transformer, or it can be made directly on the patch, by use of slots and notches. In for example Mishra et al. (2009), one patch with notch, and one patch with a slot are analyzed for multiple frequency operation.

## Multiple resonances

By introducing multiple resonances the bandwidth can be improved. Then extra resonators which have closely spaced resonance frequencies are introduced. This can be realized with use of slots in the patch, parasitic patches or stacked patches. If the different resonances are close the bandwidth increases, and if the resonances are further apart the antenna can be made for multiple frequencies.

By making slots in a patch, or changing the shape of the patch, it can obtain multiple resonant frequencies. Different dimensions of the patches will make them radiate on different frequencies. For example an H-shaped slot can be considered as two folded dipoles. In Ozkaya and Seyfi (2015), a modified leaf shaped MPA is used, more specific a tulip shape, to make an antenna that can operate in both X and Ku band. Modified leaf shaped MPAs have advantages as high radiation performance, small size and wide bandwidth or multi-band operating frequencies. The drawback is complicated analyze of its performance characteristics, due to the complex shape. Other examples where slots and different shapes are used to operate on multiple frequencies are found in Satya Dubey and Modh (2011); Samsuzzaman et al. (2013). All of these are for multiple frequency operation in the Ku-band, and can be used for satellite communication. Patches made for dual frequencies by special shape or slots cut in them, normally have a narrow bandwidth, and are therefore not interesting for the antenna in this thesis.

To obtain multiple resonances, parasitic patches can be used. The parasitic patches can be on the same plane as the main patch (the patch that is directly fed) as seen in Figure 1.5, where the parasitic patches are located on each side of the main patch. Another method is to stack the parasitic patches in layers above the main patch, as seen in Figure 1.6. The parasitic patches will radiate because of electromagnetic coupling with the main patch, and if they radiate with slightly different frequencies, the bandwidth will be increased.

As mentioned earlier, the aperture feed method can increase the bandwidth significantly when stacked patches are used. The tuning stub of the aperture coupled structure can also be set close to resonance to obtain a double tuning effect. According to Chen and Chia (2006), different factors that can be adjusted to get better bandwidth are the placement of the parasitic patches relative to the main patch, the size of the parasitic patches, and number of parasitic patches. Combinations of stacked and co-planar parasitic patches can be used to get a lower profile or a lateral smaller size. In Noh et al. (2004), three stacked patches are used to make multiple frequency antenna for the Ku-band. This antenna works on two frequencies, one frequency for transmitting and one for receiving, and a bandwidth around 10% is obtained for both frequencies. Between the patches it is placed layers of foam, which has low relative permittivity, and this gives good electromagnetic coupling. Thicker foam can give better bandwidth, but thicker foam will also reduce the electromagnetic coupling with the patch.

### 1.2.5 SSFIP principle

SSFIP is an abbreviation for *Strip-Slot-Foam-Inverted Patch*, and is the name of an MPA structure. It is a technique for increasing bandwidth of MPAs, and was introduced by Jean François Zürcher in 1988, and it is presented in Zürcher and Gardiol (1995). The

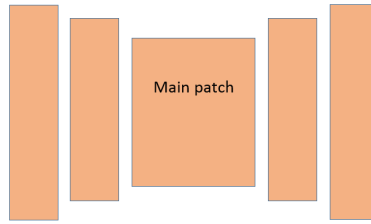


Figure 1.5: Co-planar parasitic patches

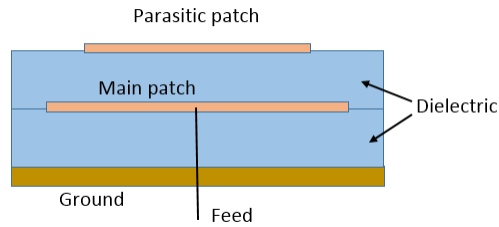


Figure 1.6: Stacked patches

abbreviation gives the order of the elements that the signal goes through. An illustration of the structure is given in Figure 1.7. The bottom-part is similar to an aperture coupled MPA, with microstrip line beneath a feed-substrate which is below a ground plane with a slot in it. Then there is a layer of foam, which makes up the patch-substrate. Foam is a good choice as substrate for the antenna, since there are foams with very low relative permittivities, which means less surface waves. Foams also allow lightweight structures even if they are thick, which is desired for patch-substrates. But foams don't have flat surfaces suited for mounting patches on, so an inverted patch is introduced, which has a thin substrate layer on its top. This substrate will be an environmental protection of the antenna, and is called radome or superstrate. It should be thick enough to give some protection, but at the same time, it's maybe desired to be so thin that it does not affect the antenna's performance significantly.

The SSFIP is, according to Kuchar (1996), further improved by adding a reflector in form of a metal plane below the structure, as seen in Figure 1.7. The reflector's purpose is to reduce back radiation. It is placed a quarter free-space wavelength below the main source of back radiation, which is the aperture. The reflected radiation will then add constructively to the field in forward direction, since the wave is travelling a half wavelength, and is phase shifted 180 degrees when it is reflected. A smaller spacing would make signals cancelling each other, and a larger spacing would give more lobes in different directions. Since the reflector is finite, not all radiation backwards is removed.

In Aliakbarian et al. (2006), a wide-band MPA array for Ku-band is made with use of the SSFIP technique. The single MPA has 25.1% bandwidth, with VSWR below 2 from 10.27 to 13.22 GHz. Air is used instead of foam, so holders are placed at the corners of the antenna to support the superstrate with the patches. A resonating aperture is the main reason for the good bandwidth.

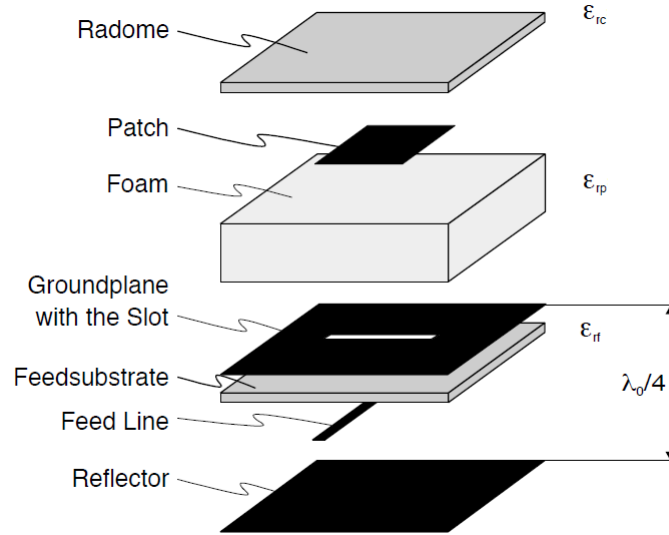


Figure 1.7: SSFIP structure with reflector. Kuchar (1996).

### 1.2.6 Polarization

In Zürcher and Gardiol (1995), the polarization of an electromagnetic wave is defined as the figure that the tip of the electric field vector makes in the space as it propagates. As said in Zürcher and Gardiol (1995), dipoles, and combinations of dipoles, have linear polarization, and basic patch antennas with rectangular, circular and triangular shapes, will also have linear polarization. Antennas can also have circular polarization due to its geometry, or the antenna can be dual polarized. A dual polarized antenna radiate with two orthogonal linearly polarized waves, which are in phase quadrature. An antenna with circular polarization will be useful in the frequency range where the input reflection coefficient is less than -10 dB, and the axial ratio is less than 3 dB, which is called the axial ratio bandwidth. A perfect circular polarization will have an axial ratio of 0 dB, and a linear polarization will have an infinite axial ratio. For a circularly polarized antenna, the polarization will normally become more elliptic further away from the main lobe. According to Lee and Tong (2012), circular polarization is more reliable to use in environments where multipathing and fading can be problematic, and for communication going through the ionosphere. A patch antenna can be made circularly polarized by generating dual polarization in three different ways. These techniques can be categorized as single feed, dual feed, and sequentially rotated.

To obtain circular polarization with a single feed structure, the patch can be almost square or almost circular, or it can be a square patch with truncated corners or a circular patch with indentations, as seen in Figure 1.8. These shapes will give two orthogonal linearly polarized waves. A patch with a slot cut in it, or a stub attached to it, can also have circular polarization. When single feed is used, the placement of the feed is crucial to obtain circular polarization. The single feed structure will then give two waves in phase quadrature with slightly different frequencies. The drawback with the single feed is the narrow bandwidth that has effective circular polarization. In Nayeri et al. (2011), a dual-

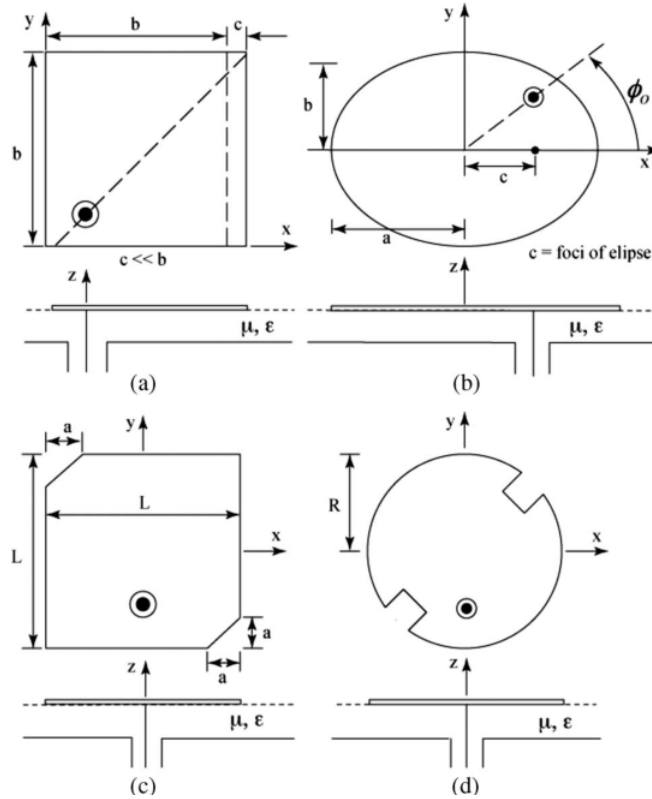


Figure 1.8: Single feed circularly polarized patches. (a) Almost square. (b) Almost circular (elliptical). (c) Square with truncated corners. (d) Circular patch with indentations. Lee and Tong (2012).

band patch antenna with circular polarization is made by use of two stacked patches with asymmetric U-slots. A probe directly feeds the upper patch, while the lower patch is excited through electromagnetic coupling with the probe. An axial ratio bandwidth of respectively 3.1% and 1.0% is achieved for the upper and the lower patch.

A dual feed structure can give better bandwidth than the single feed. A symmetrical patch is fed at two points that are located such that the cross-circular polarized components of the signal are cancelled. The method can be extended to use multiple feeds. Normally squared patches shall be avoided, since they generate high levels of cross-polarization, but when circular polarization with dual feed is desired, the patch should be symmetric. Aperture coupled antennas can be circularly polarized by the use of a split feed and apertures that is off-center or an aperture made of crossed slots. In Wu et al. (2007), a quadri-polarized aperture coupled MPA is made. This means that the antenna can use four different polarizations; one pair of orthogonal circular polarizations, and one pair of orthogonal linear polarizations. The MPA is fed through four rectangular slots in the ground plane via four feeding lines, as shown in Figure 1.9. 8 pin-diodes is used to control the feed, and in that way choose which polarization to use.

Circularly polarization can be achieved by using sequential rotation technique. Then elements in an array are fed sequentially. An example with this technique is seen in Rafii

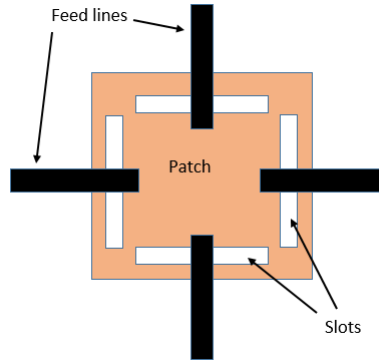


Figure 1.9: Quadri-polarized patch

et al. (2013), where a circularly polarized broadband antenna array is made. It's a  $2 \times 2$  array of squared slots. These slots are circularly polarized themselves, but by using sequential rotation in addition, the axial ratio can be improved. The four slots are spatially rotated  $90^\circ$ , and fed with a  $90^\circ$  phaseshift, and in total this will give circular polarization.

### 1.2.7 MPA Arrays

By placing patches in an array with a regular pattern, a narrower beam can be realized through combinations and cancellations of the radiated fields from the patches. In addition, the beam of the array can be electronically controlled. With electronic control, the phases and amplitudes fed to the different patches of the array can be controlled. The feed lines have to be drawn carefully if the patches shall get correct phase, and this will demand more space. Therefore, a vertical feed is desired for the array, such that feed network and patches can be placed on different layers. An example of an MPA array is seen in Figure 1.10.

An array will not only radiate with the main lobe, but will have side lobes or grating lobes too. According to Zürcher and Gardiol (1995), the side lobes are present since not all the radiated signal from the patches are adding up in one direction, and the cancellations in other directions are not complete. This a fact due to the limited size of the antenna array. A theoretical infinite array could emit only one lobe. Grating lobes occur when the patches are placed too far from each other. The patches will also affect each other through electromagnetically coupling when they are placed close to each other, and patches in the middle of the array will be affected differently than those on the edge of the array. Scan blindness can occur due to mutual coupling in arrays, and means that at certain scan angles the antenna will not work because its radiated beams are cancelled.

MPA arrays for the Ku-band already exists, as seen in for example Noh et al. (2004). This array is for both receiving and transmitting, and each element has its own feed for transmitting, and one for receiving. The array has horizontal polarization for receiving and vertical polarization for transmitting. By combining the patches into an array, the total gain increases.

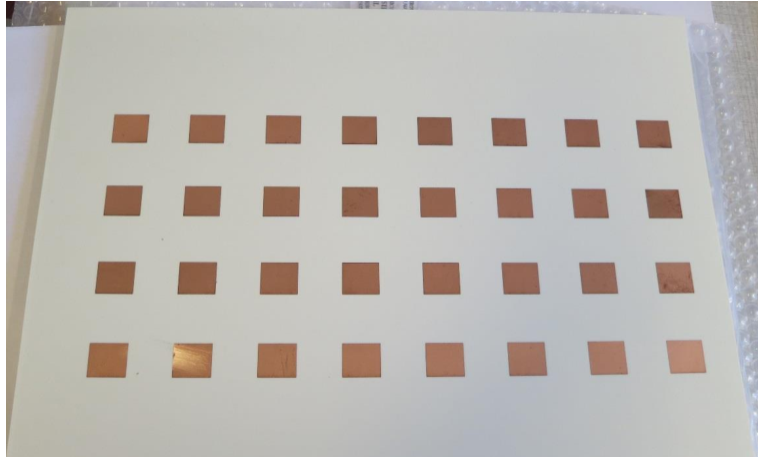


Figure 1.10: Example of MPA array

### 1.2.8 Computer tools

According to Swanson and Hofer (2003), computer aided design (CAD) for circuits started to gain momentum in the 1970s, when mainframe computers became more available. At the same time, the theory and practice of solving electromagnetic (EM) problems on computers, called numerical EM, were emerging because of increased computer power. In the 1990s, faster computers and software that was more efficient made it possible to make good planar and three-dimensional (3D) solvers. Today, radio frequency (RF) and digital design engineers use many different commercial EM field solvers to solve their problems. EM field solvers are necessary to solve analog and digital problems including high frequencies, large bandwidths, or high complexity.

### 1.2.9 Applications

In Waterhouse (2003) and in Singh and Tripathi (2011), a wide selection of different applications of MPAs are provided, and some of them are presented here. It was not before in the 1990s the MPA became a competitor to other antennas in a wide range of systems, mainly because of improvement in its bandwidth capacity. Today MPAs can be found in most kind of communication systems. Some early applications of the MPA was for fixed frequency/low bandwidth radar systems, and for telemetry on missiles and other projectiles, because of their low profile and conformal nature. An advantage the MPA has in military use is its narrow bandwidth. This makes it less vulnerable to jamming frequencies or interference. Commercial aircrafts have started to use MPAs in order to offer passengers communication services via satellite.

Due to their small size and weight, MPAs were used in some satellites in its early history, but in the mid-1990s, it became more important in satellite systems, due to development of arrays with better bandwidths and radiation performance. A famous example of a system that used MPAs is the Iridium communication system. Today most satellites use MPAs. MPAs are also used in low cost, detection systems, for example collision avoidance systems. The MPA is suited for this because of its small size, and since these systems don't require

large bandwidths and are operated at microwave frequencies. The MPA can also be found in mobile communication systems, and is commonly used in base stations. Other examples of use is for medically purposes, GPS receivers, RFID, and WiMAX.

### 1.3 Contribution

In this thesis, a wide-band, vertically fed, microstrip patch antenna element is designed simulated. It operates at both up- and downlink in the Ku-band, and it is designed with the SSFIP structure, using a resonating aperture. Another single element antenna that operates at both up- and downlink frequencies in the Ku-band is already presented in Parikh et al. (2012), but this antenna has not as wide bandwidth and as high gains as achieved in this thesis. The single element antenna presented in Aliakbarian et al. (2006), only works for the downlink frequency, but the antenna presented in Pavuluri et al. (2008) can be used for both frequencies. On the other hand it is not as well matched, and has lower gains than the antenna presented here.

It was not found many examples of antennas with patch reflectors, implying that it is not much investigated. The patch reflector presented here is special in the way that it is configured to work on the frequencies in the Ku-band.

A new qualitative design and tuning procedure for a wide/dual-band patch antenna is given in this thesis. The procedure covers design of all parts of an SSFIP structure with resonant aperture, and gives guidelines for different approaches in the tuning procedure.

Design and simulation of the feed network is not a part of this thesis. The antenna elements will neither be simulated in array here.

### 1.4 Outline

In Chapter 2 theory and models for electromagnetism, antennas and microstrip circuits that has been applied in the thesis is provided, including definition of terms and the coordinate system used here. The software utilized for design and simulation, and some of its features are presented.

Parameters from the design of the antenna is given in Chapter 3, along with parameters and simulations of the tuned antenna. A patch reflector is introduced, and simulation results of the antenna element with the patch reflector are provided. The design and tuning procedure is given in Chapter 4, after a review and discussion on effects of different antenna parts. The report is concluded in Chapter 5, together with a discussion on results and design, and recommendations for future work with the antenna.



# Chapter 2

## Preliminaries

In this chapter, theory on electromagnetism, antennas and microstrip circuits utilized in the thesis is presented. Some features and requirements for the antenna is presented, and a brief introduction to the software used for design and simulation is provided.

### 2.1 Theoretical preliminaries

#### 2.1.1 Electromagnetism

All classical electromagnetic phenomena can be described by Maxwell's equations. The four equations are coupled differential equations, and in notation of vector calculus they are given as

$$\nabla \times \mathbf{E} = -\frac{\partial \mathbf{B}}{\partial t} \quad (2.1)$$

$$\nabla \times \mathbf{H} = \mathbf{J} + \frac{\partial \mathbf{D}}{\partial t} \quad (2.2)$$

$$\nabla \cdot \mathbf{D} = \rho \quad (2.3)$$

$$\nabla \cdot \mathbf{B} = 0 \quad (2.4)$$

in Chatterton and Houlden (1995). The bold characters represent vectors.  $\mathbf{E}$  and  $\mathbf{H}$  are the electric and magnetic *field intensities*, and  $\mathbf{D}$  and  $\mathbf{B}$  are respectively the electric *displacement* and the magnetic *flux density*. The quantities  $\rho$  and  $\mathbf{J}$  are the *density of free electric charge*, and the *electric current density* of any external charges. These quantities can be thought of as the source of electromagnetic fields. A current  $\mathbf{J}$ , varying with time, will create a circulating time-varying magnetic field  $\mathbf{H}$ , and this magnetic field will generate a circulating time-varying electric field  $\mathbf{E}$ , which again will generate a magnetic field, and so on, and we have an electromagnetic wave. In a material with relative permittivity  $\epsilon_r$ , and relative permeability  $\mu_r$ , we have that

$$\begin{aligned} \mathbf{B} &= \mu_r \mu_0 \mathbf{H} \\ \mathbf{D} &= \epsilon_r \epsilon_0 \mathbf{E} \end{aligned}$$

The speed of the electromagnetic waves in free-space can be found from the equations as

$$c = \sqrt{1/\varepsilon_0\mu_0} \quad (2.5)$$

where  $\varepsilon_0 = 8.854 * 10^{-12}$  F/m, is the free-space permittivity, and  $\mu_0 = 4\pi * 10^{-7}$  H/m, is the free-space permeability. This gives  $c \approx 3 * 10^8$  m/s, which is the speed of light. The wavelength  $\lambda$  is then found from

$$\lambda = \frac{c}{f} \quad (2.6)$$

where  $f$  is the frequency of the wave. The effective wavelength, also called guide wavelength, is the wavelength in a transmission line, and it can be calculated from

$$\lambda_{eff} = \frac{\lambda_0}{\sqrt{\varepsilon_{eff}}} \quad (2.7)$$

where  $\lambda_0$  is the free-space wavelength, and  $\varepsilon_{eff}$  is the effective permittivity of the feed substrate.

As stated in Balanis (2012), Maxwell's equations are used to solve for the field vectors, assuming that the field vectors are single-valued, bounded and continuous functions and derivatives of time and space. However, Maxwell's equations are not easily solved for realistic situations, so simplifications and approximations are used for solving electromagnetic problems. At boundaries in medias where there are discontinuities in the electrical properties, the field vectors are discontinuous, and their behaviour must be found using the boundary conditions. The electromagnetic fields of boundary-value problems are obtained by using adjusted Maxwell's equations. The equations are coupled partial differential equations, so each equation has more than one unknown field. By raising the order of the equations to second-order partial differential equations, they can be uncoupled, and these equations are normally referred to as *wave equations*.

According to Yeh and Shimabukuro (2008), the electromagnetic fields in a simple medium governed by a linear vector wave equation, are linear. This means that the complete electromagnetic field can be obtained by superposing partial fields, and the electromagnetic waves can be divided into some basic wave types, which together can give the complete electromagnetic field. The different waves are also called *modes*, and for a given electromagnetic boundary-value problem, each field configuration that solves the problem is a mode. The basic wave types are as given in Yeh and Shimabukuro (2008):

1. *Transverse Electromagnetic Waves*(TEM). There is no electric or magnetic field component in the direction of propagation.
2. *Transverse Magnetic Waves*(TM or E waves). There is no magnetic field component in the direction of propagation.
3. *Transverse Electric Waves*(TE or M waves) There is no electric field component in the direction of propagation.
4. *Hybrid Waves*(HE or EH waves). All electric and magnetic fields components are contained in the wave.

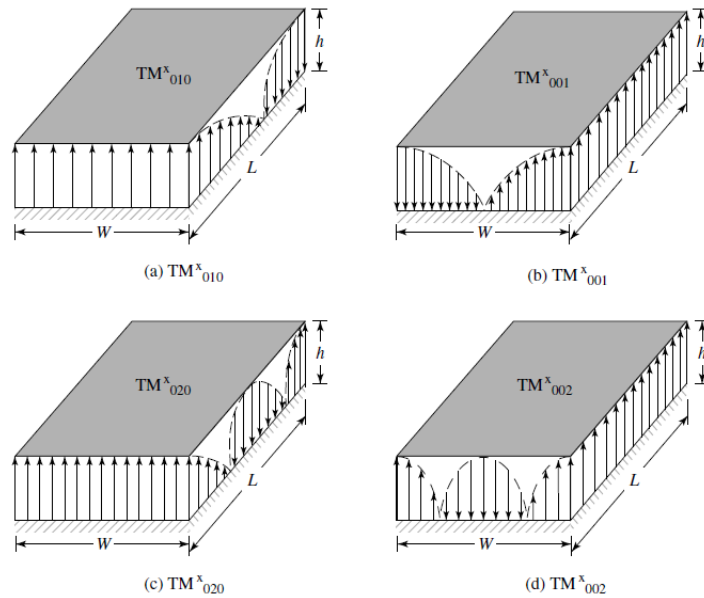


Figure 2.1: Half-wave patterns for some TM-modes. Balanis (2005)

In microstrips or patches, mode numbers are designated by three suffix numbers attached to the mode type, such as  $TE_{lmn}$  or  $TM_{lmn}$ , where  $l, m$  and  $n$  respectively represents the number of half-wave patterns across the height, the length, and the width of the microstrip or patch. The mode number for the height will usually be zero since the height of the patch is too small to support any mode, and it is therefore sometimes not written. The mode with the lowest order resonance is referred to as the *dominant* mode. In Figure 2.1 the relation between half-wave patterns and some different TM modes are seen for patches.

### 2.1.2 Antennas

In Balanis (2005) it is referred to the *IEEE Standard Definitions of Terms for Antennas*, where an antenna is defined as "a means for radiating or receiving radio waves.". The antenna is the structure between a guided wave and a space wave. It can be represented by an impedance  $Z_{ant} = (R_L + R_r) + jX_A$ , where  $R_L$  is the load resistance, representing losses in the antenna,  $R_r$  is the *radiation resistance*, which represents the radiation from the antenna, and  $X_A$  is the reactance associated with the imaginary part of the radiation. It is desired to transfer the majority of the power to the radiation resistance, so as much as possible of the power is used for radiation. Different parameters are used to tell how good the performance of an antenna is, and the parameters used here will be described next. If nothing else is stated, the definitions are taken from Balanis (2005).

#### Radiation pattern

The radiation pattern is a graphical representation of the antenna's radiation properties in space coordinates. The radiation pattern includes power, radiation intensity, field strength, directivity, phase or polarization. It is often plotted in decibels, in order to get a more

detailed view of the parts of the pattern with low values, such as side lobes. The beamwidth of an antenna is often defined as the *half-power beamwidth* (HPBW), which is the angular separation of the points where the power is half of the maximum power. In decibels, this means the points with -3dB respectively to the maximum.

### Radiation density and radiation intensity

Radiation density is radiated power per area, and is measured in  $W/m^2$ . Radiation intensity is obtained by multiplying the radiation density with the square of the distance, and it is equal to power radiated per unit solid angle. The total power radiated by an antenna can be found from integration of the radiation intensity over the entire solid angle of  $4\pi$ .

### Directivity

The directivity of an anisotropic source is the ratio between its radiation intensity in a given direction, and that of an isotropic source. An isotropic source is a hypothetic antenna, which radiates equal in all directions. Directivity is a dimensionless measure, and is often given in decibels or isotropic decibels (dBi). Isotropic decibel means that it is measured relative to an isotropic antenna.

### Gain

Gain is defined as the ratio between the radiation intensity in a given direction to the radiation intensity from an isotropic source transmitting same amount of power. It is calculated as  $Gain = 4\pi \frac{\text{radiation intensity}}{\text{total input power}}$ . If the direction not is given, it is usually in the direction of maximum radiation. The gain is a dimensionless unit, and it is often given in decibels or isotropic decibels. Gain is related to directivity, and the difference is that gain accounts for efficiency and losses, while directivity doesn't.

### Front-to-back ratio

The front-to-back ratio is the ratio between gain in (normally) the maximum gain direction, and the gain in the direction turned  $180^\circ$  relative to the maximum.

### S-parameters

According to Caspers (2011), S-parameters (Scattering-parameters), are used to describe high frequency networks. They are expressed in terms of in- and outgoing waves. A network with two ports, will give a four-pole system. In a network with  $n$  ports, the waves moving toward the  $n$  port are  $\mathbf{a} = (a_1, a_2, \dots, a_n)$ , and the waves moving away from the  $n$  port are  $\mathbf{b} = (b_1, b_2, \dots, b_n)$ . The relation between  $a_i$  and  $b_i$  is expressed by a system of  $n$  linear equations, and on matrix formulation  $\mathbf{b} = \mathbf{S}\mathbf{a}$ . A two-port system is written as

$$\begin{aligned} b_1 &= S_{11}a_1 + S_{12}a_2 \\ b_2 &= S_{21}a_1 + S_{22}a_2 \end{aligned} \tag{2.8}$$

Table 2.1: Corresponding values of  $S_{11}$  and VSWR

$S_{11}$	VSWR
-7.35dB	2.5
-9.54dB	2
-10dB	1,92
-14dB	1,5
-15dB	1.43

$S_{11}$  is the *input reflection coefficient*,  $S_{21}$  is the *forward transmission*,  $S_{12}$  is the *reverse transmission*, and  $S_{22}$  is the *output reflection coefficient*. The input reflection coefficient is often denoted by  $\Gamma$ , and it is a dimensionless number between 0 and 1. When it is given in decibels, it is more often denoted  $S_{11}$ . The amount of power that is reflected at the input terminals of the antenna is determined by the degree of mismatch, which is a function of the antenna input impedance and the characteristic impedance of the transmission line. A perfect match means that  $\Gamma = 0$ .  $S_{11}$  is a widely used measure of an antenna's bandwidth. The bandwidth is considered to be the frequency band where  $S_{11}$  is less than a given value, often -10dB. Another measurement of impedance matching is VSWR (Voltage Standing Wave Ratio), which is a function of the input reflection coefficient. The relation between power, input reflection coefficient, impedances and VSWR is as given in Balanis (2005):

$$\frac{P_{refl}}{P_{inc}} = |\Gamma|^2 = \frac{|Z_{ant} - Z_c|^2}{|Z_{ant} + Z_c|^2} = \left| \frac{VSWR - 1}{VSWR + 1} \right|^2 \quad (2.9)$$

where  $P_{refl}$  is the reflected power,  $P_{inc}$  is the incoming power,  $Z_{ant}$  is the antenna input impedance, and  $Z_c$  is the characteristic impedance of the transmission line. With a perfect match,  $VSWR = 1$ . Some corresponding values of  $S_{11}$  and VSWR are given in Table 2.1.

### Quality factor, efficiency and bandwidth

Quality factor (Q), efficiency and bandwidth are all interrelated, so it is not possible to optimize all for the same antenna. Some trade-offs must be made, but often it is desired to optimize one on cost of another. Since MPAs have narrow bandwidth, it is normally attempted to increase this, on the cost of the Q. The Q represents the antenna losses, which typically are radiation, conduction, dielectric and surface wave losses. Bandwidth (BW) is inverse proportional to Q, and is given by  $BW = \frac{1}{Q}$ . This formulation does not take impedance matching at the antenna terminals into account, but this can be done by adding the VSWR in the formula. Then the formula becomes

$$BW = \frac{VSWR - 1}{Q\sqrt{VSWR}} \quad (2.10)$$

In general, the bandwidth is inversely proportional to the volume of the antenna. Since basic MPAs have low profile, they have a small volume, and a narrow bandwidth, but the bandwidth will increase with thick substrates. The Q associated with surface wave losses will increase with thicker substrate, but the Q associated with radiation losses will decrease.

Many different efficiencies are related to antennas. Total efficiency is a product of reflection efficiency, conduction efficiency, and dielectric efficiency. Reflection efficiency is defined as  $e_r = 1 - |\Gamma|^2$ , where  $\Gamma$  is the reflection coefficient. The conduction and dielectric efficiencies are often hard to calculate, and are normally written as one single efficiency, called the antenna radiation efficiency. This antenna radiation efficiency is defined as the ratio between radiated power and the input power. Since surface waves is an important factor in an MPA, a surface wave efficiency is included for MPAs. For a microstrip antenna the radiation efficiency is written as  $e = \frac{Q_t}{Q_{rad}}$ , where  $Q_t$  is the total Q, and  $Q_{rad}$  is the Q due to radiation losses. The efficiency is also be defined as the ratio between gain and directivity, since gain includes losses in the antenna, while directivity doesn't.

### Polarization

An electromagnetic wave can be linearly, circularly or elliptical polarized. If the propagating wave oscillates parallel relative to the ground, it is horizontally polarized, and if it oscillates orthogonal relative to the ground, it is vertically polarized. When the electric field vector moves in a straight line, the wave is linearly polarized. A wave can be decomposed in two linearly polarized components, and if these two components are in phase, the wave is linearly polarized. If the two components not are in phase, the wave is elliptically or circularly polarized, and only if the two components of the wave have equal amplitude and a  $90^\circ$  phase shift (in phase quadrature), the wave is circularly polarized. If a circularly polarized wave is rotating counterclockwise when it is propagating toward the observer, the polarization is right handed circularly polarized (RHCP). Otherwise, if it is rotating clockwise when propagating towards the observer, the polarization is left handed circularly polarized (LHCP).

The desired polarization form in a case is often called co-polarization, and the opposite is called cross-polarization. Cross-polarization is the polarization that is orthogonal to the desired co-polarization. In a case with an antenna with horizontal polarization, vertical polarization is the cross-polarization, and in the case of an antenna with RHCP, LHCP will be the cross-polarization. Normally, linear or circular polarization is desired, and elliptical polarization is a result of geometric or electric imperfections.

A squared patch will have circular polarization since both fundamental modes,  $TM_{010}$  and  $TM_{001}$ , occur at the same frequency when the width and length of the patch are equal, and the two modes have the same radiation pattern, rotated  $90^\circ$  relative to each other.

### 2.1.3 Antenna measurements

Different measurements are used to tell the performance of an antenna, or to validate theoretical results, and to tune antennas corresponding to these. Many different properties of an antenna can be measured, here the focus will be on radiation pattern, gain, impedance/bandwidth, and front-to-back ratio (F/B). For measurements of for example radiation pattern and gain, the spherical coordinate system in Figure 2.2 is used. The radial distance is kept constant, so only the angular coordinates  $(\theta, \phi)$  are used for positioning. The antenna is positioned in the centre of the coordinate system, and in this thesis, the antenna element is placed with the centre of the patch in the middle of the xy-plane. The

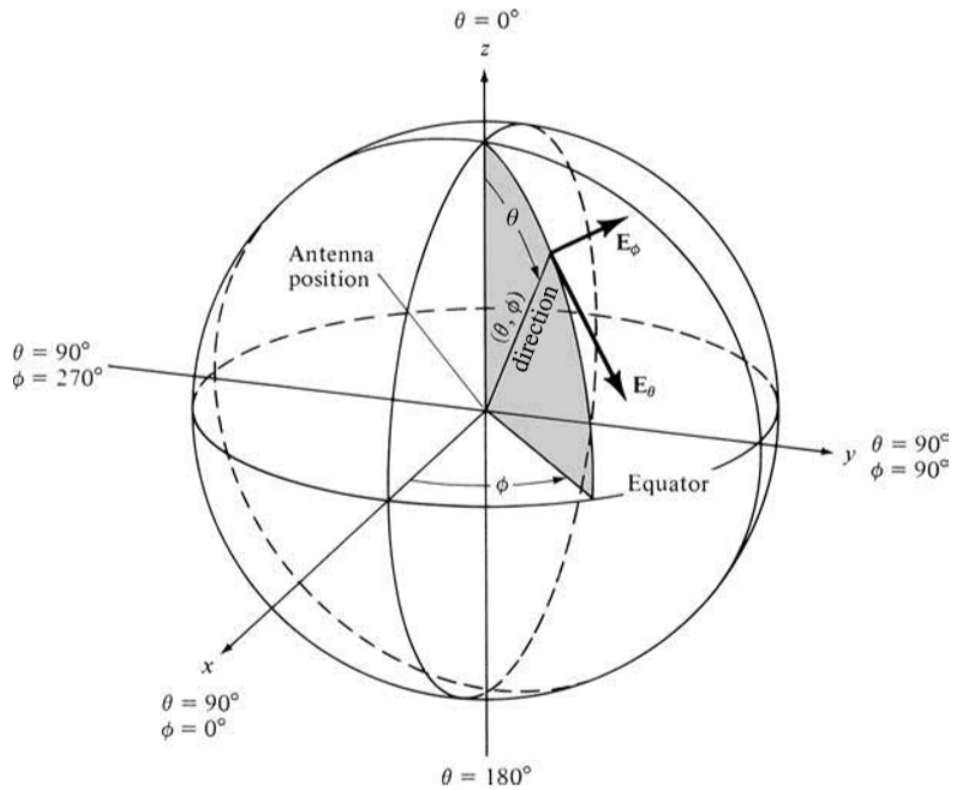


Figure 2.2: Spherical coordinate system. Balanis (2005)

patch, substrate and ground planes are all parallel to the  $xy$ -plane. The feed line and the patch will have their longitudinal direction in the  $y$ -plane.

A very helpful tool for antenna measurements is the Smith chart, shown in Figure 2.3. According to Zürcher and Gardiol (1995), the Smith chart is a conformal mapping of the horizontal and vertical coordinate lines in the complex plane of the normalized impedance,  $Z_L/Z_c$ , the load impedance relative to the characteristic impedance, onto the complex plane of the reflection coefficient,  $\Gamma$ . The diagram consists of two types of circles; resistance circles, whose centre is located on the horizontal axis of the Smith chart, and reactance circles, which appear as bows since their centre is at the outer circle of the Smith chart. In the centre of the chart  $\Gamma = 0$ , and at the edges  $|\Gamma| = 1$ . Points in the upper half is inductive, and points in the lower half is capacitive. The horizontal axis in the middle is real values. On the far left of this real axis is the point for a short circuit and on the far right is the point for an open end.

The Smith chart can be used for matching, where a perfect matching will be in the centre of the chart. Different levels of VSWR will be drawn as circles with centre in  $\Gamma = 0$ . Frequency responses of antennas can be plotted in the chart, and the closer a given frequency is to the centre, the better is the antenna matched for this frequency. When a resonator is plotted in a Smith chart, the plot can make a loop. For an aperture coupled patch, the radius of the loop can be seen as a measure of coupling between aperture and patch, where a larger radius means better coupling. In a Smith chart frequencies inside a given VSWR

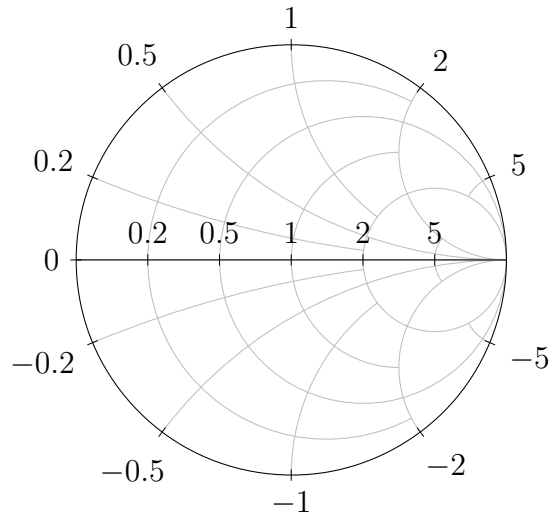


Figure 2.3: Smith chart

circle will represent the bandwidth, but the bandwidth is maybe more clearly presented in a rectangular coordinate system, with for example  $S_{11}$  in dB on the vertical axis, and the frequencies on the horizontal axis.

#### 2.1.4 Materials in microstrip structures

Microstrip circuits are normally made of two types of materials; dielectric substrates and metal conductors. The definitions of dielectrics and conductors given in Chatterton and Houlden (1995), are that when  $\sigma/\omega\varepsilon \leq 1/100$ , the material is a dielectric, and when  $\sigma/\omega\varepsilon > 100$ , the material is a conductor. Here  $\sigma$  is the conductivity of the material, and  $\omega = 2\pi f$ , with  $f$  being the signal frequency, and  $\varepsilon$  is the permittivity. Together the dielectrics and the conductors form an inhomogeneous structure, and Maxwell's equations, or the wave equations, must be solved individually for each medium, giving very complex problems. However, different approaches are used to make the calculations less complex.

To make calculations and models easier to work with, conductors can be thought of as perfect conductors. In a *perfect electric conductor* (PEC), the electric field is set to zero, and the conductivity is infinitely large. According to Zürcher and Gardiol (1995), the boundary conditions says that on the surface of a PEC, the tangential component of the electric field is continuous. Since there is no electric field inside the conductor, the electric fields does not exist tangentially on the surface of the PEC, and magnetic fields will not stay normally on a PEC and its surface impedance is zero. Most metals, such as copper, can be approximated to be PEC, since they have very large conductivity.

The complementary to the PEC, is the *perfect magnetic conductor* (PMC). According to Zürcher and Gardiol (1995), it is has a negligible internal magnetic field, and the tangential field of a magnetic field on its surface, must be normal to the PMC. This can be used for ferromagnetic materials with a very high permeability  $\mu$ . Ferromagnetic materials are seldom used in transmission lines, but the concept of PMC is usable for making models.

The dielectric substrates make the structure of the MPA, and they are support for the

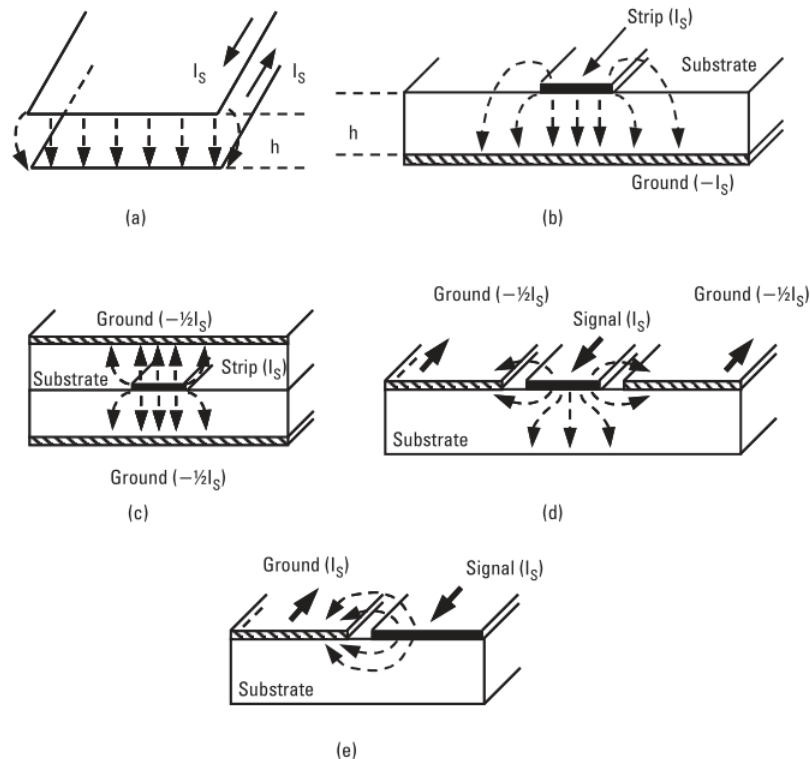


Figure 2.4: Planar transmission lines and their TEM mode E-field distributions and currents: (a) parallel-plate, (b) microstrip, (c) stripline, (d) coplanar waveguide, and (e) slotline. Holzman (2006).

conductors. The electric characteristics of a dielectric are determined by its permittivity and thickness. Its electrical function is, according to Zürcher and Gardiol (1995), to concentrate the electromagnetic fields and prevent unwanted radiation. The relative permittivity is the permittivity of the material normalized to the permittivity of free space.

### 2.1.5 Microstrip circuits

The microstrip line is a planar transmission line for microwave signals, and consists of a conductor on top of a grounded substrate. It was evolved from the stripline, which is a transmission line that is embedded in a dielectric. In Figure 2.4, some common planar transmission lines and their TEM mode electric field distributions and currents are shown. The microstrip is suited for making small and light weight circuits, and is easy to integrate with chip devices, according to Balanis (2012). Drawbacks compared to other transmission lines are high line losses, low power capabilities, and poor isolation between circuits.

Since the microstrip is placed between two different dielectric layers, and its fringing field lines will be in both of the two medias, it can be considered as a line in a homogenous dielectric, where the overall relative permittivity has a value somewhere between that of the two relative permittivities. This overall relative permittivity is called the *effective relative permittivity*, or just effective permittivity. Normally, the upper part of the microstrip

is exposed, so the top dielectric is air. The effective relative permittivity will typically be closer to that of the substrate below the line, than the relative permittivity of air. Because the microstrip is composed of two different dielectrics, it cannot support pure TEM modes, according to Balanis (2012). This is because waves in the two medias not will travel with the same velocity, and the boundary conditions gives transverse electric or magnetic components. However, since the longitudinal components of the field are much smaller than the transverse components, a quasi-TEM approximation can be used. The following formulas for microstrips are found in Hammerstad and Jensen (1980). The effective permittivity is defined as

$$\varepsilon_{eff} = \frac{\varepsilon_r + 1}{2} + \frac{\varepsilon_r - 1}{2} \left(1 + 10 \frac{h}{W}\right)^{-ab} \quad (2.11)$$

where  $h$  is the substrate thickness/height,  $W$  is the width of the microstrip,  $\varepsilon_r$  is the relative permittivity of the substrate, and  $a$  and  $b$  are given as

$$a = 1 + \frac{1}{49} \ln \left[ \frac{\left(\frac{W}{h}\right)^4 + \left(\frac{W}{52h}\right)^2}{\left(\frac{W}{h}\right)^4 + 0.432} \right] + \frac{1}{18.7} \ln \left[ 1 + \left(\frac{W}{18.1h}\right)^3 \right] \quad (2.12)$$

$$b = 0.564 \left( \frac{\varepsilon_r - 0.9}{\varepsilon_r + 3} \right)^{0.053} \quad (2.13)$$

Normally  $ab \approx \frac{1}{2}$  is a good approximation. It is reported that the accuracy of this model is better than 0.2% when  $\varepsilon_r \leq 128$  and  $0.01 \leq \frac{W}{h} \leq 100$ . For  $\frac{W}{h} \leq 1$ , an extra term should be added according to Balanis (2012), though in most cases  $\frac{W}{h} > 1$ .

The characteristic impedance  $Z_c$  for an infinitely thin microstrip is approximated by

$$Z_c = \frac{1}{2\pi} \sqrt{\frac{\mu_0}{\varepsilon_0 \varepsilon_{eff}}} \ln \left( F_1 \frac{h}{W} + \sqrt{1 + \left(\frac{2h}{W}\right)^2} \right) \quad (2.14)$$

where

$$F_1 = 6 + (2\pi - 6) \exp \left[ - \left( 30.666 \frac{h}{W} \right)^{0.7528} \right] \quad (2.15)$$

and  $\varepsilon_0$  is the free-space permittivity and  $\mu_0$  is the free-space permeability. The accuracy of this model is reported to be better than 0.03% for  $\frac{W}{h} \leq 1000$ . This quasi-TEM assumption is for low frequencies. When the frequencies are higher, the fields concentrate in the dielectric substrate and the effective permittivity increases. An approximation of the effective permittivity with this increase is given in Zürcher and Gardiol (1995) as

$$\varepsilon_{eff}(f) = \varepsilon_r - \frac{\varepsilon_r - \varepsilon_{eff}}{1 + G(f/f_p)^2} \quad (2.16)$$

where  $f$  is the signal frequency, and

$$f_p = Z_c / (2\mu_0 h) \text{ and } G = 0.6 + 0.009 Z_c \quad (2.17)$$

The effective permittivity is frequency dependent because velocity of a signal varies with frequency. Higher frequency components travel faster than lower frequency components.

## Surface waves

Based on the direction an electromagnetic wave is transmitted in the microstrip, the waves can be categorized as in Zürcher and Gardiol (1995). The direction is defined by the angle  $\theta$  about the axis normal to the ground plane. The waves that propagate toward open space, and thus make antennas radiate, are called space waves, and have an elevation angle  $\theta$  between 0 and  $\pi/2$ .

Surface waves have an elevation angle  $\theta$  between  $\pi/2$  and  $\pi - \arcsin(1/\sqrt{\epsilon_r})$ . These waves are reflected by the ground plane and then back by the dielectric-to-air boundary, such that the amplitude will build up and cause excitation of *surface wave modes*. The fields made by the surface waves will mainly stay trapped in the dielectric, and take up a part of the energy of the signal. This gives the antenna lower efficiency. Surface waves will also increase coupling between patches on the same substrate, and in large phased arrays, this can lead to blind spots, meaning that the array cannot transmit or receive in certain directions. Surface waves at the edges of patches will increase side lobes and cross-polarization levels. These effects makes surface waves unwanted in antenna systems, so the levels of surface waves should be kept as low as possible. Use of thicker substrates gives more surface waves, and according to Waterhouse (2003), printed antennas with a thickness greater than  $0.2\lambda_0$ , will have relatively low surface wave efficiencies. However, if there are multiple resonators in the antenna, the efficiency can be improved, because the radiators can couple power from the surface waves.

There is also a category of waves called leaky waves; these are more sharply directed downward in the media. The leaky waves does not have as great impacts as the other two types, and will not be focused on in this thesis.

### 2.1.6 Methods and models

The MPA radiates when electric currents flow on the metal plate it is consisted of. A basic MPA radiates with a relatively broad 3-dB beamwidth, between  $70^\circ$  and  $90^\circ$ , according to Zürcher and Gardiol (1995). The length of the MPA is important for the resonance frequency, and the width is defining the input impedance of the MPA. A square patch has almost uniform fields along the edges which makes up the width of the MPA, and a sinusoidal variation along the edges which makes up the length of the MPA, as seen in Figure 2.5. The magnetic currents at the edges of an MPA is seen in Figure 2.6.

To find the electromagnetic fields of an MPA, Maxwell's equations must be solved and the boundary conditions must be appropriate. This process is complicated since there are three different inhomogeneities in the structure; between dielectric(s) and air, between metal conductors and other medias, and at the edges of the structure itself. Anyway, good approximate models can be made with the use of sophisticated computing techniques. There are different methods and models for analysing the fields radiated by microstrip antennas, and they vary in accuracy and complexity. The methods can be divided, similarly as in Pozar and Schaubert (1995), into simplified methods (analytical models) and full-wave methods. The simplified methods give easier calculations due to approximations in the models, but they are not as accurate as the full-wave methods.

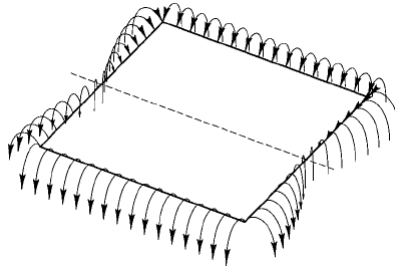


Figure 2.5: Fringing electric fields of a squared patch. Milligan (2005)

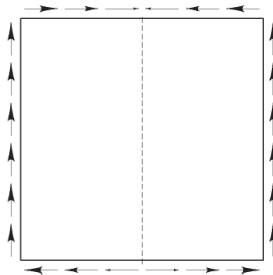


Figure 2.6: Magnetic current on the edges of a squared patch. Milligan (2005)

### Simplified methods

The simplified methods include *transmission line models* and *cavity models*. The transmission line model is the simplest model used for analyse of patch antennas. In this model, a rectangular patch is regarded as a low-impedance microstrip line that radiates at its two extremities, and whose width determines the impedance and effective relative permittivity. The lowest order mode,  $TM_{010}$ , radiates when the effective length across the patch is a half wavelength. The radiating edges of the patch are loaded by a combination of parallel-plate radiation conductance, and capacitive susceptance. According to Milligan (2005), the transmission line model can be used when designing MPAs with a bandwidth between 1 and 4 %, and if the bandwidth percentage is lower or higher the cavity model should rather be used.

In Kuchar (1996) an example of a transmission line model is given. The model is assuming that the radiation from the patch is caused by the fringing fields at the ends of the patch. The fields at the end of the patch can be split into tangential and normal components, with respect to the patch plane. The normal components will be out of phase since they are spaced by a half-wavelength, and therefore not contribute to the radiation in the far field in broadside direction. The tangential components that are in phase will combine and give the radiation normal to the patch surface. This gives a model where the patch is regarded as two parallel slots placed a half-wavelength apart (at each end of the patch). The far-field pattern,  $F(\theta)$ , in the H-plane of the antenna can then be approximated by

$$F(\theta) = \frac{\sin\left(\frac{\pi W}{\lambda_0} \sin \theta\right)}{\frac{\pi W}{\lambda_0} \sin \theta} \cos \theta \quad (2.18)$$

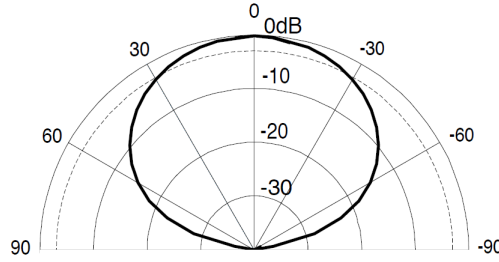
Figure 2.7: Far-field pattern for a patch with  $W_p/\lambda_0 = 0.4$ . Kuchar (1996)

Table 2.2: Comparison of analytical models

Application	Transmission line model	Cavity model
Patch shapes analyzed	Rectangular only	Regular shapes
Substrate thickness	Thin	Thick
Feed types used	Microstrip, probe	Microstrip, probe, aperture coupling
Circularly polarized antenna	No	Yes
Stacked antennas	No	Yes
Mutual coupling between edges	Explicitly included	Implicitly included
Application to arrays	Yes	No

The model is sensible for  $|\theta| \leq 90^\circ$ . The pattern is governed by the ratio between the width and the wavelength. In Figure 2.7, the far-field pattern for an MPA with  $W_p/\lambda_0 = 0.4$  is given.

In the cavity model, the space between the patch and the ground plane is considered as a resonant electromagnetic cavity, which radiates from its edges. According to Milligan (2005), the tangential electric fields on the sidewalls of the cavity are replaced by the equivalent magnetic currents. The sidewalls of the cavity are assumed to be perfect magnetic conductors, while the patch and the ground plane are considered to be perfect electric conductors. The cavity model is suitable for patches with geometries as disks, rectangles, ellipses and triangles. Shapes that are more complex can be analysed by segmentation into smaller and simpler shapes.

In Garg et al. (2001), different simplified methods are compared, and this comparison is presented in Table 2.2. Only the basic transmission line model and the cavity model are included in Table 2.2. Different versions of the models exist, and they can have some other properties than those given here. For example, the cavity model can be generalized for use on shapes of separable geometries, not only regular shapes. From the table it is seen that the cavity model can be used for aperture coupling and antennas with thick substrates, whereas the transmission line model cannot. Compared to the full-wave methods, the major drawback of the simplified methods is the limited accuracy for resonant frequency and input impedance for antennas with thick substrates. The simplified methods also lack good analysis of mutual coupling, large arrays, surface wave effects and different substrate configurations, while the full-wave methods includes such effects through the use of accurate Green's functions.

## Full-wave methods

The full-wave methods include among other numerical methods; the *method of moments* (MoM) and the *finite element method* (FEM). These methods are accurate, but require heavier and more complex computations than the simplified methods, so computer programs are used for the calculations. According to Swanson and Hofer (2003), MoM was introduced in 1968. The MoM is used to solve an integral equation, by use of Green's functions for the dielectric substrates. Green's functions can be used to calculate fields from current distributions. According to Milligan (2005), the MoM starts with assuming currents over small regions of the antenna. It then expands the currents in a sum of basis functions, and solves for the coefficients of the expansion. It is important with a good choice of basis functions for an efficient evaluation of the fields. In the process of MoM, matrices that require time-consuming numerical methods for inversion are obtained and used.

According to Yeh and Shimabukuro (2008), the FEM was first used to solve electromagnetic problems in 1975. As stated in Milligan (2005), the structure of the problem is divided into cubic cells when FEM is used, so this require a program that can divide the structure into a mesh before starting to solve. The analysis is performed in the frequency domain, and must be repeated for every frequency of interest. Currents on boundary surfaces are calculated by use of the *equivalence theorem* with the incident fields, and then the far-field radiation pattern is calculated from these boundary currents. By use of the equivalent theorem, electric fields can be replaced with fictitious magnetic currents, which makes the calculations easier.

### 2.1.7 Design of MPAs

#### General design

According to Balanis (2005), the design procedure of a basic rectangular MPA with  $TM_{010}$  as dominant mode, is made up of the following steps;

1. Some values must be found or decided before any designing can start. The relative permittivities,  $\epsilon_r$ , of the substrates must be known, and the height of these substrates must also be chosen. The operating frequency for the antenna must also be decided.
2. The width of the patch,  $W$ , for effective radiation is calculated from

$$W = \frac{c}{2f_r} \sqrt{\frac{2}{\epsilon_r + 1}} \quad (2.19)$$

where  $f_r$  is the resonant frequency of the fundamental mode of the patch antenna.

3. The effective relative permittivity is found using

$$\epsilon_{eff} = \frac{\epsilon_r + 1}{2} + \frac{\epsilon_r - 1}{2} \frac{1}{\sqrt{1 + 12 \frac{h}{W}}} \quad (2.20)$$

which is a variant of (2.11).

4. The length-extension of the patch due to the fringing effect is found from

$$\Delta L = 0.412 \cdot h \frac{(\varepsilon_{eff} + 0.3) \left(\frac{W}{h} + 0.264\right)}{(\varepsilon_{eff} - 0.258) \left(\frac{W}{h} + 0.8\right)} \quad (2.21)$$

5. The length of the patch antenna is then

$$L = \frac{c}{2f_r \sqrt{\varepsilon_{eff}}} - 2\Delta L \quad (2.22)$$

A design procedure for making a circular patch is also given in Balanis (2005). The relative permittivity and the height of the patch substrate, and the operation frequency must be known. Then the radius,  $a$ , of the patch with  $\text{TM}_{110}$  as dominant mode, and fringing effect included, is found from

$$a = \frac{F}{\left(1 + \frac{2h}{\pi \varepsilon_r F} \left[\ln\left(\frac{\pi F}{2h}\right) + 1.7726\right]\right)^{1/2}} \quad (2.23)$$

where the height,  $h$ , is in centimetres, and

$$F = \frac{8.791 \times 10^9}{f_r \sqrt{\varepsilon_r}} \quad (2.24)$$

### Design of the aperture coupled MPA

When designing an aperture coupled microstrip patch antenna (ACMPA) there are many parameters to adjust. These parameters for a rectangular patch and aperture can be seen in Figure 2.8 and Figure 2.9, and are as listed in Pozar (1996):

- Relative permittivity of antenna/patch substrate,  $\varepsilon_{rp}$ : lower permittivity gives wider bandwidth and less surface waves.
- Thickness of antenna/patch substrate,  $H_p$ : thicker antenna/patch substrate gives better bandwidth, but less coupling.
- Relative permittivity of feed substrate,  $\varepsilon_{rp}$ : for good microstrip circuit qualities this will typically be relatively high, in the range 2 to 10.
- Thickness of feed substrate,  $H_f$ : thinner feed substrate results in less spurious radiation through surface waves, but gives higher loss. Should be between  $0.01\lambda$  and  $0.02\lambda$ .
- Length of microstrip patch,  $L_p$ : the length of the patch determines the resonant frequency of the antenna.
- Width of microstrip patch,  $W_p$ : the width of the patch affects the resonant resistance of the antenna. A wider patch gives less resistance, and can increase directivity and bandwidth.

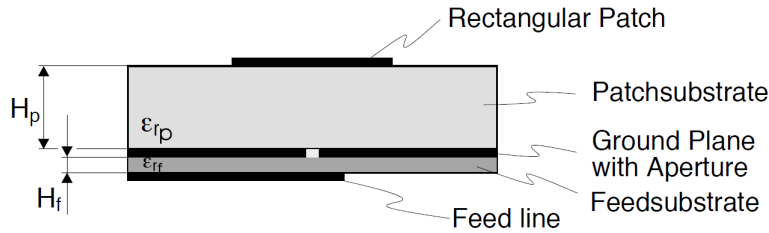


Figure 2.8: Side view of an ACMPA. Kuchar (1996).

- Length of slot/aperture,  $L_a$ : the length of the slot primarily determines the coupling level and the back radiation level. A larger slot will increase the coupling, but the slot should be no longer than what is required for impedance matching.
- Width of slot/aperture,  $W_a$ : the width of the slot is influencing the coupling level, and it is normally circa 1/10 of the slot length.
- Width of feed line,  $W_f$ : the characteristic impedance of the feed line depends on its width. The width of the feed line also affects the coupling with the slot, and a thinner feed line will give a little better coupling.
- Position of feed line relative to slot: best coupling is achieved when the feed line is positioned at right angle to the centre of the slot.
- Position of the patch relative to the slot: best coupling is achieved when the patch is centred above the slot.
- Length of tuning stub,  $L_{stub}$ : the tuning stub is used to tune excess reactance of the aperture coupled antenna. Best coupling is achieved when the slot is excited from a standing wave on the microstrip, with its maximum located under the slot. This is achieved with a quarter-wave stub, though the length of the stub will be less than  $\lambda/4$  long, since the open-circuit end has fringing capacitance.

Other shapes of the aperture can give better coupling between feed line and patch. A rectangular aperture is better than a circular, but for example H-shape, bow tie, dog bone or hourglass shapes, shown in Figure 2.10, can increase the coupling even more. According to Pozar and Targonski (1991), the magnetic polarization is the dominant coupling mechanism between feed and patch, and the shapes with enlarged ends will give more uniform shapes of the fields. Another advantage with these shapes is that the antenna can be matched with a smaller sized aperture. A smaller aperture will radiate less, and the F/B will be improved. According to Garg et al. (2001), a patch shaped as a circle, an annular ring, a square or a patch with a quarter-wave length, have an inherently lower Q than a rectangular patch with a length of a half-wavelength, and thus they can give a larger bandwidth.

### Antenna equivalent circuit

To get a better understanding of how the aperture coupled antenna behaves, an equivalent circuit model of such an antenna is presented in Figure 2.11. The feed line has a

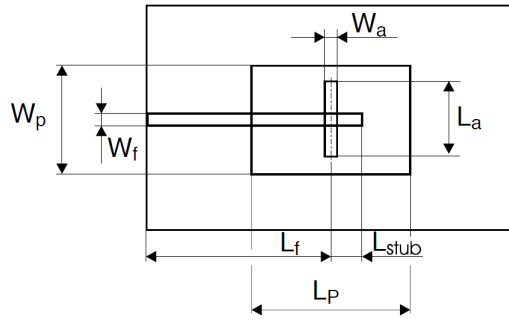


Figure 2.9: Top view of an ACMPA. Kuchar (1996).

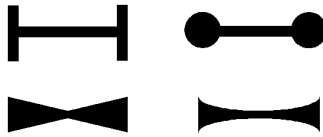


Figure 2.10: Different aperture shapes. Top left: H-shape. Top right: dog bone. Bottom left: bow tie. Bottom right: hourglass.

characteristic impedance,  $Z_{0,f}$ , and has length  $L_f$ . The stub is the open end with length  $L_{stub}$ . The aperture is represented by a parallel tank circuit with the inductance  $L_{ap}$  and the capacitance  $C_{ap}$ , since a half-wavelength aperture will be resonant. If the aperture is not resonant, it will normally be inductive. The patch is viewed as an open-ended transmission line of length  $L_p$ , with a characteristic impedance  $Z_{0,p}$ . To represent the fringing fields at the open ends of the patch, the capacity  $C_{ap}$  and the resistor  $R_{rad}$  are added. The transformer is included to represent the difference in impedance level between the aperture and the patch transmission lines. Its turn ratio is  $N$ .

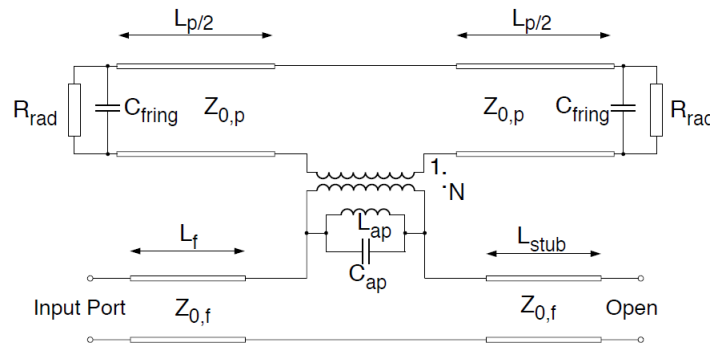


Figure 2.11: Equivalent circuit for the aperture coupled antenna. Kuchar (1996).

## 2.2 Technologic preliminaries

### 2.2.1 Antenna configuration and requirements

The antenna element designed in this thesis shall be a part of an array. This implies some physical restrictions and requirements. The distance from center to center between two antenna elements shall be no larger than  $\sim 1.2\lambda$ , meaning the antenna element for Ku-band frequencies not should be longer than 30 mm. In an array with many antenna elements closely positioned, it is challenging to make the feed network and to give more space for this, it is placed below the antenna element, and a vertical feeding technique shall be used. The antenna element must be made such that the feed network can be vertically connected to the feed line in the antenna element when the two are coupled together. It is desired that the antenna has as low profile and weight as possible to make it more portable. To keep the price of production low, the complexity of manufacturing should also be kept low. But foremost it is concentrated on obtaining the best possible antenna performance and radiation characteristics.

The antenna shall radiate in the Ku-band, where frequencies for downlink are from 10.7 to 12.75 GHz, and for uplink are from 14.0 to 14.5 GHz. It is desired with a wide/dual-band antenna, which can operate at both uplink and downlink. An accepted input reflection coefficient,  $S_{11}$ , for frequencies in the operation bandwidth must be below -10dB. The bandwidths presented in this thesis are the -10dB bandwidths. The antenna element shall radiate in broadside direction, meaning tangential to the patch plane, and the majority of the power should be concentrated in this direction, and it is therefore desired to have a high F/B.

### 2.2.2 Program for design and simulation

To perform simulations of the antenna, software from AWR was used. The AWR corporation is a National Instruments (NI) company, which makes the *NI AWR Design Environment*<sup>TM</sup> (NI AWRDE) software. This software includes *Microwave Office* for circuit simulation, and the electromagnetic (EM) analysis tools *AXIEM*<sup>®</sup> and *Analyst*<sup>TM</sup>. The software is used for RF and microwave designs, and you can make layouts and simulate circuits with it. There is a good variety of components for microstrip circuits in its libraries, and it is possible to design your own components. Here the most important functions and programs relevant for this thesis will be presented in more detail. The information about the software is taken from Sim (2016).

#### AXIEM

AXIEM is a 3D planar EM analysis software, which is based on the Moment of Methods (MoM). It can solve for stackups of planar dielectrics and conductors, where dielectrics extend infinitely in the plane. The space above, below and the walls of the stackup can be set as PEC, copper or approximate open. AXIEM uses a mesh of triangles and rectangles on the surface of the conductors when solving, and effects of the dielectrics are included through Green's functions. The surface currents modeled in AXIEM contain all x, y and

z components. Metal traces can be simulated with or without thickness. In both cases, losses in the metal are calculated accurately, but coupling between lines that are close is not included when thin metal is used. With thin metal, only the bottom of the metal is conducting in the simulations, and this is mostly true for low frequencies, but not at higher frequencies. However, for thick metals, Analyst can be faster to use than AXIEM. The accuracy of AXIEM is good for most types of problems, and should be good for the problems in this thesis.

### Analyst

Analyst 3D is another EM simulator in the NI AWR Design Environment. It uses frequency-domain Finite-Element Method (FEM) on a tetrahedral mesh in a three-dimensional volume. Analyst makes no approximations regarding geometry, and can be used on any kind of model. Analyst will compared to AXIEM use longer time for a simulation, and use more computer memory.

### Simulations in this thesis

These are the recommendations/guidelines for choosing between Analyst and AXIEM:

- Analyst should be used for problems with 3D effects such as thick metal, many ground planes and metal enclosures.
- AXIEM should be used for problems containing only planar metal and dielectrics and open boundaries, especially when the metal is modeled as zero-thickness. It is also more efficient for planar radiators.

Based on the information given above, the AXIEM tool was chosen to use in this thesis. It was chosen because it is recommended for planar structures and radiators. Since AXIEM works slower when simulating with thick metal, it was decided to simulate without the effects of metal thickness, and rather take a look at this effect in future works.

All simulations in this thesis are simulated in the frequency range from 10 GHz to 16 GHz. The simulator decides which frequencies in this range it needs to simulate to get an accurate response. Thus, not all frequencies are simulated, and in the simulation results presented here, the closest simulated frequency to the one of interest is used. The edges of the simulation area were selected as approximately open, except from when it was simulated with a metal plane reflector. Then the bottom edge was set as a copper plane.

The mesh made by the simulator was limited to have a minimum edge length of 0.5 mm, and the maximum size is determined by the maximum frequency simulated. The minimum was chosen based on information from Swanson and Hoefler (2003), saying that the cell size should be between  $\lambda/10$  and  $\lambda/30$  of the highest frequency of interest to capture the guide wavelength. At the highest simulated frequency, 16 GHz, this means that the cells should be between 0.6 mm and 1.9 mm. The minimum was chosen as 0.5 mm, in order have a chance to capture variations across the width of lines also, which normally requires smaller cells than the guide wavelength according to Swanson and Hoefler (2003).

**TX-Line**

*TX – line*<sup>®</sup> is a free-to-use transmission line calculator included in Microwave Office. It can calculate electrical and physical characteristics of transmission lines, based on the input given. TX-Line can do calculations for many types of transmission lines, such as microstrip, CPW, stripline, coplanar waveguide, and slotline. The microstrip line in Microwave Office is based on the models in Hammerstad and Jensen (1980) and Bahl and Garg (1977).

# Chapter 3

## Antenna design

In this chapter, the design process of the antenna element is reviewed, and afterwards the antenna element is tuned. A reflector patch is designed and simulated, and it is looked at some other alternative designs of the antenna element. Results from simulations of the antenna element are presented.

### 3.1 Initial design of the antenna

The design procedure should build on simple models and formulas, which give an approximation to what the antenna should be like. Before the tuning process starts, it is important to have a good approximation of the antenna design, since starting out with a design far from any working antenna, will make the tuning process like shooting blindly. However, it is not necessary to use full-wave analysis for initial designing, since that would be a time consuming and very complex way to make a design. To use full-wave analysis for the tuning was considered a better approach. Previously made antennas with desired characteristics and similar structures were used as references during the design process.

#### 3.1.1 Choice of feeding technique and structure

The literature survey, on vertical feeding techniques and design strategies of patches, which was carried out in the beginning of the work with this thesis, gave a good starting point for designing the antenna. In the literature survey different techniques and designs for MPAs were investigated, and among the feeding techniques considered, the most interesting turned out to be the aperture coupled feed. The technique has many good characteristics for use in an antenna array like the one of this project. Aperture coupled feed gives good bandwidth, space for layout of the feeding network, and it is possible to make antennas with several types of polarization. Many parameters can be adjusted when making an aperture coupled antenna, and many variations are possible with this feeding technique. A drawback is the extra layers needed, giving it a higher profile, and that it is quite complex to analyse.

Another feeding method that could be interesting to use is the CPW feed, which requires fewer layers than the aperture coupled feed, but which has fewer parameters to adjust, and therefore not the same possibilities as with an aperture coupled antenna. According to

Garg et al. (2001), CPW feed will not give as good bandwidth as the aperture coupled feed. The coaxial probe feed has the drawback of many soldering points, making it less suitable for arrays, so it was decided not to use probe feed. Based on this, it was decided to start out designing an aperture coupled antenna. Since the goal of the project was to make a wide-band or dual-band MPA, the most promising structure was the SSFIP, which has been proven to give large bandwidths with the use of aperture coupling.

To ease the design process, it was decided to start with a rectangular shaped patch, since these are most widely used, and therefore their characteristics are better known. The steps of the general design presented in 2.1.7 were used to start designing the MPA. The antenna in Aliakbarian et al. (2006) was used as a reference for the initial antenna structure, and some of the dimensions were set according to this paper. This antenna was used as reference since it is a wide-band antenna for Ku-band, and it has a structure similar to SSFIP. It would be much easier to make the MPA wide- or dual-banded by using a resonating aperture. Then the MPA would have two resonances, one for the patch and one for the aperture. The operating frequencies of the antenna were already known; 10.7 to 12.75 GHz for downlink, and 14 to 14.5 GHz for uplink. It was decided to make the patch with a resonance in the center of the uplink frequencies, 14.25 GHz, and the aperture with a resonance at the center of the downlink frequencies, 11.7 GHz, similarly as the antenna in Pavuluri et al. (2008).

### 3.1.2 Substrates

An aperture coupled antenna needs one feed substrate and one patch substrate, as described in 2.1.7. The patch substrate should be a material with low permittivity, and ideally, it would be air, but that can be unpractical since it would demand some extra support for the structure. Therefore, foam is a good alternative, since there are foams with low relative permittivity, and they are quite robust. *ROHACELL*<sup>®</sup>31HF is a polymethacrylimid foam designed for antenna applications. It has a very low relative permittivity and loss tangent of respectively 1.046 and 0.0017 at 10 GHz. It is possible to get it cut to a desired thickness, and therefore it was chosen as antenna substrate. Initially, the thickness of the foam was set to 3 mm, the same thickness as the antenna substrate used in Aliakbarian et al. (2006). Although air was used as antenna substrate for that antenna, the relative permittivity of the foam was considered to be so low that the same thickness could be used. The thickness have to be adjusted through tuning, since no methods for calculation of substrates was found.

The feed substrate should have a rather high relative permittivity, in the range of 2 to 10, and it should be thin to reduce surface waves, typically 0.01 to 0.02  $\lambda$ . The free-space wavelengths for the frequencies of the antenna are 23.5 to 28.0 mm for downlink, and 20.7 to 21.4 mm for uplink. A feed substrate with thickness between 0.2 and 0.5 mm could then be respectable for both downlink and uplink frequencies. The *Rogers Corporation* has several dielectrics to use in microwave circuits, and their RO3035<sup>TM</sup> was chosen since it has an appropriate relative permittivity of 3.6, and it is available in layers as thin as 0.127 mm, which can work as superstrate. A thickness of 0.508 mm was chosen for the feed substrate, which is the same thickness as the feed substrate of the antenna in Aliakbarian et al. (2006), where RO4003<sup>TM</sup> are feed substrate, which has almost the same relative permittivity as RO3035<sup>TM</sup>. RO3035<sup>TM</sup> has a very low water absorption, so some other material must be

used for the superstrate if it must be 100% waterproof.

### 3.1.3 Patch

First, the width of the patch was approximated by (2.19), with  $f_r = 14.25$  GHz,  $h = 3$  mm, and the relative permittivity of the foam/patch substrate  $\epsilon_r = 1.046$ . This gave the patch width  $W = 10.4$  mm. Then the effective permittivity of the patch substrate for low frequencies was found using (2.11), where  $ab = \frac{1}{2}$ , which gave  $\epsilon_{eff} = 1.035$ . By using (2.14), (2.15), (2.16) and (2.17), the effective permittivity at 14.25 GHz was calculated to 1.044, which is slightly smaller than the relative permittivity of the foam. When the effective permittivity is known, the length of the patch can be calculated from (2.21) and (2.22). It was calculated that  $\Delta L = 1.85$  mm and  $L = 6.6$  mm. Thus, the formulas gives a patch that is 6.6 mm long and 10.4 mm wide. This is some millimeters shorter length than used in Pavuluri et al. (2008), and some millimeters wider than the patch in Aliakbarian et al. (2006). When  $W > L > h$ , the dominant mode of the patch is  $TM_{001}$ , according to Balanis (2005), and its resonant frequency is given by

$$f_r = \frac{c}{2L\sqrt{\epsilon_r}} \quad (3.1)$$

where the fringing effect not is considered. With this formula, the frequency of the antenna should be 14.1 GHz. But the formula the length was calculated from, was for a patch operating in  $TM_{010}$  mode, where  $L > W > h$ . In the tuning procedure it was found that the patch should be longer and less wide to obtain a satisfactory operation.

### 3.1.4 Stub and feed-line

The chosen feed substrate, which the feed-line would be on, had a height  $h = 0.508$  mm, and a relative permittivity of 3.6. The other side of the feed-line would be covered by foam, which was lying between it and the reflector and it would therefore be a microstrip with superstrate. But since the relative permittivity of the foam was very low, close to that of air, the feed line could be treated as a microstrip with one side exposed to air.

With a given characteristic impedance, the width of the feed-line could then be found from (2.14), as a function of  $Z_c$ ,  $\epsilon_{eff}$ , and  $h$ . But  $\epsilon_{eff}$  is a function of  $h$  and  $W$ , as seen in (2.11), so the effective relative permittivity of the feed substrate and the width of the microstrip must be found in an iterative way from the formulas. However, several free calculators that can do this calculation. The TX-line calculator finds the width based on  $Z_c$ ,  $\epsilon_r$ ,  $h$ , and the operating frequency.  $50\Omega$  is a standard input/termination impedance of high frequency systems, so it was chosen as the desired  $Z_c$ . TX-line calculated the width of the feed line to  $\sim 1.08$  mm for the frequencies of the Ku-band. The length of the feed-line was set to 12 mm for the simulations, about one effective wavelength. Different lengths of the feed-line will affect the phase of the input, but the tuning stub shall compensate for this by having a length that gives somewhat same phase at the input.

In order to get best possible coupling between feed and patch, the tuning stub should be a little shorter than a quarter effective wavelength in the feed. Then a standing wave will

have its maximum right beneath the aperture. Because of the fringing effect at an open-ended microstrip, the stub must be a little shorter than a quarter effective wavelength. The effective wavelength/guide wavelength was calculated from (2.7). The effective permittivity of the feed substrate for low frequencies was calculated from (2.11), with  $ab = \frac{1}{2}$ ,  $\epsilon_r = 3.6$ ,  $h = 0.508$  mm and  $W = 1.08$  mm. This gave  $\epsilon_{eff} = 2.85$ . From (2.14), (2.15), (2.16) and (2.17), the effective permittivity at the Ku-band frequencies was calculated to be equal to the relative permittivity of the substrate, 3.6. For the patch substrate, only a slight change between the relative and the effective high frequency permittivity was obtained, so for frequencies in the Ku-band the change can be negligible, since the frequencies are relatively high.

The effective wavelength was calculated to 11.1 mm for the center uplink frequency, and 13.5 mm for the center downlink frequency. Using the wavelength in the middle between them, 12.3 mm, should work well for both. The fringing effect at an open-ended microstrip must be taken into account when calculating the length of the tuning stub. This is found from (2.21), the same formula used to find the length-extension of the patch. For the stub, this length was found to be 0.2 mm. Then the quarter-wave stub would be  $(12.3\text{mm}/4) - 0.2\text{mm} \approx 2.9\text{mm}$ . The calculated stub length is too long when compared to the tuning stub of Aliakbarian et al. (2006), where it is 0.9 mm, and where the substrate parameters are almost equal to the ones used here, and those are the most important parameters for the stub-length. This difference between calculated quarter-wavelength and a well working tuning stub is also observed in Kuchar (1996), where the calculated effective quarter wavelength is  $\sim 18$  mm, and the tuning stub is set to 8.32 mm. Based on this the tuning stub was initially set to 0.9 mm, the same as in Aliakbarian et al. (2006). The suggested method to find the length of the tuning stub is then to use simulations to adjust the length until a current maximum is obtained directly beneath the aperture, and look at measurements of the input impedance as a function of the stub-length to find the length for maximum coupling.

### 3.1.5 Aperture and reflector

#### Resonating aperture

A general advice for ACMPCAs is that the aperture not should be resonant. A resonant aperture will give unwanted radiation to the back of the antenna, since slots radiate in both directions. If the aperture has the same resonant frequency as the patch, the radiation from the aperture would interfere with the radiation from the patch. For the antenna of this thesis, the idea was to use a resonating aperture at the downlink frequency, and let the patch resonate at the uplink frequencies, and thus avoid interference since they work on different frequencies. However, there will still be radiation backwards, and to remove some of this a reflector was used.

#### Slot antennas

The guidelines for dimensioning the aperture of an ACMPCA given in most literature are intended for non-resonant apertures, generally saying that a larger slot gives better coupling, but more back radiation. However, there are a type of antennas called microstrip slot

antennas. They consists of a slot/aperture cut in a ground plane on a dielectric substrate, that is fed by a microstrip which sits under the same substrate, as seen in Figure 3.1. The shorting strip is the same as the tuning stub. The microstrip slot antenna structure is a part of the ACMPA, and in order to make a resonant aperture, theories and design methods for the slot antenna can be applied.

To make a resonating aperture, its length can be a half wavelength, a quarter wavelength, or a multiple of these. Similarly as a patch can be viewed as a wide microstrip, the slot antenna can be seen as a slotline. Slotlines are transmission lines which consists of a dielectric substrate with a narrow slot etched in the metal on one side, as seen in Figure 3.2. According to Gupta et al. (1996), the electric field component in a slot is mainly across the slot in the plane of metallization, and these fields are shown in Figure 3.3, for a microstrip slot antenna.

Similarly to the microstrip, slotlines does not support pure TEM propagation, and the propagation mode of the slotline is almost TE. In Figure 3.4 the tangential component distribution of the electric field in  $TE_{010}$ -mode is shown. The aperture on the figure is a half-wavelength long. Closed-form expressions for slotlines on low permittivity substrates are given in Gupta et al. (1996). These expressions are obtained by curve fitting of numerical results from Galerkin's method in Fourier transform domain, which is an accurate analysis of slotlines. The expression for normalized slot wavelength,  $\lambda_s/\lambda_0$ , valid for

$$\begin{aligned} 0.006 &\leq h/\lambda_0 \leq 0.06 \\ 0.0015 &\leq W/\lambda_0 \leq 0.075 \\ 2.22 &\leq \epsilon_r \leq 3.8 \end{aligned}$$

is given as

$$\frac{\lambda_s}{\lambda_0} = 1.045 - 0.365 \cdot \ln(\epsilon_r) + \frac{6.3(W/h)\epsilon_r^{0.945}}{238.64 + 100(W/h)} - \left(0.148 - \frac{8.81(\epsilon_r + 0.95)}{100\epsilon_r}\right) \ln(h/\lambda_0) \quad (3.2)$$

With a free-space wavelength,  $\lambda_0$ , at 11.7 GHz of 25.6 mm, height of substrate  $h = 0.508$  mm, an assumed width of the slot,  $W$ , between 0.04 mm and 1.92 mm, and a relative permittivity of the substrate,  $\epsilon_r = 3.6$ , this holds. The equation is reported to have an average absolute percentage error of 0.37%. Similarly as for the feed-line, the side of the slot covered with foam, was considered as air in the calculations. From (3.2), the wavelength in the slot was calculated to  $\lambda_s = 20.8$  mm. In Garg et al. (2001), page 455, it is said that the resonant length of the slot in its dominant mode is given by

$$L_r = \frac{\lambda_s}{2} - \Delta L_s \quad (3.3)$$

where  $\Delta L_s$  is the equivalent length associated with the inductance at the two shorted ends of the slotline. This is somewhat similar to the capacitive length extension of the microstrip. The inductive extension is a result of stored magnetic energy, which comes from current flowing in the metal around the end of the slot. It was not found any simple and accurate way to calculate the inductive length extension in any literature, but it is mentioned in Gupta et al. (1996) that the equivalent length of the short end increases when  $W$  or  $h$  is

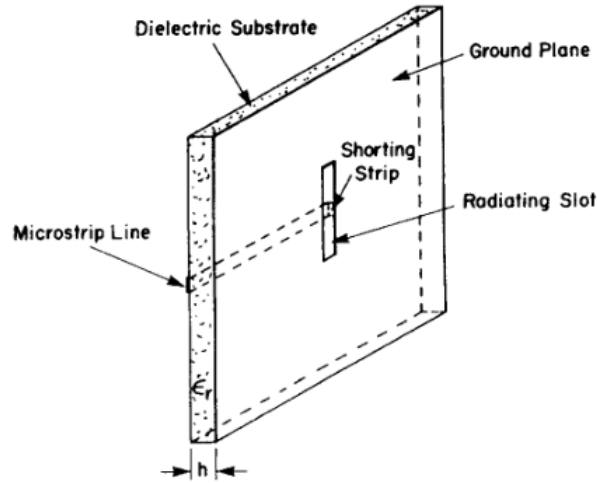


Figure 3.1: Structure of a microstrip slot antenna. Garg et al. (2001)

increased. It is said that the inductive length extension is significant and can may be up to  $0.1\lambda_s$ . Considering a wide slot to get better coupling, it can be assumed that the length extension will be approximately  $0.1\lambda_s$ . Then the extension on each side of the slot would be 2.08 mm, and (3.3) gave  $L_r = 6.24$  mm. Compared to the resonant aperture in Aliakbarian et al. (2006), which is 6.61 mm long and 0.926 mm wide, the length is close on. Based on this the initial length was set to 6.24 mm, and the width to 0.9 mm as in the reference.

### Babinet's principle

A principle often used for slots in electromagnetic, is *Babinet's principle*, and it can help to give an understanding of how a slot antenna works. According to Balanis (2005), the principle was originally made for optics, where it says that "when the field behind a screen with an opening is added to the field of a complementary structure, the sum is equal to the field when there is no screen". This means that the diffraction pattern from, and the sum of waves transmitted through, the two complementary screens are equal. An electromagnetic version of the principle was made by Booker, where the symmetry in the expressions for  $\mathbf{E}$  and  $\mathbf{H}$  of Maxwell's equations are exploited. It makes it possible to change between two complementary perfect conducting screens, where the first has an aperture cut in it, and the other screen is obtained by changing the regions of conductor and space in the first screen. According to Chatterjee (1988), the complementary of a perfect conducting electric screen, is a perfect conducting magnetic screen. A perfect electric conductor can represent this, where all electric and magnetic quantities are interchanged everywhere. Thus the electric source  $\mathbf{J}$  is changed with the magnetic source  $\mathbf{M}$ ,  $\mathbf{E}_m$  by  $\mathbf{H}_e$ ,  $\mathbf{H}_m$  by  $-\mathbf{E}_e$ ,  $\varepsilon$  by  $\mu$ , and  $\mu$  by  $\varepsilon$ , where subscript  $\mathbf{m}$  denotes fields on the perfect magnetic conductor, and  $\mathbf{e}$  denotes fields on the perfect electric conductor. This means that a slot antenna has a complementary flat dipole, shown in Figure 3.5. The solution of  $\mathbf{E}$  for the slot will be proportional to that of  $\mathbf{H}$  for the dipole, and vice versa. The electric field pattern of the slot will look like the

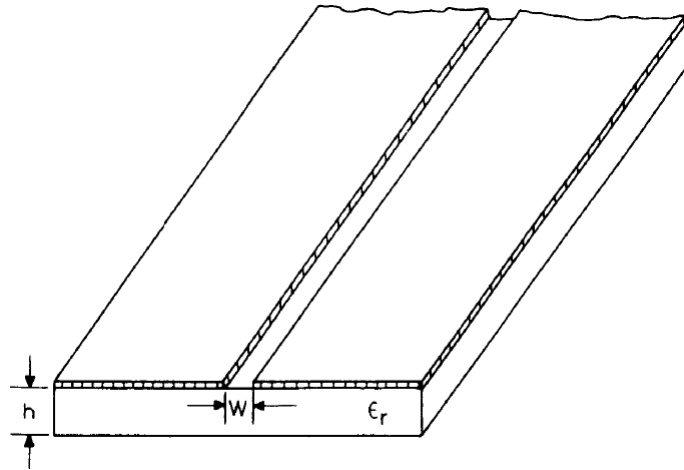


Figure 3.2: Structure of the slotline. Gupta et al. (1996)

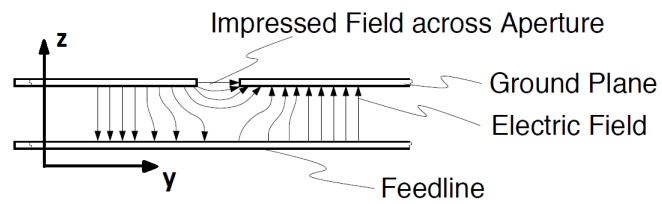


Figure 3.3: The electric fields in a microstrip slot antenna. Kuchar (1996)

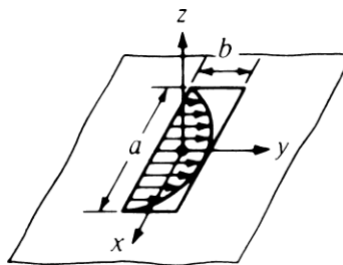


Figure 3.4: Electric field in a half-wave aperture. Balanis (2005)

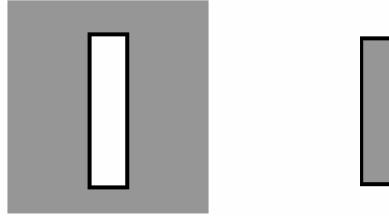


Figure 3.5: Slot antenna and complementary dipole.

magnetic field of a dipole. These opposite characteristics was observed where the slotline has an inductive extension at shorted ends, while the microstrip has capacitive extension.

Considering this symmetry, the length of the aperture can be calculated by assuming it as a microstrip dipole. From (2.7), with  $\varepsilon_{eff} = 3.6$ , the effective wavelength at 11.7 GHz is 13.49 mm, with a half wavelength of 6.75 mm. If the width of the slot/microstrip dipole was set to 0.9 mm, the length extension for an ordinary microstrip on the chosen feed substrate, was calculated from (2.21) to be 0.19 mm. Then the physical length of the microstrip dipole would be 6.37 mm. This is only 0.13 mm longer than the length that was calculated for the aperture from (3.3). Therefore, it seems the aperture length can be calculated in this simpler way too.

### Improving front-to-back ratio

A large resonating aperture gives better bandwidth and coupling to the patch. The disadvantage of the resonating aperture is that it radiates somewhat equally to the front and the back of the antenna, causing a poor front-to-back ratio (F/B). One possible way to achieve a better F/B is by using a reflective metal plane under the aperture, as mentioned in 1.2.5. According to Waterhouse (2003), this metal plane must have a large extension relative to the aperture, in order to avoid deformation of the radiation pattern caused by diffraction at the edges of the plane. The edges of the metal plane can also be covered by an absorbing material, or they can be shaped and cut to avoid edge currents. In an array the metal plane will be large seen from elements in the middle, but at the edges there may be some unwanted effects. A shielding metal plane may give propagation of *parallel plate waveguide modes*, which will reduce the radiation efficiency of the antenna. These modes appear since the space between the ground plane with the aperture and the metal reflector plane acts as a parallel plate waveguide.

Other methods for improving the F/B is to use a cavity backed solution, or place another MPA element beneath the aperture as a reflector. With a cavity-backed solution, the aperture is enclosed in a cavity, which will eliminate fields radiated directly backwards. This method is more complex in its structure, and will therefore be more expensive. The method of using an MPA element as a reflector is quite similar to the principle of the reflector

in a Yagi-Uda antenna. Between the feed-line and the reflecting element, a thick layer of foam is used to keep the level of coupling between them low. The directive patch is shielded from the reflecting element by the ground plane. The reflecting element will therefore mainly interact with the aperture. For the Ku-band antenna, the solution with reflector elements was considered more practical. Since the main part of the feed-network would be placed below any reflecting structure, separately spaced reflector elements would make it possible to have vertical connections from the feed-network to the feed-lines between the elements. A complete metal plane would only allow connections at its edges. Then effects of mutual coupling between antenna elements in an array due to excitation and propagation of parallel plate modes between the reflecting metal plane and the ground plane with the aperture would be avoided.

But what should the dimensions of the reflecting element be? According to Waterhouse (2003), the reflecting element should have its own resonant frequency at a lower frequency than what it is reflecting. It is also shown that the magnitude and phase for the far-fields of the reflecting patch, remains mostly constant above its operating frequency, and the element will work for a wide frequency band. The length of the reflecting patch controls the relative phase between it and the aperture, while the width and the spacing control the relative magnitude between reflecting element and aperture. The space between the reflecting patch element and the aperture is not bound in the same way as for a metal plane, where it must be  $\lambda_0/4$ , but the spacing should be more than  $0.1\lambda_0$  according to Waterhouse (2003). In an array, the use of reflecting patches gives the ability to reduce radiation in any angle toward the back, and get maximum reflection in a desired angle. This can be achieved by adjusting the dimensions, spacing and position of the reflecting elements.

It was decided to start the simulations with a complete metal plane, and try with a reflecting patch when the rest of the antenna was finished. The metal plane was to be distanced  $\lambda_0/4$  from the aperture, with  $\lambda_0 = 25.6$  mm, so the distance had to be 6.4 mm. Under the aperture it was already a 0.5 mm substrate, and for the remaining 5.9 mm, the same foam as in the patch substrate was used. Since most of the antenna elements in the array will be far from the edges of the metal plane, the simulations could be executed with an infinite sized copper plane, which is easy to simulate in AXIEM. Eventual effects of the elements on the edges can be evaluated later when the array will be made.

### 3.1.6 Superstrate

A dielectric cover, called superstrate or radome, can be used to protect the MPA from the environment, or for supporting the patches and hold them in place. A superstrate is used in the SSFIP structure to hold the patches in place and protect them. Other elements can have the same effects as superstrates, for example painting or naturally occurring ice layers. Superstrates will affect the characteristics of the antenna, so they are often made very thin to avoid change of the antenna's performance, and thin films or foils can be used. There is a trade-off between protection, and effect on antenna performance, that must be considered. Thicker superstrates is more robust, but will affect the antenna more than a thin superstrate. The relative permittivity will change, and it changes more with a superstrate with high relative permittivity. It was decided to use the same substrate as superstrate as

that used for the feed substrate.

The most significant effect of a superstrate is lower resonant frequency. So when a superstrate is added, the rest of the antenna must be tuned. In addition superstrates can be used actively to enhance gain, efficiency, eliminate surface waves, and get an omnidirectional beam pattern, as shown in Alexopoulos and Jackson (1984). The same paper provides a method to find the optimal superstrate thickness in terms of maximizing the efficiency. As said in Section 2.1.2, the efficiency and the bandwidth cannot be optimized at the same time, and since the main objective for the antenna in this thesis is to have a large bandwidth, it is not desired or possible to have a 100% efficiency. Therefore, the superstrate thickness for 100% efficiency is not necessary to use here. Anyway, it can be of interest to look at this before deciding a thickness of the superstrate, or it can be used for future work.

To get an optimum thickness for efficiency it is desired to find the substrate thickness,  $h$ , for which the antenna operates at the dominant TM mode, and the attenuation constant go to zero. To eliminate surface waves, the substrate thickness must be less than the thickness at which the first TE mode turns on, denoted by  $h_{max}$ . The maximum substrate height for a non-magnetic substrate, is derived from

$$\frac{1}{\sqrt{n_2^2 - 1}} \arctan \left\{ \frac{\sqrt{n_1^2 - 1}}{\sqrt{n_2^2 - 1}} \cot \left[ 2\pi \left( \frac{n_1 h_{max}}{\lambda_0} \right) \sqrt{1 - \frac{1}{n_1^2}} \right] \right\} = \frac{1}{\sqrt{n_2^2 - n_1^2}} \arctan \left( \frac{\varepsilon_2 \sqrt{n_1^2 - 1}}{\sqrt{n_2^2 - n_1^2}} \right) \quad (3.4)$$

where  $n_1 = \sqrt{\varepsilon_1}$  and  $n_2 = \sqrt{\varepsilon_2}$ , and with the relative permittivity of the patch substrate  $\varepsilon_1 = 1.046$ , the relative permittivity of the superstrate  $\varepsilon_2 = 3.6$ , and  $\lambda_0 = 21.05$  mm, the wavelength for the upper/patch resonance, this gave  $h_{max} = 4.131$  mm. So with  $h = 3$  mm, the substrate thickness is less than the maximum thickness. The general rule for optimizing the efficiency given in Alexopoulos and Jackson (1984), says that when  $h \leq h_{max}$ , the normalized superstrate thickness shall be equal to the normalized critical superstrate thickness, given by  $n_2 t / \lambda_0 = n_2 t_c / \lambda_0$ , where  $t$  is the superstrate thickness, and  $t_c$  is the critical superstrate thickness. The value of the normalized critical superstrate thickness was found from investigation of the graph in Figure 3.6, and with the given relative permittivities it was found to be 0.09. This means that  $n_2 t / \lambda_0 = 0.09$ , and the superstrate thickness for optimum efficiency was calculated to be  $t = 0.997$  mm.

In Alexopoulos and Jackson (1984), it is also stated a way to optimize gain and radiation resistance. This is obtained by choosing the thicknesses such that a resonance condition is made. The resonance conditions occur when  $n_1 h / \lambda_0 \cong 0.50$ , and  $n_2 t / \lambda_0 \cong 0.25$ , where  $h$  is the substrate thickness and  $t$  is the superstrate thickness. The antenna must be located in the middle of the substrate, and  $\varepsilon_2 \gg \varepsilon_1$ . This will cause a large voltage at the location of the antenna, and give increased gain and radiation resistance. To meet the requirements for thickness, the layers must be thick, about half a wavelength in the media, which will give the antenna a much higher profile, and that is unwanted.

It was decided to try with a very thin superstrate that would have little effect on the antenna performance. The radiation characteristics were favoured over protection. It was decided that the support of the antenna element would come from the foam used as antenna substrate, and that this could be robust enough. The thinnest available layer of the chosen dielectric was 0.127 mm, so this was used for the simulations. This would make it possible to ignore effects of the superstrate when the design was made.

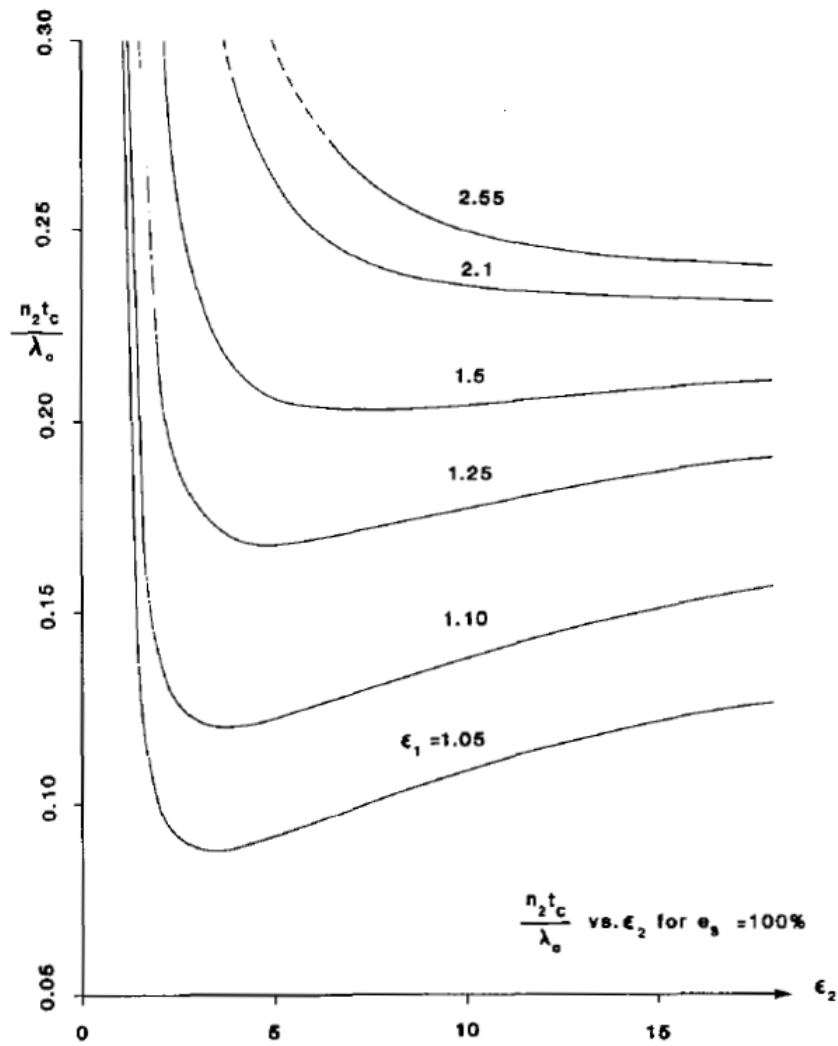


Figure 3.6: Normalized critical thickness versus  $\epsilon_2$  for 100% efficiency. Alexopoulos and Jackson (1984)

Table 3.1: Geometric parameters of initial antenna design

Antenna part	Parameter	Value
Superstrate	Relative permittivity	3.6
	Height	0.127 mm
Patch	Length	6.6 mm
	Width	10.4 mm
Patch substrate	Relative permittivity	1.046
	Height	3 mm
Aperture	Length	6.24 mm
	Width	0.9 mm
Feed substrate	Relative permittivity	3.6
	Height	0.508 mm
Feed line	Width	1.08 mm
	Length	12 mm
Stub	Length	0.9 mm
Foam layer above reflector	Relative permittivity	1.046
	Height	5.9 mm
Reflector	Type	Infinite copper plane

### 3.1.7 The initial design

An overview of the initial antenna geometry and structure is given in Table 3.1.

## 3.2 Tuning

With the initial design of the antenna in place, the tuning could start. Since the design was made with use of simple models and formulas, the tuning was performed with simulation tools based on full-wave methods, to get a more accurate result.

Simulation result of the initial design are seen in Figure 3.9, and it shows a quite good resonance, with best matching around 12 GHz, but good response up to almost 14 GHz. This was probably an effect of a low patch resonance, which was close to the aperture resonance, so at first the dimensions of the patch were changed to move its resonant frequency up. The width was decreased, since the frequency of a patch with  $TM_{001}$  as dominant mode is controlled by the width. At the same time the length was increased, and after also decreasing the thickness of the patch substrate, two resonances were observed, one around 11.7 GHz caused by the aperture, and one around 13.9 GHz, caused by the patch. These are shown in Figure 3.10.

The resonance frequency of the patch had to be moved up to the desired center frequency of 14.25 GHz, and when this was conducted, the patch changed dominant mode to  $TM_{010}$ , since its length was set longer than its width during the tuning process. After that was achieved, it was attempted to obtain a better matching for both frequencies, and simultaneously maintain a good bandwidth. Most parts of the antenna had to be tuned during this process, and when the simulation results were satisfying, it could be attempted to make a reflecting

patch. More knowledge on how the different parts of the antenna were tuned can be found in Section 4.1, where the effects of each part of the antenna are reviewed.

### 3.3 Tuned antenna design

An overview of the geometry of the tuned antenna is given in Table 3.2. It can be compared to Table 3.1 to see the changes made during the tuning process. Performance parameters of the antenna are presented in Table 3.3, and in Figure 3.11 - 3.16, plots from the simulations of the tuned antenna are provided. Figure 3.7 and Figure 3.8 gives a view of the antenna structure. It is only the metal parts that are shown, the substrates are made transparent in these figures. In the top view, the patch is visible, and in the bottom view, the feed line is seen. The ground plane with the aperture is  $(30 \times 30)$  mm, which is the size used during simulation. The mesh made by the simulator is visible.

With the characteristics and performance of this design, it was chosen to not start on any new design, since the requirements for frequency range and bandwidth were met. It would be more fruitful to go on working with this antenna, and possibly improve some of its characteristics. One task would be to make a patch reflector.

Table 3.2: Geometric parameters of tuned antenna design

Antenna part	Parameter	Value
Superstrate	Relative permittivity	3.6
	Height	0.127 mm
Patch	Length	7.3 mm
	Width	6.8 mm
Patch substrate	Relative permittivity	1.046
	Height	2.6 mm
Aperture	Length	6.2 mm
	Width	1.1 mm
Feed substrate	Relative permittivity	3.6
	Height	0.508 mm
Feed line	Width	1.1 mm
	Length	12 mm
Stub	Length	0.8 mm
Foam layer above reflector	Relative permittivity	1.046
	Height	5.9 mm
Reflector	Type	Infinite copper plane
Overall height	10.13 mm	

Table 3.3: Performance parameters of tuned antenna design

Parameter	Upper/patch resonance	Lower/aperture resonance
Center frequency	14.4 GHz	11.5 GHz
$S_{11}$ at center frequency	-39.74 dB	-33.28 dB
Directivity	9.30 dBi	7.00 dBi
Gain	8.90 dBi	6.72 dBi
Efficiency	91.20%	93.76%
Half power beamwidth (x-axis)	45.2°	64.6°
Half power beamwidth (y-axis)	29.7°	54.3°
Bandwidth	4.33 GHz (33.0%)	

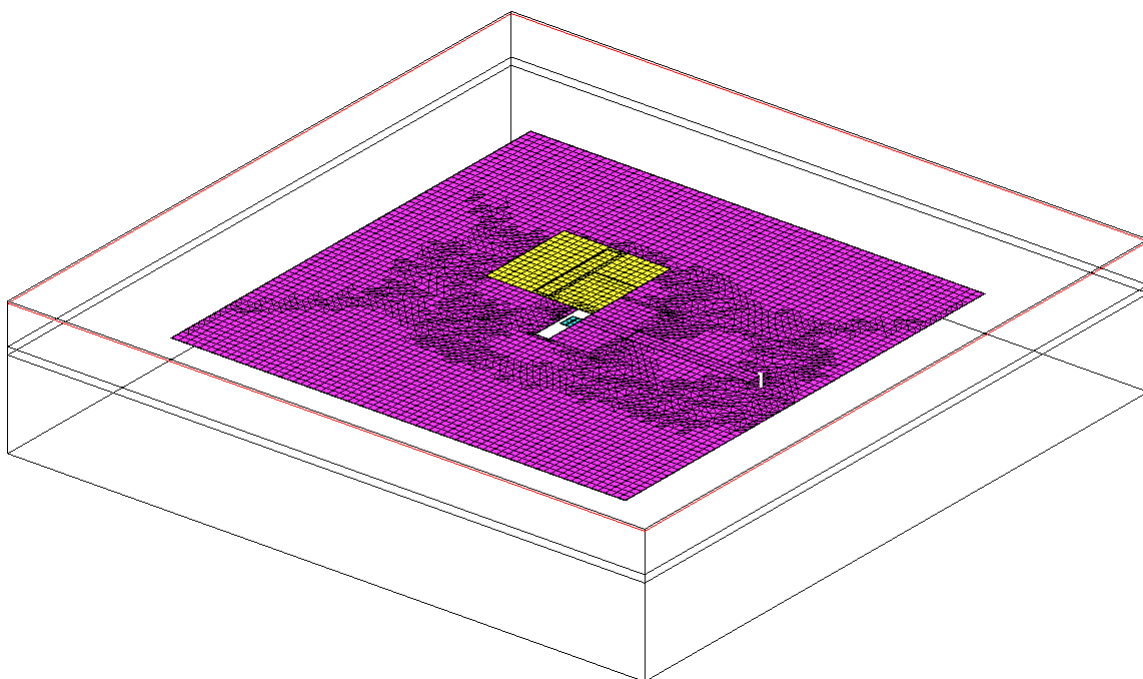


Figure 3.7: Top of the antenna element seen from the side.

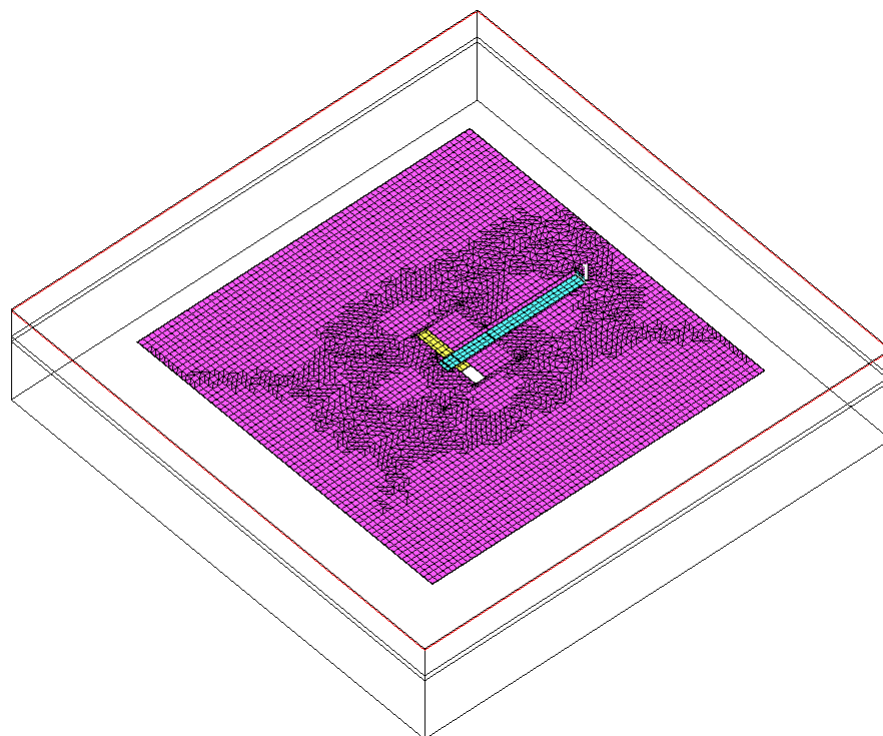


Figure 3.8: View of bottom of antenna element.

### 3.3.1 Simulation results

On the following pages, simulation results of the antenna element are given.

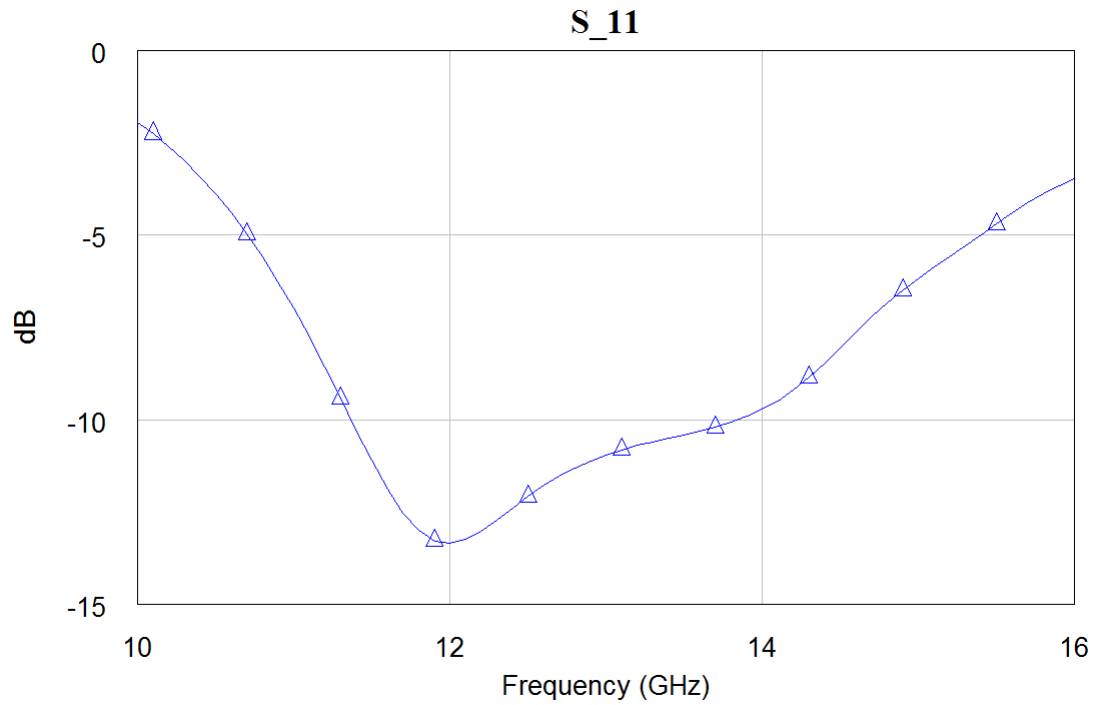
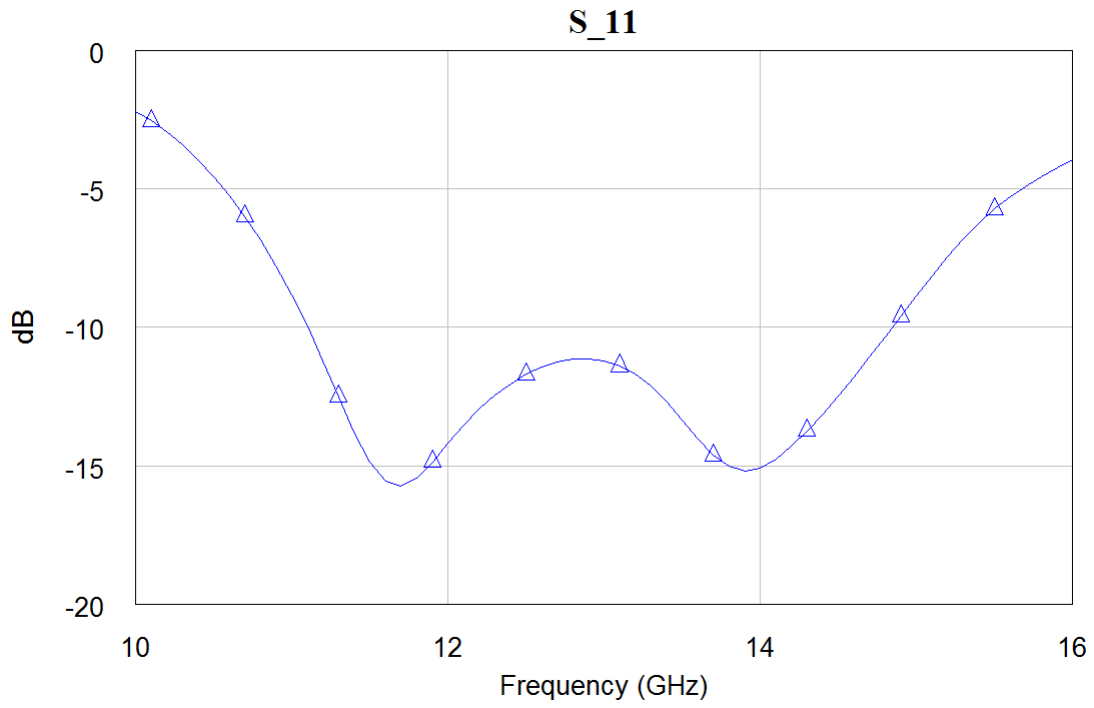
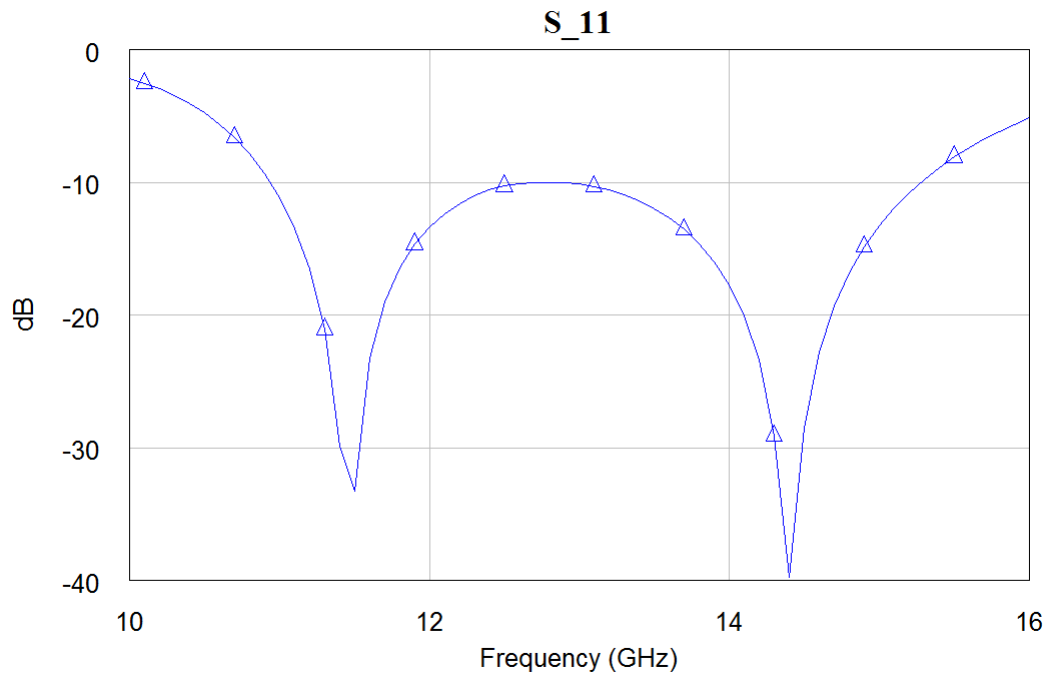


Figure 3.9:  $S_{11}$  of the initial design.

Figure 3.10:  $S_{11}$  after first part of tuning.Figure 3.11:  $S_{11}$  of the tuned antenna.

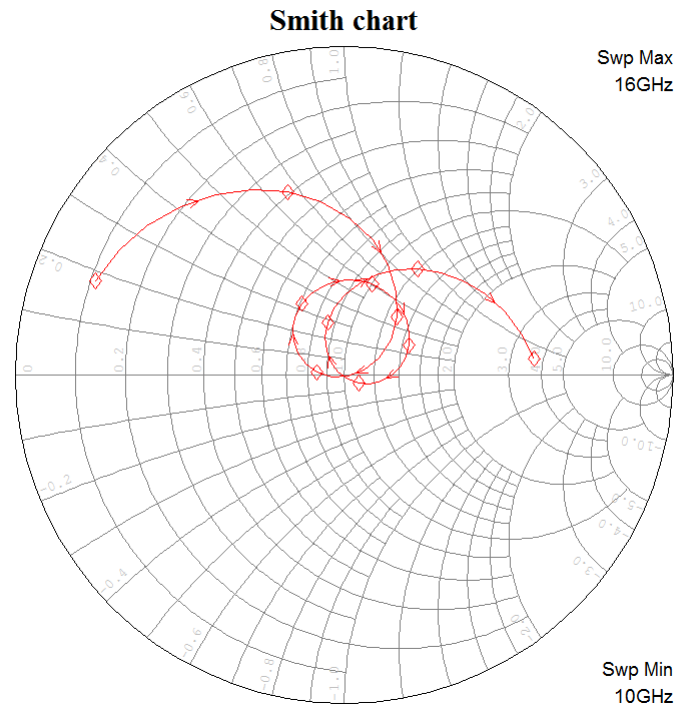


Figure 3.12: Smith chart of the antenna.

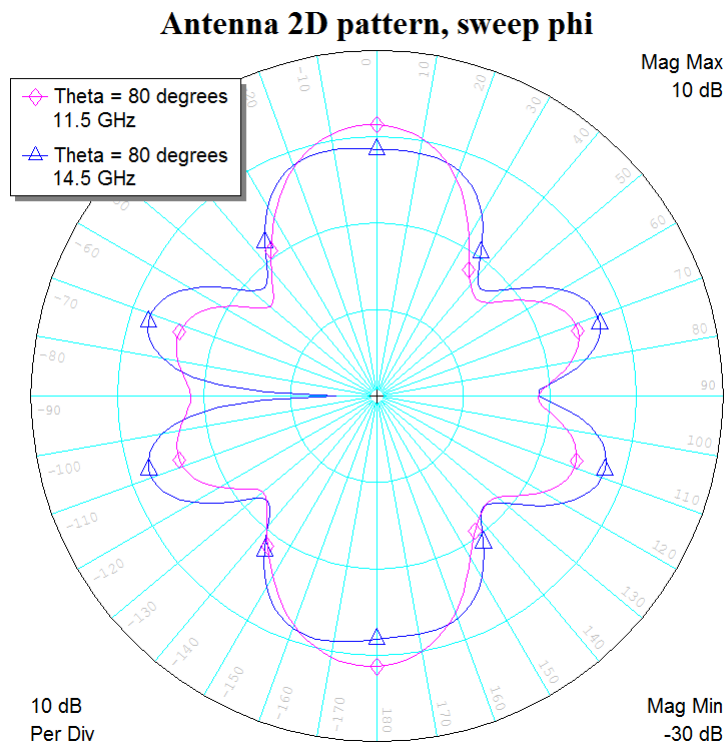
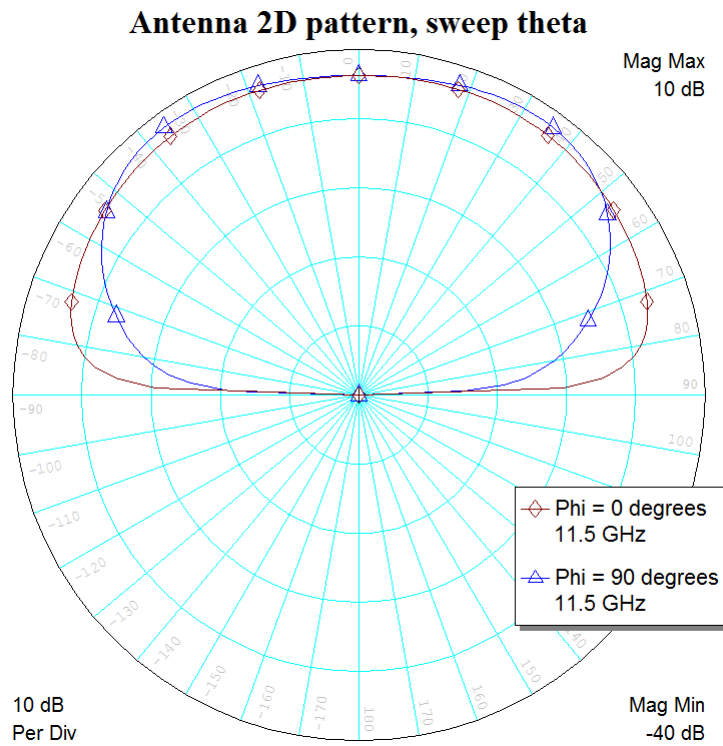
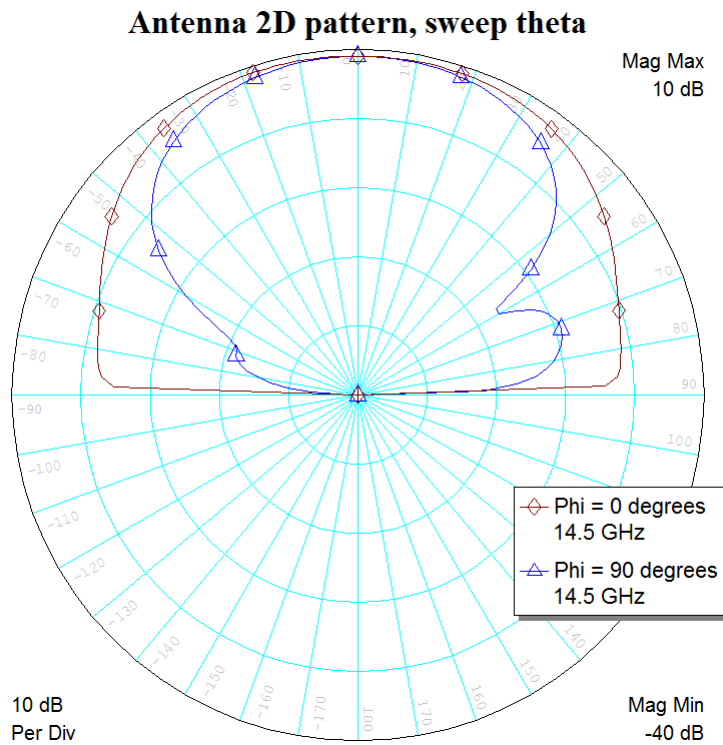


Figure 3.13: Horizontal radiation pattern for  $\theta = 80^\circ$ .

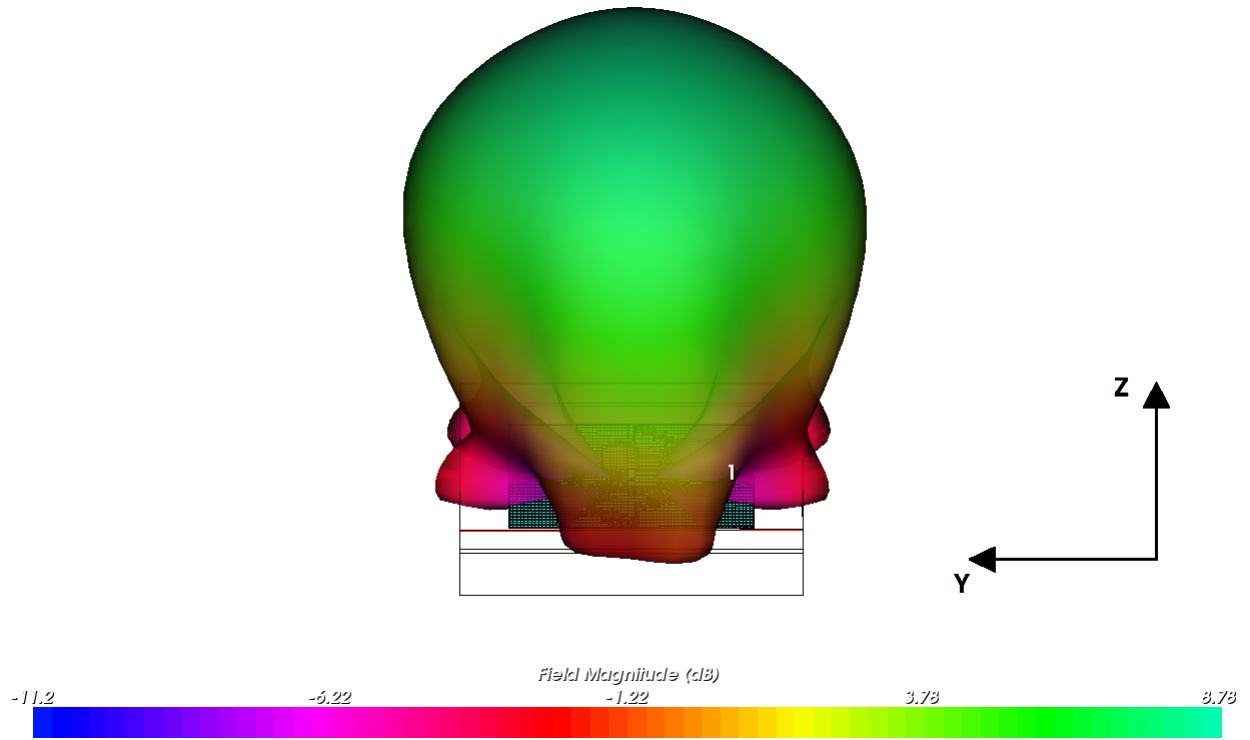


(a) Vertical radiation pattern at 11.5 GHz.

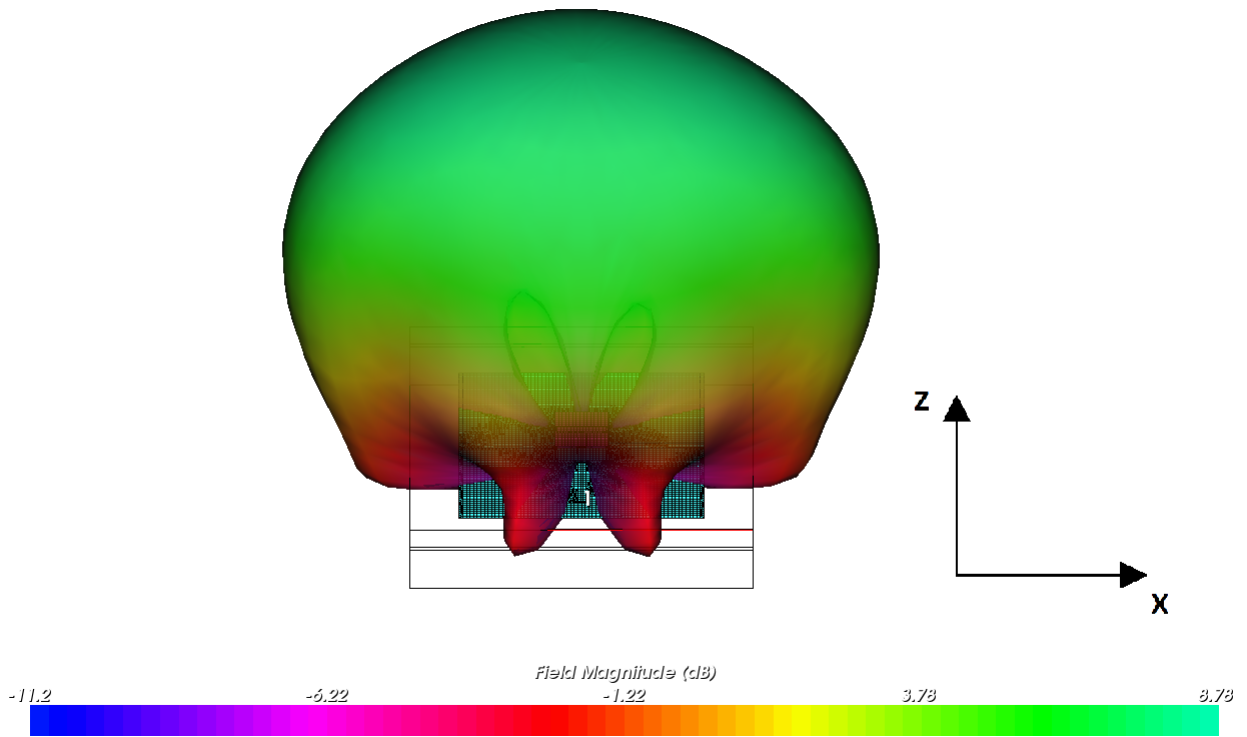


(b) Vertical radiation pattern at 14.5 GHz.

Figure 3.14: Vertical radiation patterns.

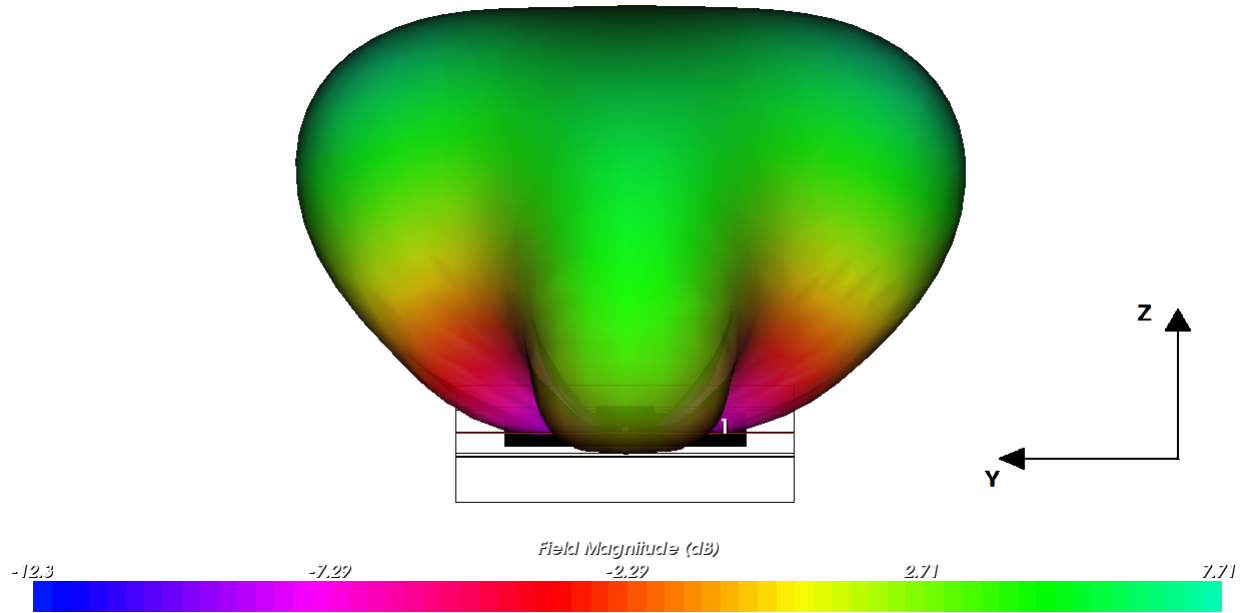


(a) 3D radiation pattern at 14.5 GHz.

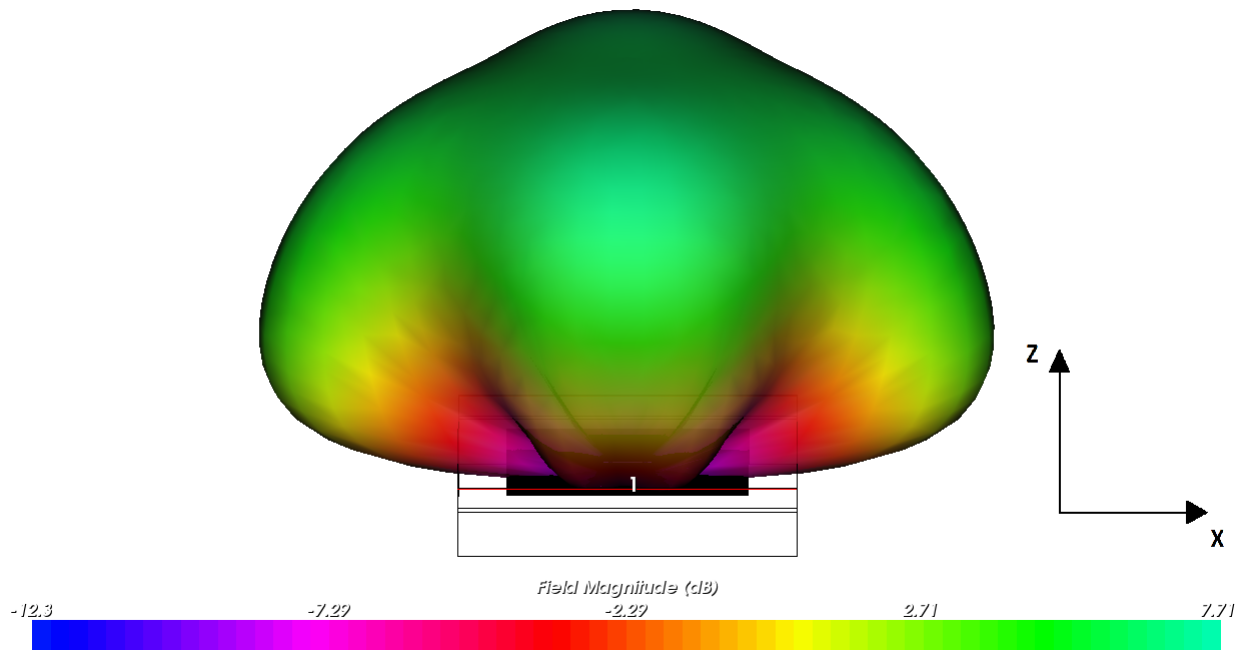


(b) 3D radiation pattern at 14.5 GHz.

Figure 3.15: 3D radiation pattern at 14.5 GHz.



(a) 3D radiation pattern at 11.5 GHz.



(b) 3D radiation pattern at 11.5 GHz.

Figure 3.16: 3D radiation pattern at 11.5 GHz.

## 3.4 Antenna with patch reflector

In Section 3.1.5 the back radiation of the aperture was reviewed, and the solution with a patch reflector was introduced. A patch reflector should at least have a  $0.1\lambda_0$  distance from the resonating aperture, and with a maximum wavelength in the Ku-band of 28 mm, a 3 mm thick foam as spacing would work. This would almost halve the thickness of the foam above the reflector for the complete metal plane reflector, and the overall height from reflector to superstrate was reduced to 7.23 mm. With the thickness set, the length and the width of the patch reflector could be found through experimental simulations in AXIEM.

It was not only the aperture that radiated backwards, simulations showed a significant back radiation from the patch too. This meant that the reflector had to be constructed in a way that it would reflect well at both patch and aperture resonance frequencies. The final length was set to 14 mm, and the width to 0.5 mm, so it was actually a patch dipole. It might seem counter-intuitive that a patch with shorter length or width will reflect better than a larger one, but the reflecting patch is a radiator in itself, and can therefore function better when it is tuned to give a desired magnitude and phase in the far-field of the antenna element.

The back-radiation was divided in three lobes, one directly to the back at  $\theta = 180^\circ$ , and two at  $\theta = \pm 130^\circ$ . The lobe in the direction  $\theta = 130^\circ$  was larger than the other two, and in order to reduce that lobe, the patch reflector was offset by 1 mm from the center of the antenna in the direction of the larger lobe. This reduced the lobe to the same magnitude as the other backward side lobe.

The introduction of the patch reflector in the system caused the frequencies to shift, and gave poorer matching. This was probably due to a reactive shift of the input impedance, since these effects were mostly compensated for by adjusting the length of the stub up to 0.85 mm.

The geometry of the antenna with the patch reflector was the same as for the antenna with infinite reflector, except for the foam above the reflector, which was reduced to 3 mm, the tuning stub that was increased to 0.85 mm, and of course the size of the reflector, which was set to  $(14 \times 0.5)$  mm. The patch reflector is seen in Figure 3.17. The performance parameters of the antenna with the patch reflector are provided in Table 3.4. The values can be compared to those for the antenna with an infinite reflector in Table 3.3. The F/B is the simulated power gain in the direction  $\theta = 0^\circ$  relative to the power gain in the direction of  $\theta = 180^\circ$ . In comparison with the F/B given in the table, the F/B without any reflector was 15.7 dB at 14.5 GHz, meaning an improvement of 2.8 dB, while at 11.5 GHz the F/B was 8.6 dB without reflector, meaning an improvement of 5.7 dB. In Figure 3.20 - 3.25, plots from simulations of the antenna with patch reflector are given. As a reference, simulations of the antenna without any reflector are provided in Figure 3.18 and Figure 3.19.

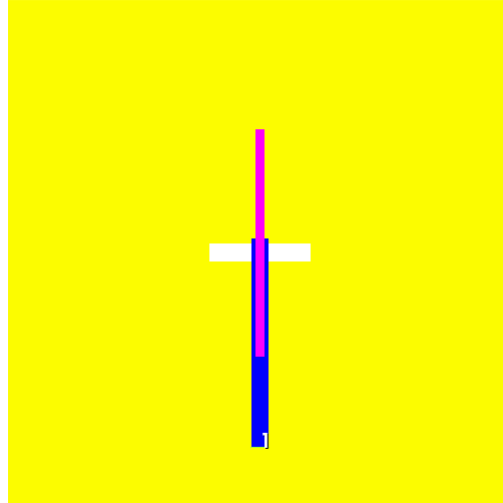
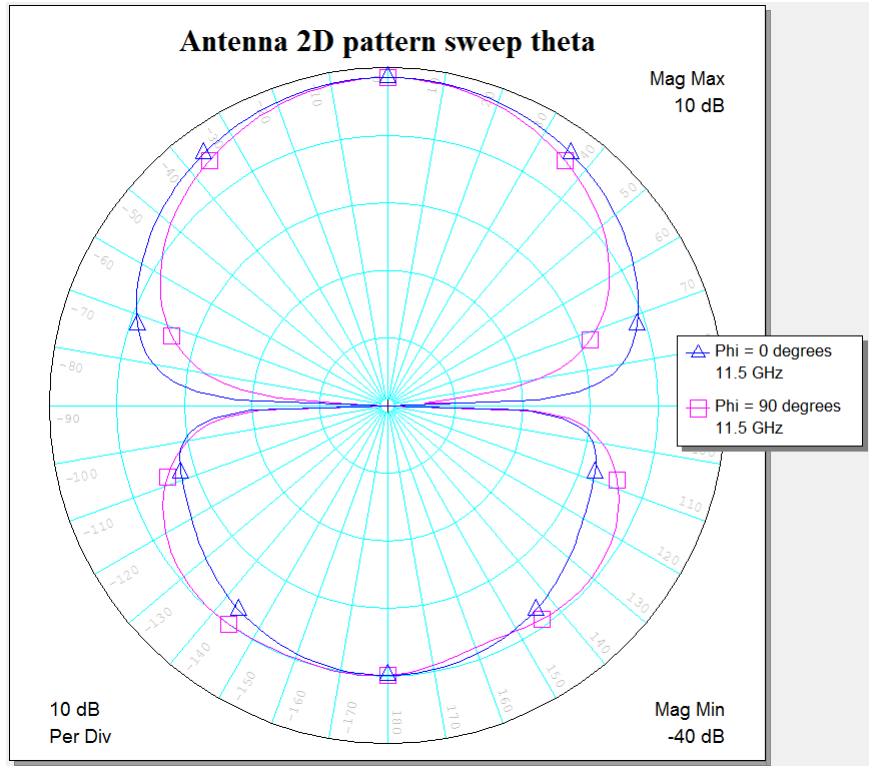


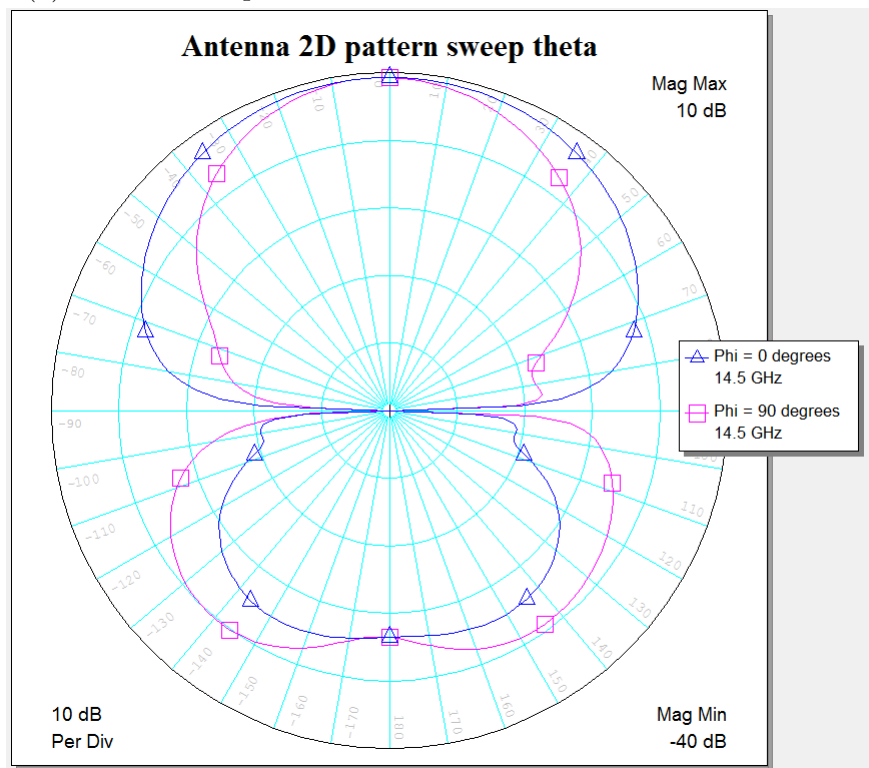
Figure 3.17: Bottom view of antenna element with patch reflector.

Table 3.4: Performance parameters of the antenna with patch reflector

Parameter	Upper/patch resonance	Lower/aperture resonance
Center frequency	14.3 GHz	11.6 GHz
$S_{11}$ at center frequency	-30.42 dB	-23.36 dB
Directivity	9.51 dBi	8.73 dBi
Gain	9.08 dBi	8.32 dBi
Efficiency	90.57%	90.99%
Half power beamwidth (x-axis)	40.3°	41.7°
Half power beamwidth (y-axis)	22.8°	31.3°
Bandwidth	4.05 GHz (30.9%)	
F/B	18.5 dB	14.3 dB

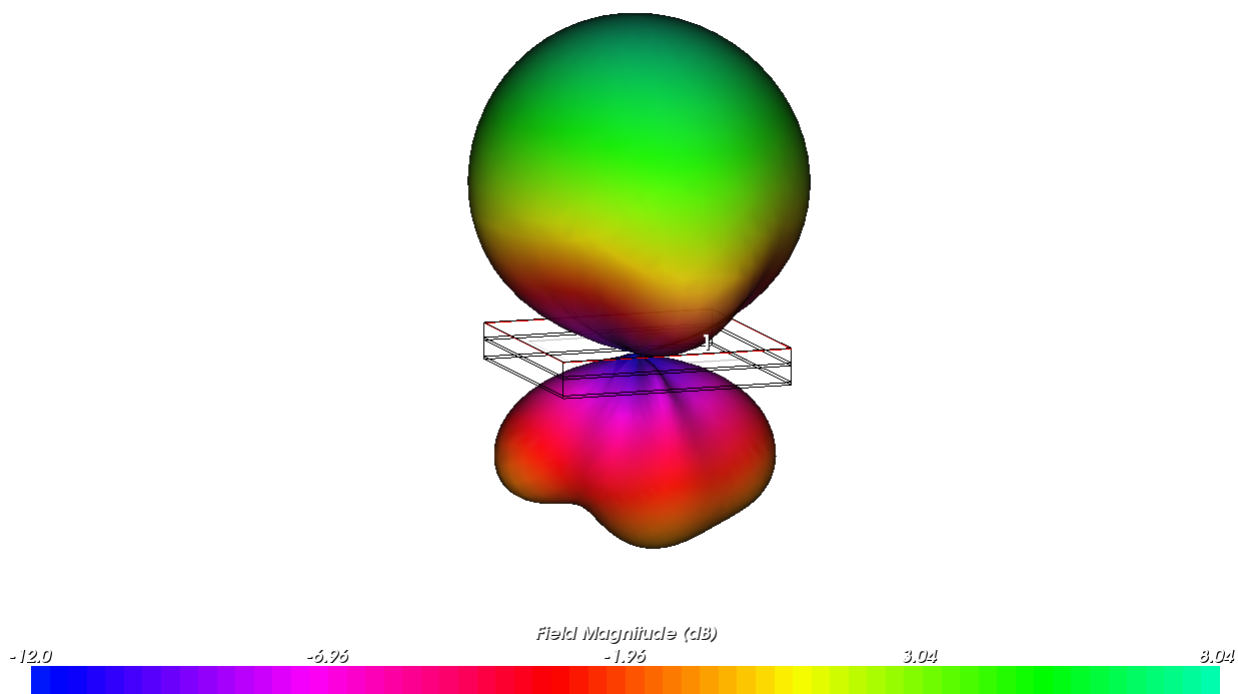


(a) 2D radiation pattern at 11.5 GHz without reflector.

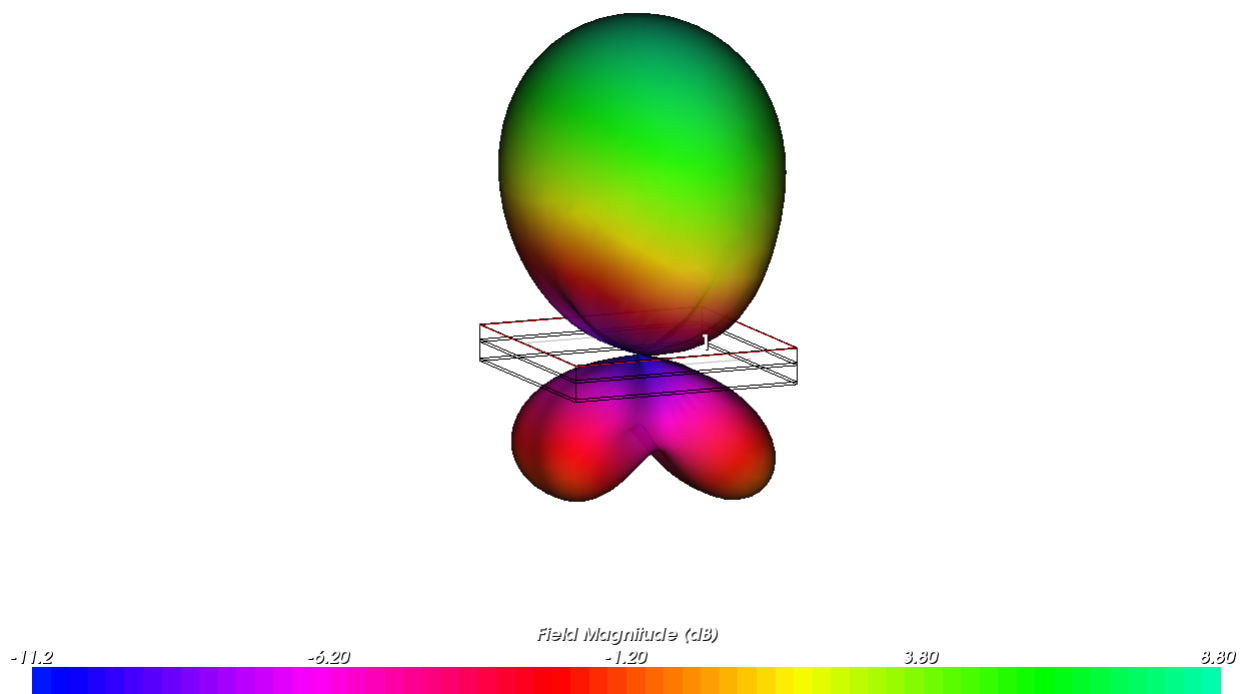


(b) 2D radiation pattern at 14.5 GHz without reflector.

Figure 3.18: 2D radiation patterns without reflector.



(a) 3D radiation pattern without reflector at 11.5 GHz.



(b) 3D radiation pattern without reflector at 14.5 GHz.

Figure 3.19: 3D radiation patterns without reflector.

### 3.4.1 Simulation results

On the following pages, simulation results of the antenna element with a patch reflector are given.

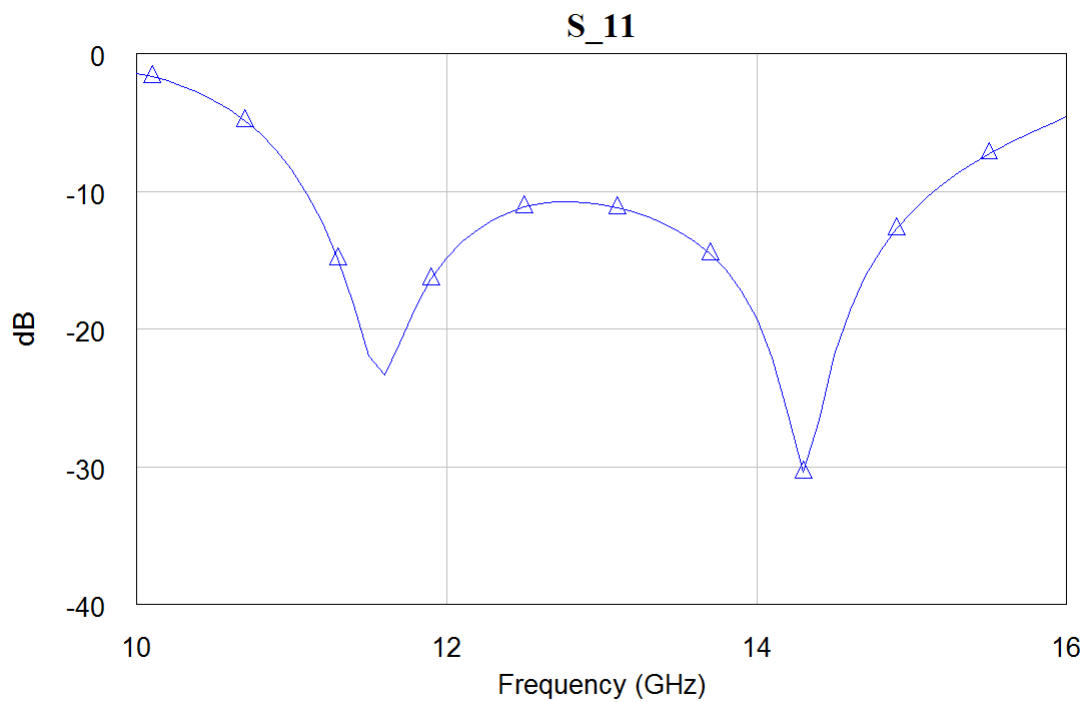


Figure 3.20:  $S_{11}$  of the antenna.

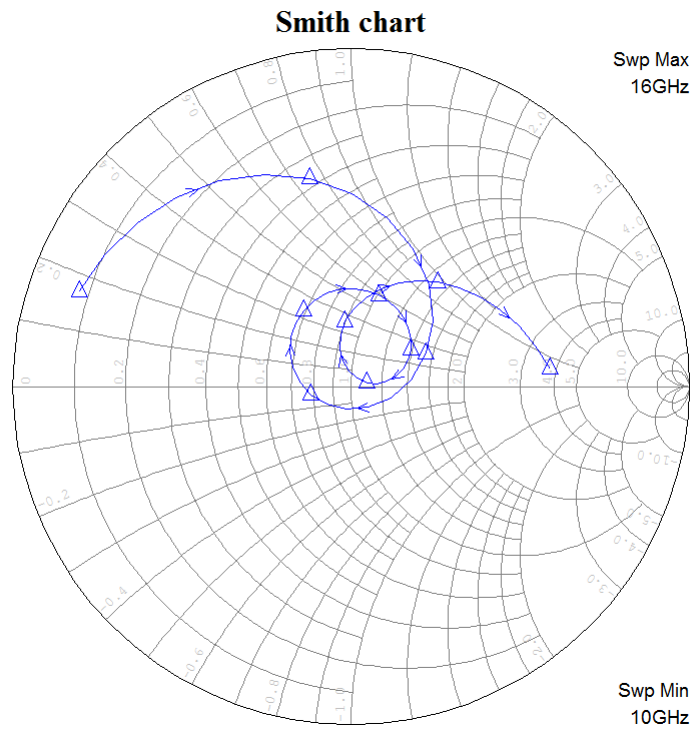


Figure 3.21: Smith chart of the antenna.

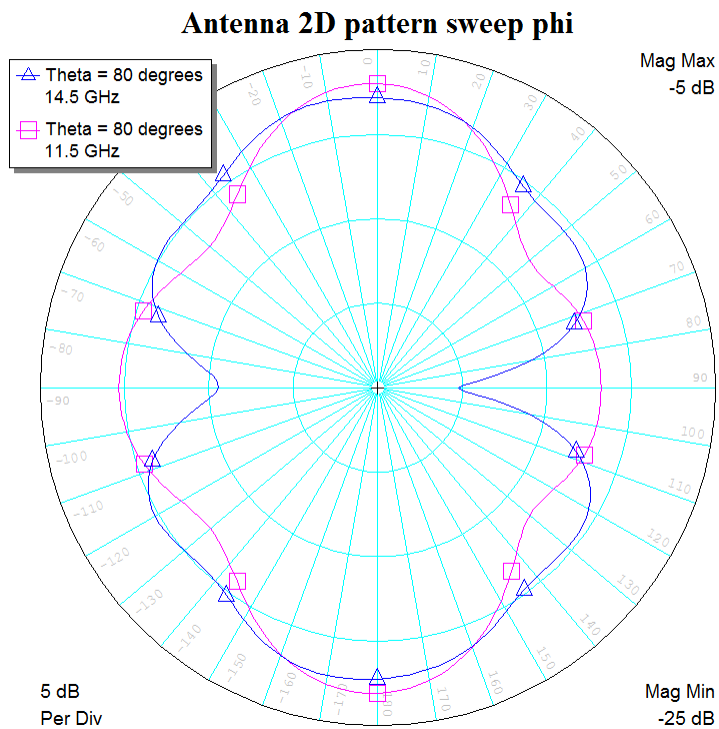
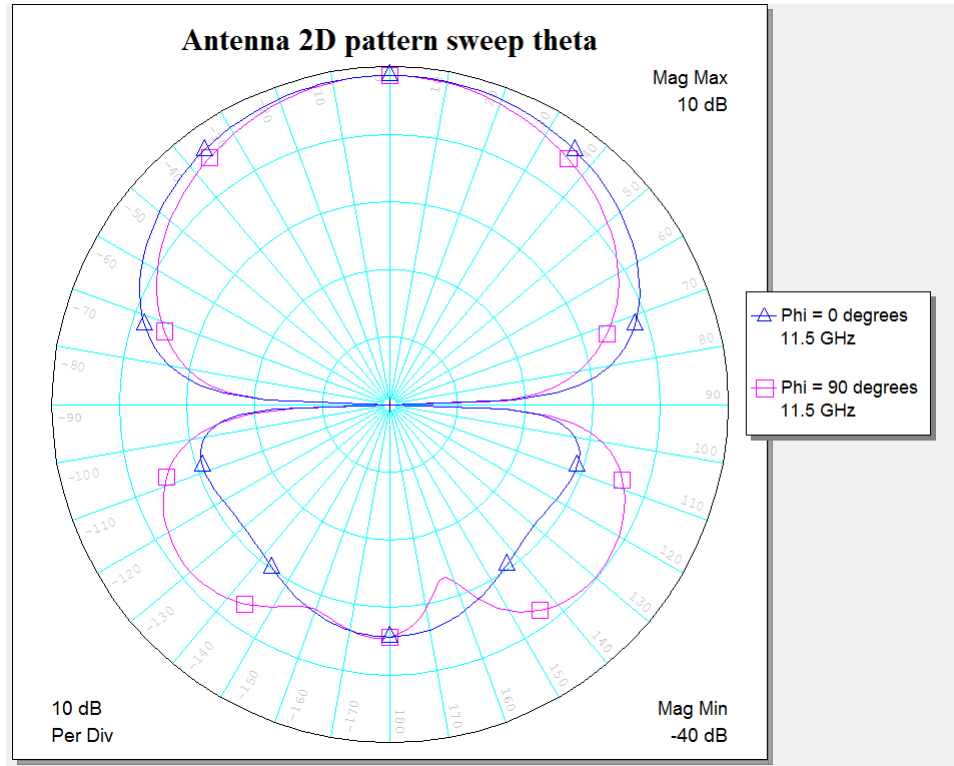
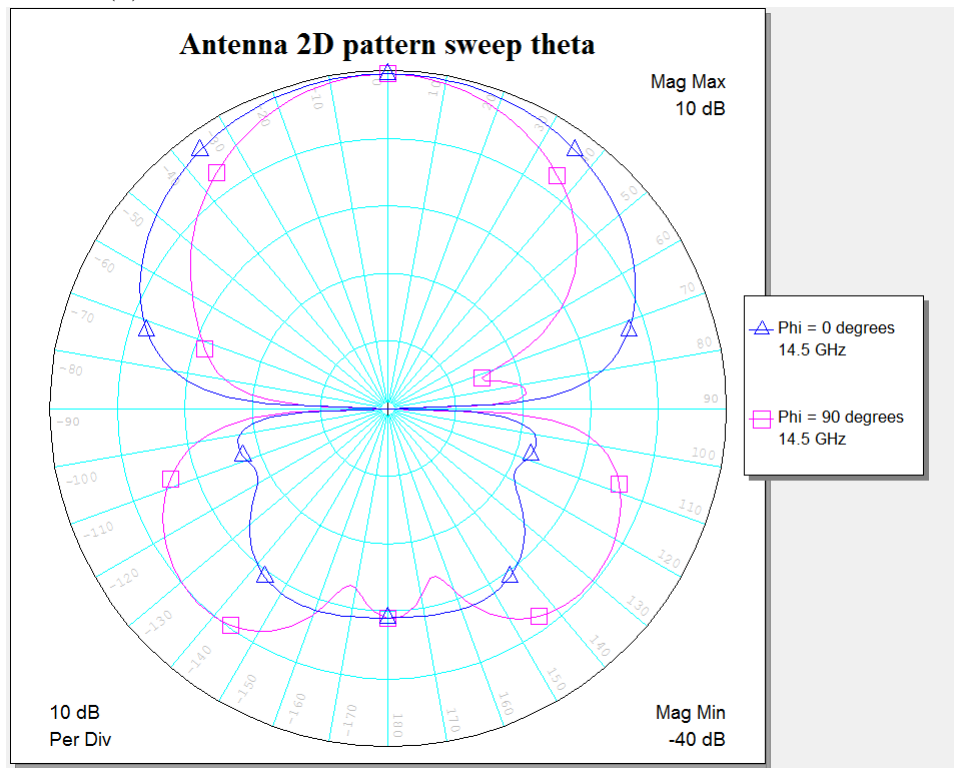


Figure 3.22: Horizontal radiation pattern for  $\theta = 80^\circ$ .

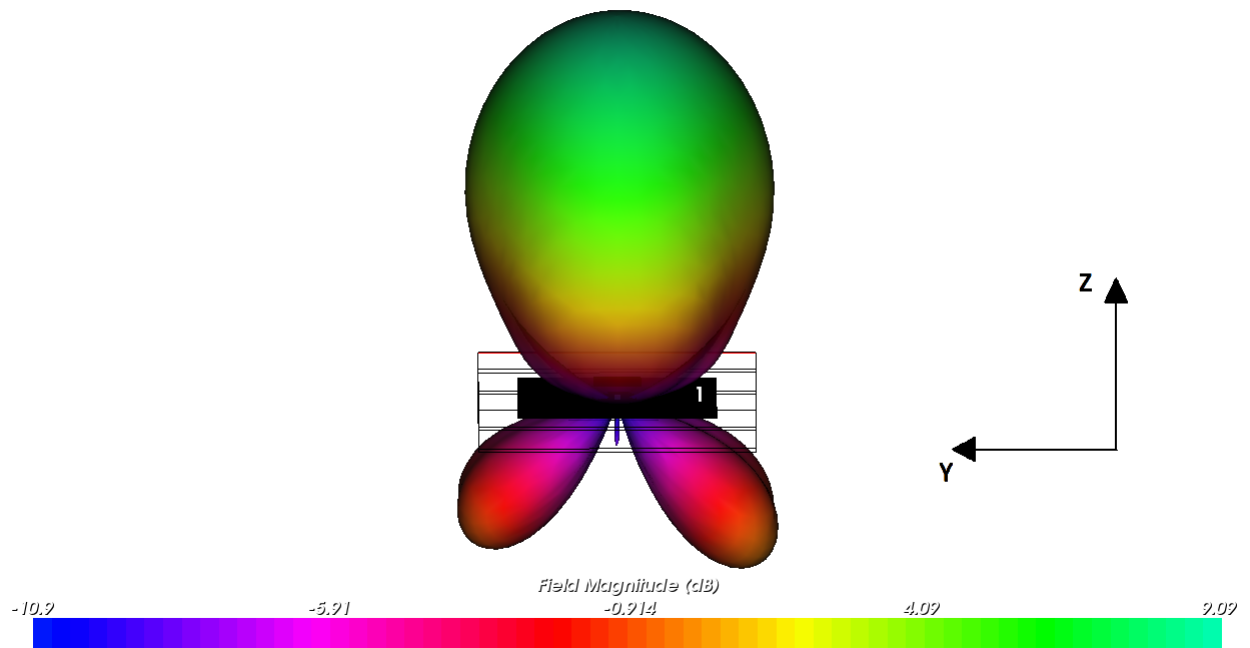


(a) Vertical radiation pattern at 11.5 GHz.

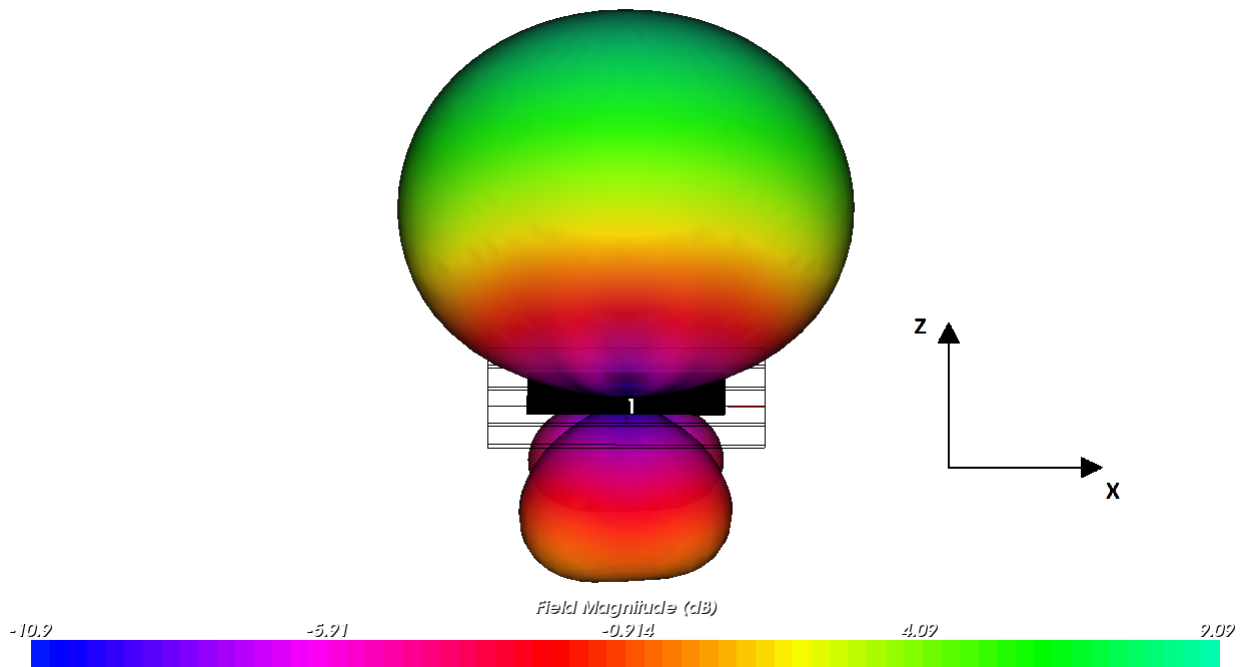


(b) Vertical radiation pattern at 14.5 GHz.

Figure 3.23: Vertical radiation patterns.

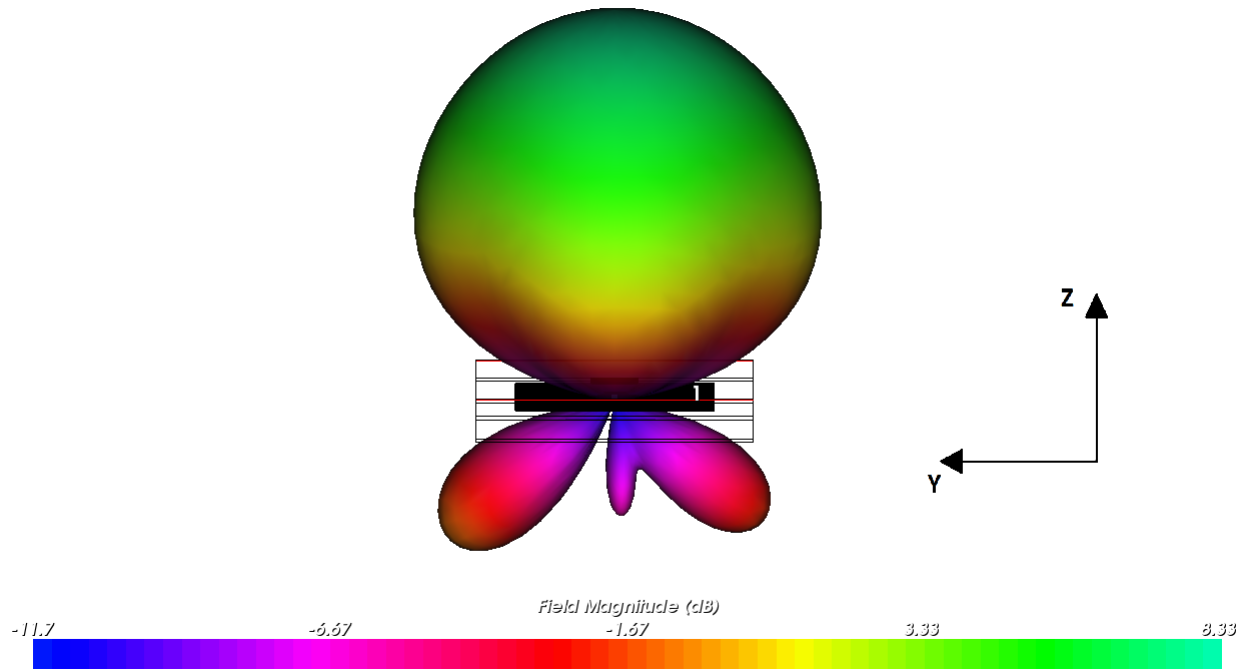


(a) 3D radiation pattern at 14.5 GHz (x-plane).

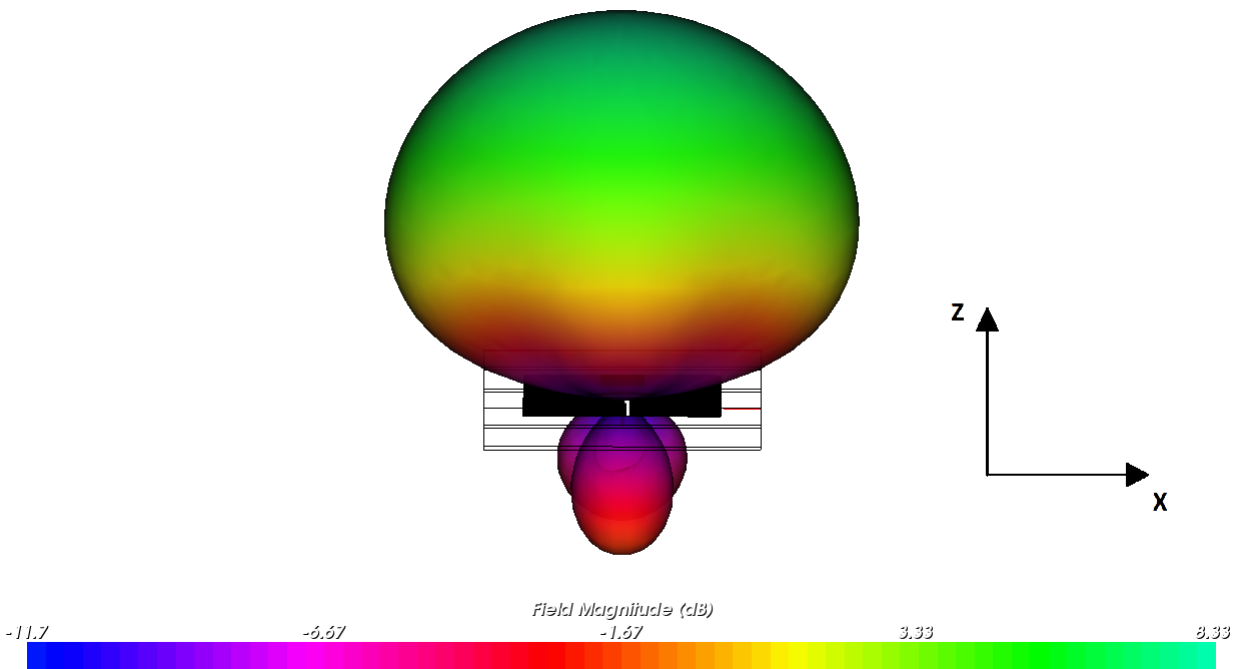


(b) 3D radiation pattern at 14.5 GHz (y-plane).

Figure 3.24: 3D radiation pattern at 14.5 GHz.



(a) 3D radiation pattern at 11.5 GHz (x-plane).



(b) 3D radiation pattern at 11.5 GHz (y-plane).

Figure 3.25: 3D radiation pattern at 11.5 GHz.

## 3.5 Comments on results

The presented simulations of the antenna element shows that it works good for a broad frequency band, and covers both uplink and downlink frequencies in the Ku-band. The matching levels and input reflection coefficients are very good at both frequencies, and a total bandwidth over 30% is achieved. This is true for both designs, with metal plane reflector, and with patch reflector. The directivities and gains are good at both resonance frequencies, when looking at other comparable works. The directivity and gain at the uplink frequency are very good. Efficiencies over 90% are good, especially since bandwidth has been favoured over efficiency in the process of making the antenna element. From the simulation plots and the HPBW, it is observed that the beam is narrower for the uplink frequency, and it is narrower when the patch reflector is used. The configuration with the patch reflector also gave a smoother radiation pattern with less difference in power radiated in different directions. With the patch reflector, better directivity and gain are obtained, but the input reflection coefficients are less good, and there is a small decrease in bandwidth and efficiency, compared to using the metal plane reflector. The patch reflector will most certainly give some more back radiation than the metal plane reflector, but it will give more freedom in adjusting radiation characteristics. The levels of F/B with the patch reflector can be acceptable, and the increase seen in F/B for the aperture resonance frequency were good.

## 3.6 Other design considerations

### 3.6.1 Different shaped aperture and patch

Another thing that was proposed to test was different shapes of the aperture, but this was discarded. Other shapes can improve the coupling, and improve the bandwidth of the aperture, and it was attempted to implement a dog bone shaped aperture in the simulation program. However, this shape was very hard to work with, because the combination of circular and straight edges were hard to change in the program. The improved F/B obtained with such shapes are mostly due to a smaller aperture which radiates less, and that is unwanted here, since the aperture is used as a resonator. Also, according to Aliakbarian et al. (2006), the effects of using such shapes are small. Therefore, it was decided to not spend time on making a new aperture.

It was attempted to use a circular patch, instead of a rectangular, since it according to Garg et al. (2001) has a larger bandwidth. The radius was calculated by use of (2.23) and (2.24), and was found to be 2.8 mm. Simulations with this radius showed no patch resonance near 14.25 GHz. The radius had to be tuned up to 4.6 mm to get a resonance near 14.25 GHz. It is possible that this large difference in computed and tuned radius is due to the patch operating at a different mode. The simulations with the circular patch showed no significant difference in any performance parameters when compared with the rectangular patch, so both shapes could be used. The circular patch is seen in Figure 3.26.

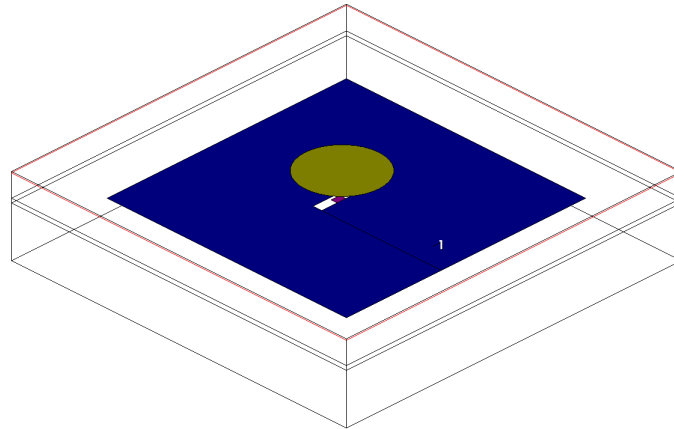


Figure 3.26: Antenna element with circular patch

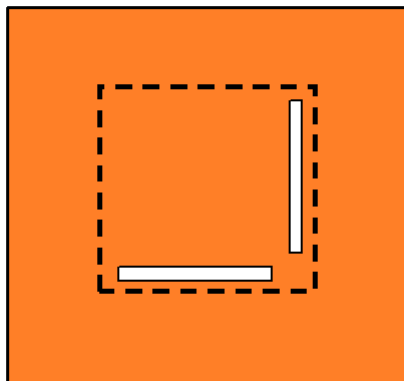
### 3.6.2 Alternatives for polarization

To make a wide/dual-band SSFIP antenna dual or circularly polarized, two orthogonally oriented apertures can be used. An alternative with a single feed is to use stacked patches with slots cut in them to make them dual polarized. Then each patch has its own resonance, making the antenna dual-banded. However, introducing another patch would give a higher profile to the antenna of this thesis, and making patches with slots is a complicated process, so a solution with two feeds seemed more attractive. The two apertures of a dual polarized antenna are fed with equal power from power splitting, and with a  $90^\circ$  phase shift. The two apertures can be positioned in a number of different ways, for example they can be shifted away from the center of the patch to the edges of the patch, as seen in Figure 3.27a, but this will give an unsymmetrical feed which reduces the polarization purity. The apertures can instead be placed centrally, forming a cross, shown in Figure 3.27b, or the two slots can be divided into four smaller slots, a double crossed slot as in Figure 3.27c. The feed must be made such that cross coupling between the feeds and the apertures are avoided.

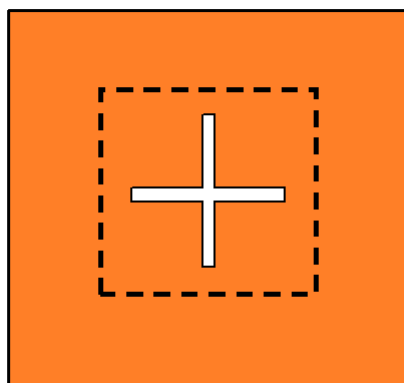
Using stacked patches is most common with the solution of two feeds and dual resonance, but that is not considered here, since the second resonance comes from the aperture. Therefore, both the patch and the aperture must be made for dual polarization, and how can an antenna with a resonating aperture be made dual or circularly polarized? An example with a resonating aperture and somewhat equal structure as the antenna here, is found in Kirov and Mihaylova (2010), where a crossed resonant aperture is used. The patch and aperture dimensions are chosen in a way such that both  $TM_{010}$  and  $TM_{001}$  are excited, and in combination gives a circular polarization. The antenna is operating at only the downlink frequency of the Ku-band. Any examples where the aperture and patch are working at different frequencies, and at the same time is circularly polarized for each frequency was not found. It was also desired to look at possibilities of switching between different polarizations, as seen in Wu et al. (2007). Since using four resonating apertures would take up much space, it can be hard to make the same structure here, and the apertures would have to be placed close to each other, which would give high levels of coupling between them. To realize different polarizations in an antenna with resonating apertures will be a demanding task,

and a solution with this was not found here.

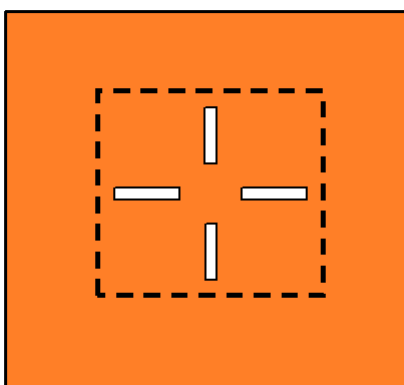
To improve any circular polarization the antenna elements can be placed sequentially rotated in the array. That is only used to improve already circular polarized antenna elements. It is possible to try with resonating aperture(s) organized as in Figure 3.27a or Figure 3.27b, to make a dual polarized wide-band antenna. Due to limited time, this was not implemented here, but this can be attempted in any future work with the project. A way to achieve different polarizations in the same antenna with resonating apertures must be found before it can be thought of making ways to switch between polarizations.



(a) Off-center dual aperture.



(b) Cross aperture.



(c) Double crossed aperture

Figure 3.27: Different aperture configurations for dual polarized patch antennas.

# Chapter 4

## Design and tuning procedure

In this chapter a design and tuning procedure for a wide/dual-band patch antenna element is presented. The procedure is divided in two; one for design and one for tuning, but at some points, the design must be made directly through tuning. The procedures are given in a qualitative way, since combinations of effects from different parameters are hard to take into account in a quantitative procedure. The procedures can be regarded as general guidelines, and can be used for wide/dual-band SSFIP antennas with resonating aperture. But first it is looked at the effects of each part of the antenna element.

### 4.1 Effects of parts

In this section, the effects of tuning on different antenna parts are presented. The results are based on experimental tuning performed on the antenna(s). The most significant effects observed in the simulations are also presented in figures found in Section 4.1.8.

#### 4.1.1 Patch

The length of the patch affects the frequency response. A longer patch reduces the center frequency of the patch, and also the center frequency of the aperture, but less. A shorter patch will increase the frequencies. This is seen from the  $S_{11}$  measurement in Figure 4.3. The width of the patch has the same effect on frequencies as the length has, but not in the same degree. To see the same change in frequencies as if the length is changed by 0.2 mm, the width must be changed 1 mm. With a decreased width, the loops in the Smith chart grows, meaning better coupling, as observed in Figure 4.4. The radiation pattern becomes a little narrower with a wider patch, giving somewhat higher directivity.

#### 4.1.2 Aperture

The effects on frequency response of different aperture lengths is shown in Figure 4.5. The length of the aperture is mainly controlling the resonant frequency of the aperture, where a larger aperture gives lower frequency. Changing the aperture length gives worse matching for the patch resonance, since the antenna is tuned to work optimal with a specific aperture

length. A less wide aperture will make the two resonant frequencies move closer, giving a narrower bandwidth. The upper frequency becomes lower, and the lower frequency becomes higher, as shown in Figure 4.6. The opposite effect is observed when the aperture is widened. In the Smith chart the loops are increased by increased size of the aperture, due to better coupling, shown in Figure 4.7. A smaller aperture was observed to give a slightly more narrow radiation pattern, and increased directivity.

### 4.1.3 Stub

The stub is perhaps the part of the antenna that needs most fine-tuning. The resonances are shifted upward in frequency with a shorter stub length, and opposite for a longer stub, as seen in Figure 4.8. The patch resonance is shifted most. The level of matching is decreased when the length is varied, and in a higher degree for the aperture resonance. The most interesting effect of the tuning stub is the effect on the location of maximum and minimum current. Figures Figure 4.1 and Figure 4.2 show the absolute value of the current on the feed line with the tuned stub. The currents are mostly concentrated at the edges of the feed line. Figure 4.1 shows a current maximum beneath the aperture at the patch resonance frequency. A current maximum will lead to good coupling between feed line and patch. In Figure 4.2, a current minimum is beneath the aperture at the resonance frequency of the aperture. This is surprising, since theory for slot antennas says that there should be a current maximum for a resonant slot. Recalling from Figure 2.11 that the aperture was represented as a parallel tank circuit and resonance in a parallel circuit means a minimum current. It is then possible to think that a minimum current on the line coincides with the resonant frequency of the aperture, but this is just some speculative thoughts. Obviously then, the stub must be of a length that makes a minimum in current at the aperture frequency, and a maximum at the patch frequency, and this makes the stub very fine tuned. It is also seen in Figure 4.2 that the current is concentrated on each edge of the aperture, which is the expected current distribution of a slot at resonance frequency.

### 4.1.4 Feed-line

The length of the feed line affects the radiation pattern in the simulations, but not the frequency responses. A longer feed line makes the radiation pattern narrower in the direction of the feed length, the y-axis. This is due to effects of radiation from the feed line. How long the feed line will be, depends on the feed network, and where it will couple to the feed line, so this must be checked when the feed network and the antenna elements are connected. The loops in the Smith chart will rotate as the length of the feed is changing, as seen in Figure 4.9, but the position of the resonant frequencies is rotating about the center of the Smith chart, maintaining a good matching, due to the effect of the tuning stub.

The width of the feed is depending on frequency and substrate, and it was mostly held constant in the tuning process. However, the feed line can be made wider to shift the frequencies down, or thinner for a shift upwards.

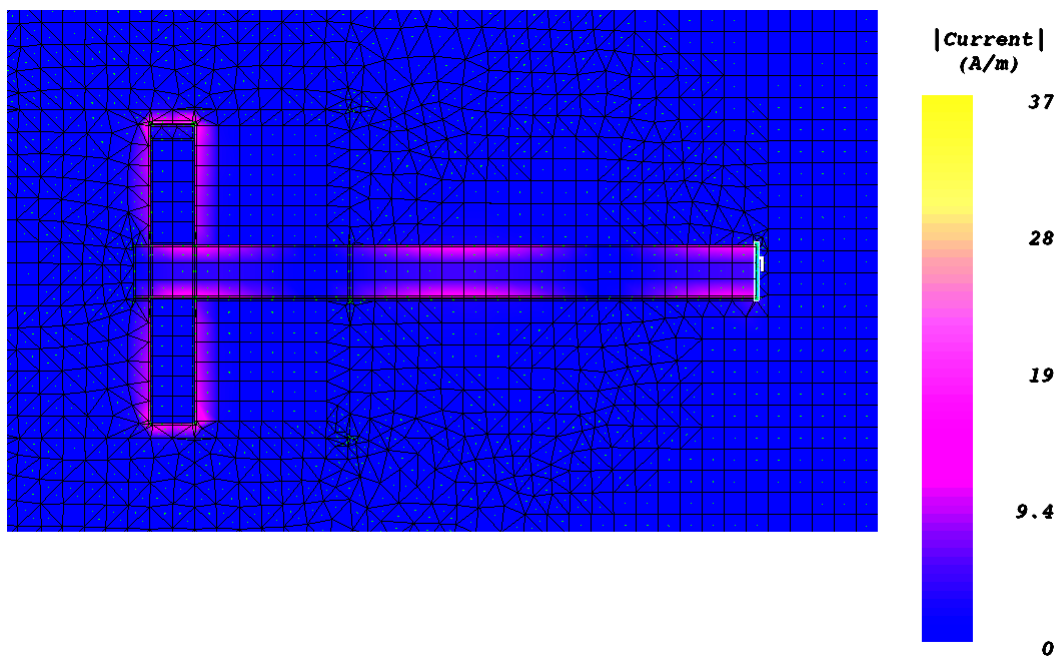


Figure 4.1: Current on feed line at 14.5 GHz

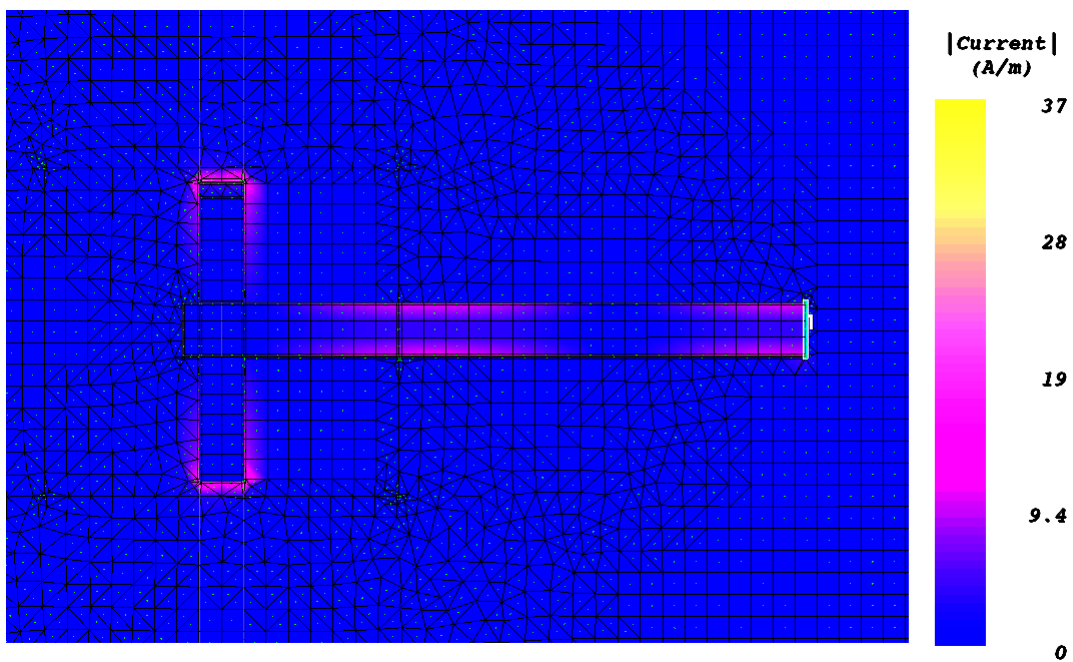


Figure 4.2: Current on feed line at 11.5 GHz

### 4.1.5 Substrates

One of the first things that was chosen in the design process was type of substrates, and their thickness. The feed substrate will reduce the resonant frequencies if it is thinner, and it will increase them if it is thicker. However, the thickness of the feed substrate is limited to the thicknesses available from the manufacturer, and thickness of feed substrate is therefore not a practical parameter to tune. Change of dielectric material can be considered, but the electrical characteristics should be quite similar, or else much of the tuning process must be implemented again. Therefore, the feed substrate should be kept constant through all simulations.

The thickness of the foam used in the patch substrate can be changed to improve the antenna's performance. This material is available in more finely divided thicknesses, down to 0.25 mm difference, so tuning of this is possible. A thinner patch substrate will shift the patch resonance down and the aperture resonance slightly up, giving less bandwidth. The opposite happens with a thicker foam, but the bandwidth can only be widened to until a point where the resonances are separated too much, and the band between them gets too high reflection. The coupling is considerably increased with a thinner patch substrate, which can be observed in Figure 4.10. A thinner foam gave higher gain for the patch resonance, but lower gain for the aperture resonance. The opposite was observed for a thicker patch substrate. The use of foam as substrate enabled large bandwidth, and gave freedom in choice of superstrate thickness, which made the design easier, and its thickness could be adjusted, making the tuning easier.

### 4.1.6 Superstrate

The simulations were carried out with a very thin superstrate, to avoid any effects it would have on the performance. It was tested to increase the thickness, and as expected this shifted the resonance frequencies down, as seen when comparing Figure 4.11 and Figure 3.11. But thicker superstrate also gave higher gain, so it can be desired to make it a little thicker. The frequency shift obtained by a slightly thicker superstrate can be compensated for by small adjustments on patch, aperture and stub.

### 4.1.7 Reflector

In the simulations an infinite copper plane spaced a quarter wavelength from the aperture was used. In order to get a lower profile antenna, it was attempted to switch the foam above the reflector with a dielectric with higher permittivity. This would make the quarter wavelength distance shorter, since wavelength is inverse proportional to the relative permittivity in the medium. These tests changed the radiation and frequency characteristics of the antenna lot, and many adjustments would have to be made to make the antenna work properly, so this was discarded. The way to go for a lower profile would be to make a patch reflector.

### 4.1.8 Simulation of different parts

The purpose of these simulations is to show effects of varying different parts in the antenna, and only one parameter is varied at the time to show its effects more clearly, while the other parameters are held constant. Small adjustments on parameters have been done during the tuning process, causing some variations in the simulation results given here. Mainly the parameters used in the simulations here are the same as in Table 3.2.

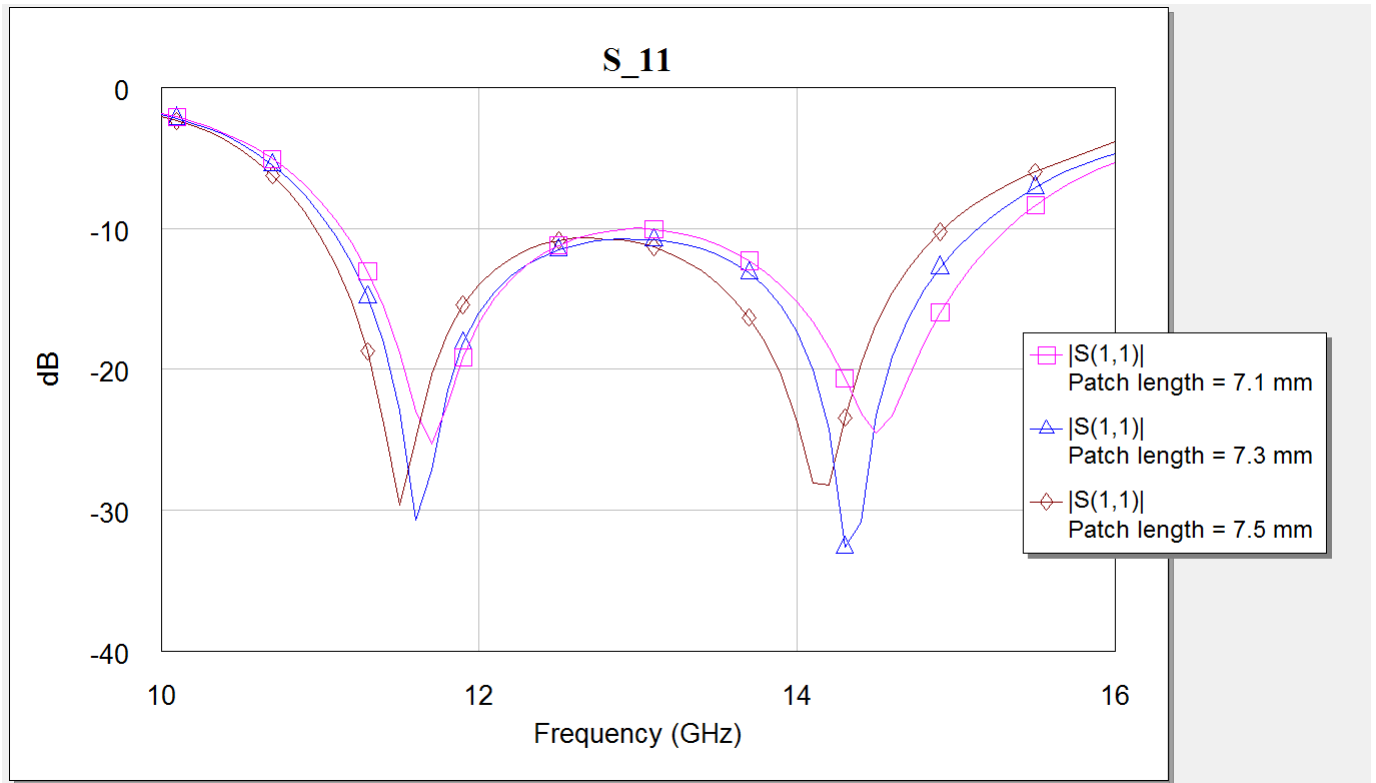


Figure 4.3: Comparison of  $S_{11}$  for different patch lengths.



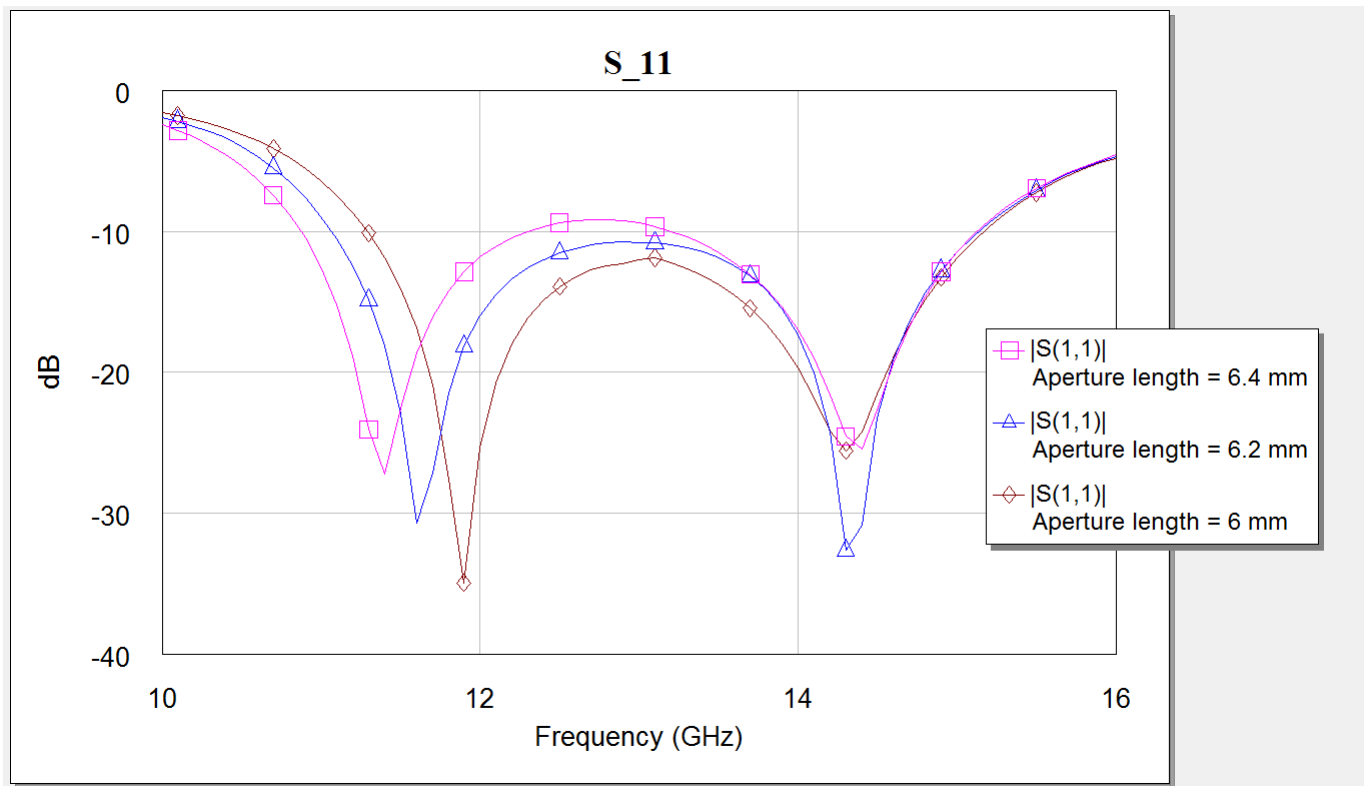


Figure 4.5: Comparison of  $S_{11}$  for different aperture lengths.

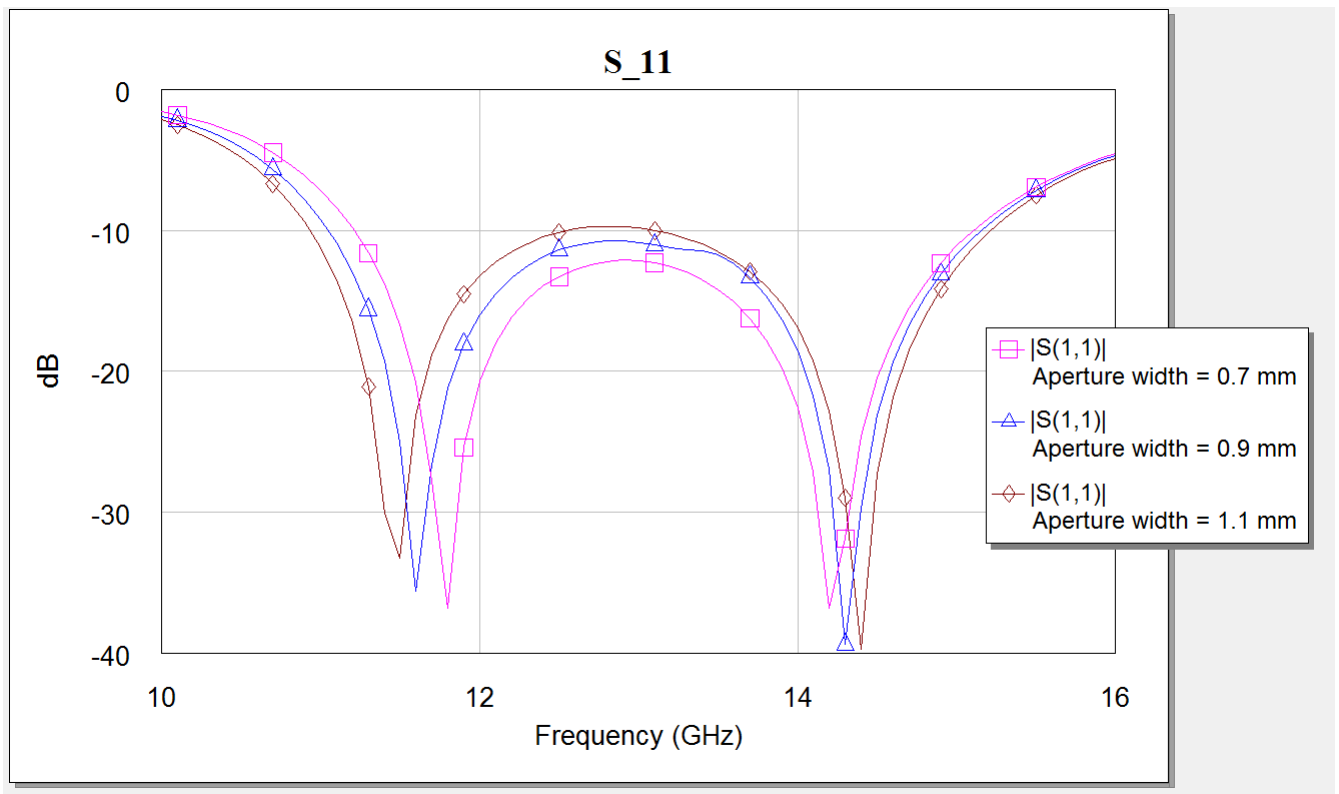
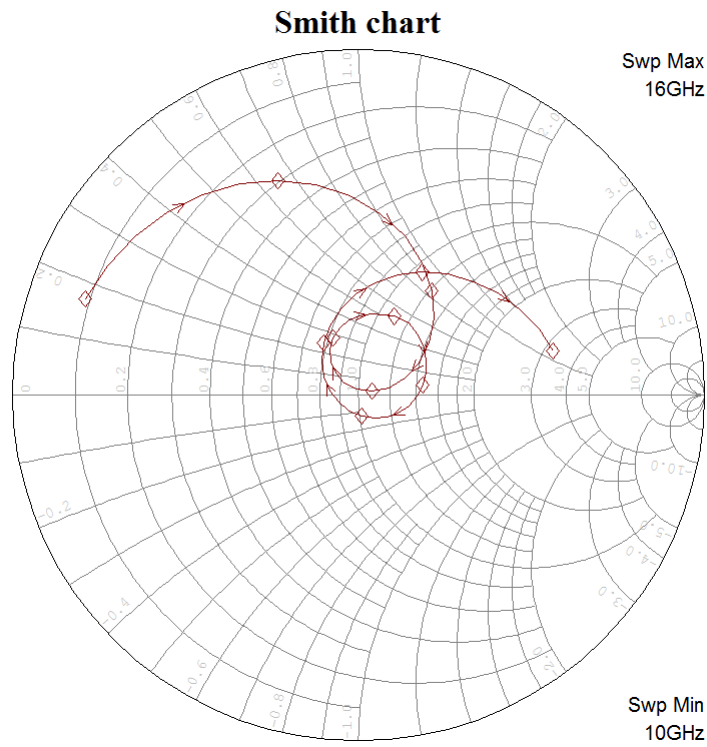
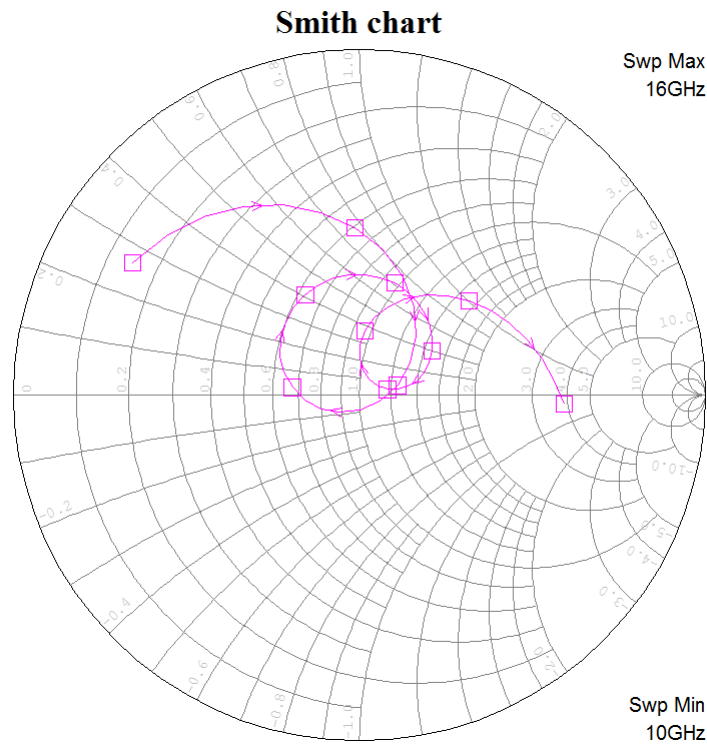


Figure 4.6: Comparison of  $S_{11}$  for different aperture widths.



(a) Smith chart for aperture length 6 mm.



(b) Smith chart for aperture length 6.4 mm.

Figure 4.7: Smith chart for different aperture lengths.

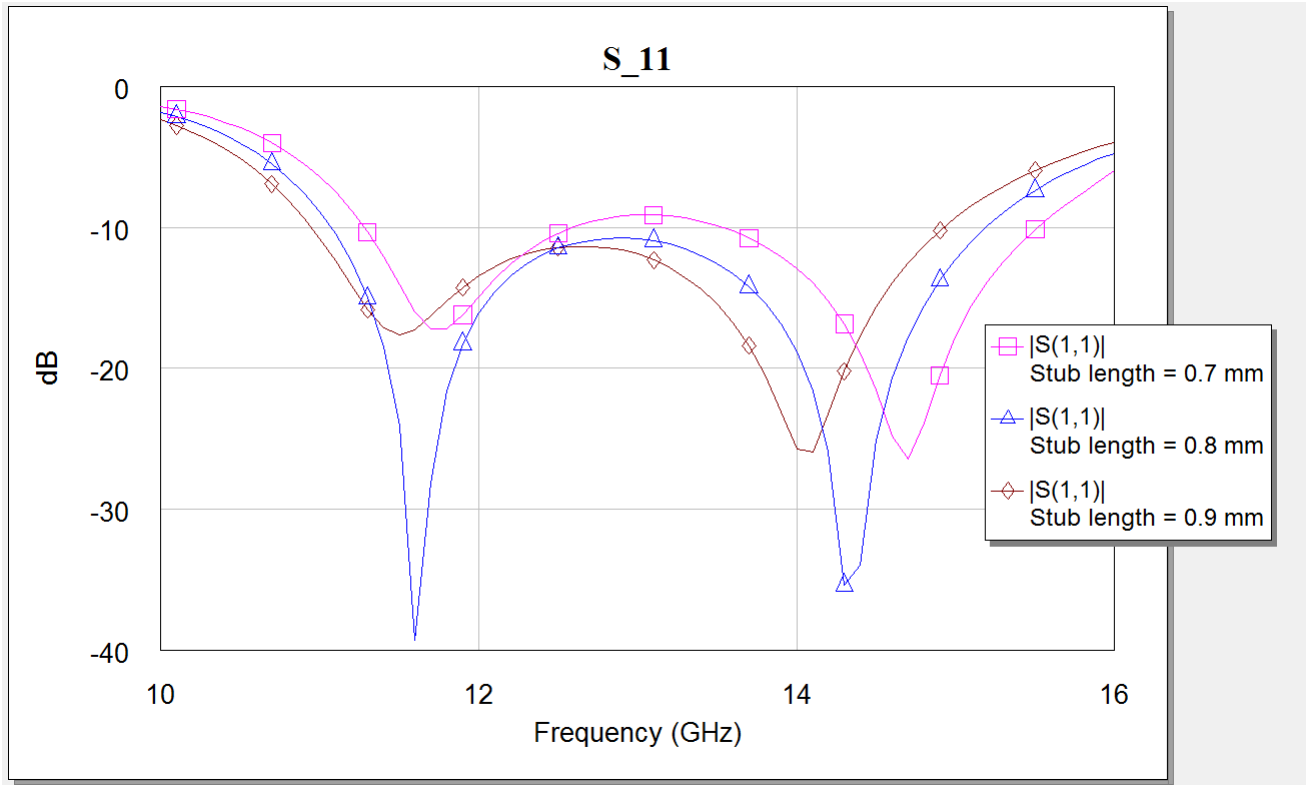


Figure 4.8: Comparison of  $S_{11}$  for different stub lengths.

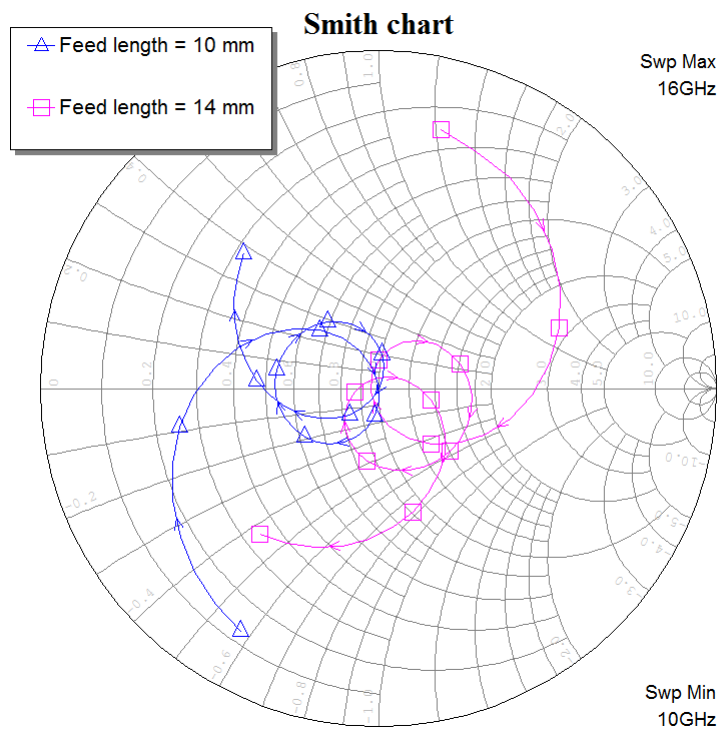
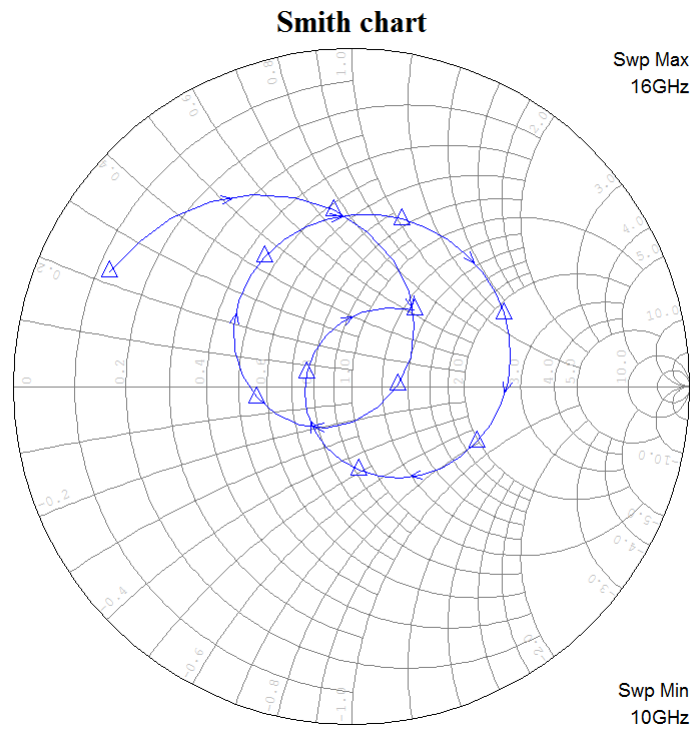
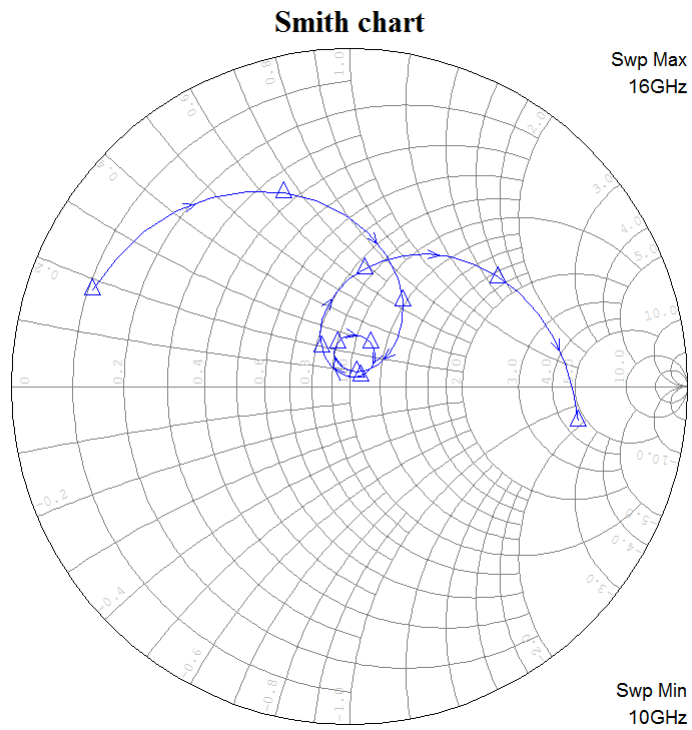


Figure 4.9: Smith chart for different feed lengths.



(a) Smith chart for a 2 mm thick patch substrate.



(b) Smith chart for a 3 mm thick patch substrate.

Figure 4.10: Smith chart for different thicknesses of patch substrate

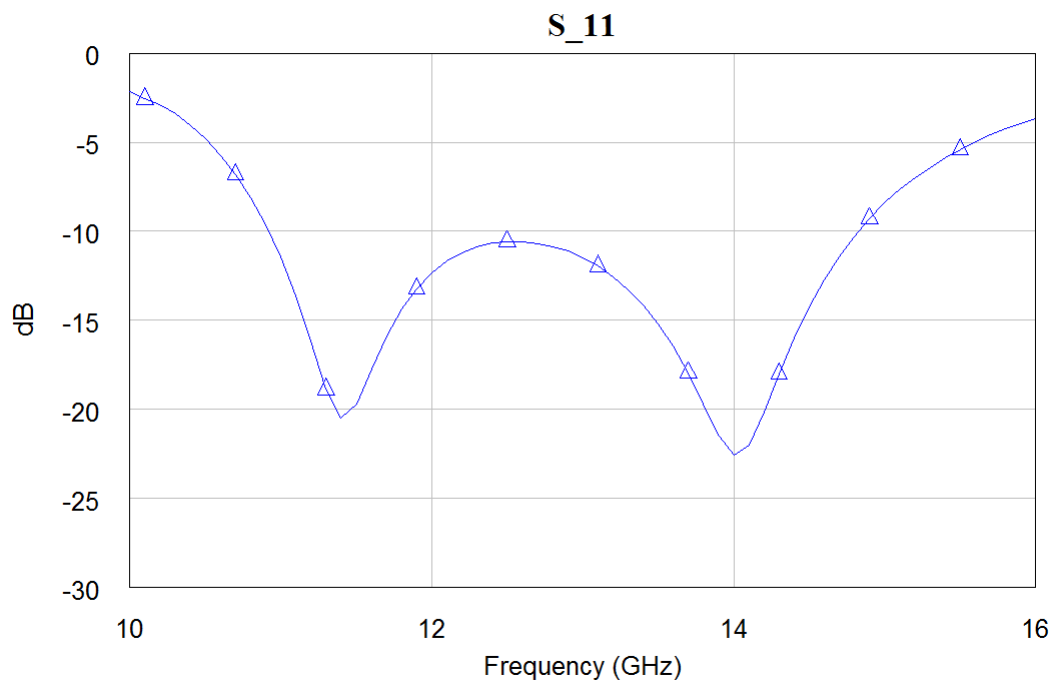


Figure 4.11:  $S_{11}$  for a 0.25 mm thick superstrate.

## 4.2 Design procedure

The SSFIP structure with aperture coupling is the recommended structure for a wide/dual-band patch antenna. To obtain better bandwidth or dual-band operation, at least two resonators must be used. The simplest method is possibly to use the patch and the aperture as resonators. Then no extra layers need to be introduced for extra stacked patches, less space is used than with parasitic elements, and it is not necessary with complex shapes, such as patches with notches and different shapes to obtain multiple resonances. The biggest drawback is the poor F/B due to the resonating aperture. This can be reduced by a reflector, either it is a complete metal plane or a patch reflector. That will give a higher profile, so the structure will maybe lose its advantage of lower profile than a structure with stacked patches. Nevertheless, a configuration with stacked patches will also produce back radiation, and without any reflector in a stacked patch structure, the antenna with resonating aperture and reflector will possibly show a better F/B.

The patch substrate must be a low permittivity dielectric and for an array antenna of a certain size, it is recommended to use foam as patch substrate in order to get a structural support. It is especially practical if the superstrate is very thin, which maybe is desired, to have support from the foam. There is no clear answer to how thick the patch substrate shall be, it is depending on how large bandwidth that is desired on cost of better coupling. The thickness of the patch substrate is varying with the operation frequency as seen in Table 4.1, where the substrate is thinner for higher frequency antennas. For the antennas at higher frequencies, the antenna with thickest substrate has the largest percentage bandwidth. This can give an impression of how thick the patch substrate should be.

For the feed substrate, the general guidelines for choosing a dielectric should be followed. Then the dielectric should have a relative permittivity in the range of 2 to 10, and a thickness of about 0.01 to 0.02  $\lambda$ . The thickness of the feed line for a specified impedance can then be calculated, either iterative from (2.11) and (2.14), or by use of some transmission line calculator.

The dimensions for a rectangular and a circular patch that were found from (2.19)-(2.24), were not very close to the patch dimensions that were obtained after tuning. This is probably due to the low relative permittivity and large thickness of the patch substrate. The formulas are not specifically made for this kind of patch substrates, and will give a too wide rectangular patch, and a too small circular patch. If you get a longer width than a length from the formulas for the rectangular patch, you can set the width to be shorter than the length, and then have a patch operating in the  $TM_{010}$ , which may be more correct

Table 4.1: Thickness of patch substrates compared to operation frequency

Thickness of patch substrate [mm]	Operation frequency [GHz]	Bandwidth	Material	Source
6.6 - 8.1	2.45	6.2%	Foam	Kuchar (1996)
2	9.5	13.2%	Foam	Zürcher and Gardiol (1995)
3	10 - 13	30%	Air	Aliakbarian et al. (2006)
1.5	12 - 14.5	19%	Air	Pavuluri et al. (2008)

than a patch operating in the  $TM_{001}$  mode. In the case of this thesis, this worked fine, and gave a patch with resonance much closer to the desired frequency. As for a circular patch, the advice will be to simulate the patch with a gradually reduced size until the resonance is satisfying.

The tuning stub is perhaps the hardest parameter to determine. The general advice of using a stub length that is a little shorter than a quarter wavelength will not help a lot. In most cases, the stub will be much shorter than a quarter wavelength. Searches through literature gave few specific results or methods to determine the stub length. The best method will be to simulate the current for different stub lengths, and find when it has maximum or minimum. What makes this extra hard for an antenna with two resonances is that the stub must have a length that works for both resonance frequencies. As seen in Section 4.1, the stub should have a length that gives a current maximum beneath the aperture at the patch resonance frequency, and a current minimum at the aperture resonance frequency.

To find the length of a resonant aperture, the simplest way to calculate it is to consider it as a microstrip dipole. Then its length will be a half-effective wavelength minus the length extension, calculated from (2.21), at each side of the aperture/dipole. The width of the aperture is not a very critical parameter, and it will not alter the antenna's performance too much. The aperture width can be used actively in the tuning process to adjust the frequencies and the coupling level. An advice is to start with an aperture width a little larger than  $1/10$  of the aperture length, to ensure good coupling, and rather reduce it later. The superstrate doesn't need to be very thick when foam is used as patch substrate, since the foam gives structural support. But if it is desired with a very robust antenna, it can be considered to have a relatively thick superstrate. The superstrate's function is to hold the patches in place, and it will be accomplished with the patches printed on the superstrate. A thin superstrate eases the antenna design, since it will have a negligible effect on the antenna performance. If desired, it can be made a little thicker to increase directivity and gain of the antenna.

A reflector is recommended if a resonating aperture is used, and it is desired that the antenna radiates broadside relative to its substrate plane. The most common alternative reflector types are a metal plane, a cavity backed solution, and a patch reflector. Which type to choose depends on placement and connection to the feed network, and complexity. A metal plane will give very good reflection for the central part of an array, but unwanted effects may occur at the edges. In addition, propagation of parallel plate waveguide modes can appear, and these are unwanted. The cavity backed solution is very effective, but is complex to design and manufacture. A patch reflector is much easier to make than a cavity, and it makes coupling with feed network easier than with a metal plane, and a thinner spacing is necessary than with a metal plane. Based on this the patch reflector was used here. The patch reflector should be placed at least  $0.1\lambda_0$  from the aperture. The dimensions and placement of the reflector can be found through simulations. It will probably be a microstrip dipole.

In short, the design procedure will be:

- Use SSFIP structure with a resonating aperture.
- Use a relatively thick foam as patch substrate.

- Use a thin, relatively high permittivity feed substrate.
- Calculate the patch dimensions and adjust them.
- Consider the aperture as a resonating microstrip dipole.
- Look at currents to determine the length of the tuning stub.
- Use a thin superstrate.
- Choose type of reflector.

### 4.3 Tuning procedure

The best will be to do the tuning in a good simulation program. The possibility of setting dimensions and parameters as variables and obtain many simulation results at once is timesaving. It's important to choose the right simulation tool for your project. It should give somewhat accurate results without running for too long time. A very complicated and accurate simulator will take too long time to run. A simulator like AXIEM is a good choice for microstrip antennas, since they are planar, and AXIEM gives accurate results in relatively short time, unless the structure contains very many layers and is very big. You should not simulate with a larger structure than needed, for example, a ground plane the size of approximately one wavelength should be good enough for one antenna element.

To make a wide/dual-band MPA, the focus must first be on getting the desired resonance frequencies, and then you can go on with enlarging bandwidth. Next step will be optimizing the matching at the center frequencies, while still maintaining a good bandwidth. Then you may want to improve radiation pattern, gain and F/B. After this, the whole process may be repeated multiple times until a satisfying characteristic and antenna performance is obtained. Since improving one parameter may reduce another, some compromises must be made, and some performance parameters must be reduced in favour of others, it all depends on your goal. For a wide-band antenna the efficiency will be reduced in favour of the bandwidth. In addition, the F/B will be reduced when a resonating aperture is used, but the bandwidth is significantly improved.

The following tips can be used to perform more effective tuning:

- Adjust the resonance frequencies by tuning patch dimensions and aperture length.
- Patch substrate and aperture width can be varied to adjust the bandwidth.
- The tuning stub is used for fine tuning the level of matching.
- Tune the reflector dimensions and position to get a maximum F/B.
- Reflector, superstrate and foam thicknesses can be adjusted to improve directivity and radiation pattern.



# Chapter 5

## Concluding remarks

In this chapter, the methods used and the results obtained in the thesis are discussed and concluded. In the end, recommendations for future work are presented.

### 5.1 Discussion

With the SSFIP structure, the advantages of aperture coupling with respect to bandwidth are maximized. Choosing this structure for a wide-band antenna is recommended. The choice of using a resonating aperture to obtain two resonances has some advantages and some disadvantages. The best alternative to a resonating aperture must be to use stacked patches. Stacked patches will introduce extra layers in the antenna, and give a higher profile. A resonating aperture will require a reflector, and that will give a higher profile. In most cases where a wide bandwidth is achieved, the aperture is resonant, and even if it not is made resonant, it will give some radiation to the back of the antenna. Both the configuration with stacked patches and with resonating aperture can be made with different polarizations. Based on this, both alternatives can be used, and using a resonant aperture with a reflector is not a bad choice. What type of reflector to use will depend on the rest of the antenna structure, and the complexity of implementing the reflector. The radiation characteristics were also slightly different based on type of reflector. A patch reflector will most probably give some lower F/B than a metal plane reflector, but it can be used actively to improve other radiation characteristics.

Implementation of a solution for switching between different polarizations was not made. First of all a single antenna element must be made with possibility to use different polarizations, and for the antenna in this thesis it was not found a solution for how this could be made.

The design and tuning procedure provided are given in a qualitative way, since a quantitative procedure most probably would not work for much higher or lower frequencies, because of different effects that are present at lower and higher frequencies.

## 5.2 Conclusions

The SSFIP structure has once again proven to give microstrip antennas with large bandwidths. Two alternative designs with different sort of reflectors were presented. The simulations of the antenna elements showed that they are usable for both up- and down-link in the Ku-band, with bandwidths over 30%. Simulations of the antenna elements showed that they were well matched, and had high gain, directivity and efficiency for being a broadband MPA. With a resonant aperture, a broad bandwidth was achieved on the cost of higher back radiation. But the use of a reflector gave good F/B levels. On the other side, a reflector gave a higher profile to the antenna, but it must be used for an antenna radiating in broadside direction. Use of a patch reflector improved gains and radiation pattern. The SSFIP structure is made up of many parts, making the design process more complicated. Parameters of each part had to be approximated before the tuning could start. Thus designing an SSFIP antenna from scratch requires knowledge about electromagnetism, and what mission and effects different parts of the antenna have. Studies of earlier work with this category of antennas has helped, and the use of earlier designs as references has given good guidance, especially during the design process. The EM simulator AXIEM was a good tool for the tuning process, where the use of variable parameters made the process faster and easier. Based on the results and experiences obtained in this thesis, a qualitative design and tuning procedure for a wide/dual-band antenna element was derived. The procedure was made for an MPA with SSFIP structure and a resonating aperture, and can be used as guidelines for making this type of antennas for other frequency bands.

## 5.3 Recommendations for future work

One of the next steps in the project will be to simulate an array with the antenna elements to see how it will work in an array. It must be checked for any unwanted side lobes or grating lobes, and how much mutual coupling there is between the elements.

The antenna must be connected with the feed network, and it must be decided if the solution with a metal plane where the feed network and the feed line is connected at the edges of the metal plane, or a patch reflector where the connections can be made between each element, shall be used. The configuration with feed network and antenna element should be analyzed, to see if any unwanted coupling between feed network and antenna occurs.

It can be tested to implement different polarizations in the antenna, primarily multiple polarizations with possibility to switch between them. The best examples with multiple polarizations use PIN-diodes to control multiple feed lines, and multiple apertures, but this seems to be complicated to implement in a wide/dual-band antenna. A solution of this kind would be very attractive, if it is possible to implement in an antenna with wide/dual-band operation.

# Bibliography

- (2016). *Simulation and Analysis Guide*. NI AWR, v12 edition.
- Alexopoulos, N. and Jackson, D. (1984). Fundamental superstrate (cover) effects on printed circuit antennas. *IEEE Transactions on Antennas and Propagation*, 32(8):807–816.
- Aliakbarian, H., Aghdam, K. M. P., and Razavi, S. F. (2006). A wideband strip-slot-air-inverted patch antenna array using resonant aperture. In *IEEE Antennas and Propagation Society International Symposium*, pages 1515–1518.
- Bahl, I. J. and Garg, R. (1977). Simple and accurate formulas for a microstrip with finite strip thickness. *Proceedings of the IEEE*, 65(11):1611–1612.
- Balanis, C. A. (2005). *Antenna Theory*. John Wiley & Sons, 3rd edition.
- Balanis, C. A. (2012). *Advanced Engineering Electromagnetics*. John Wiley & Sons, 2nd edition.
- Caspers, F. (2011). RF engineering basic concepts: S-parameters. *CERN Yellow Report*, 7:67–93.
- Chakravarthi, P. (1992). The history of communications from cave drawings to mail messages. *AES Magazine, IEEE*, 7:30 – 35.
- Chatterjee, R. (1988). *Advanced Microwave Engineering*. Ellis Horwood Limited.
- Chatterton, P. A. and Houlden, M. (1995). *EMC Electromagnetic Theory to Practical Design*. John Wiley & Sons.
- Chen, Z. N. and Chia, M. (2006). *Broadband Planar Antennas*. John Wiley & Sons.
- Consonni, D. and Silva, M. (2010). Signals in communication engineering history. *Transactions on Education, IEEE*, 53:621 – 630.
- Evans, B., Thompson, P. T., Corazza, G. E., Vanelli-Coralli, A., and Candreva, E. A. (2011). 1945-2010: 65 years of satellite history from early visions to latest missions. *Proceedings of the IEEE*, 99:1840 – 1857.
- Garg, R., Bhartia, P., Bahl, I., and Ittipiboon, A. (2001). *Microstrip Antenna Design Handbook*. Artech House.

- Gupta, K. C., Garg, R., Bahl, I., and Bhartia, P. (1996). *Microstrip Lines and Slotlines*. Artech House.
- Hammerstad, E. and Jensen, O. (1980). Accurate models for microstrip computer-aided design. In *IEEE MTT-S International Microwave symposium Digest*, pages 407–409.
- Hettak, K., Delisle, G., and Stubbs, M. (2001). A new type of dual frequency CPW-coupled patch antenna configurations. *Antennas and Propagation Society International Symposium*, 3:386 – 389.
- Holzman, E. (2006). *Essentials of RF and Microwave Grounding*. Artech House.
- IEEE (2012). *A Brief History of Communications*. IEEE Communications Society.
- Kevin, C. C. H. (2007). *Designs of Wideband Differential-Fed Patch Antennas: Analysis and Application*. PhD thesis, City University of Hong Kong.
- Kirov, G. S. and Mihaylova, D. P. (2010). Circularly polarized aperture coupled microstrip antenna with resonant slots and a screen. *Radioengineering*, 19:111 – 116.
- Kuchar, A. (1996). Aperture-coupled microstrip patch antenna array. Master’s thesis, Technischen Universität Wien.
- Kumar, A., Kaur, J., and Singh, R. (2013). Performance analysis of different feeding techniques. *International Journal of Emerging Technology and Advanced Engineering*, 3:884 – 890.
- Lee, K.-F. and Tong, K.-F. (2012). Microstrip patch antennas - basic characteristics and some recent advances. *Proceedings of the IEEE*, 100:2169 – 2180.
- Milligan, T. A. (2005). *Modern Antenna Design*. John Wiley & Sons, 2nd edition.
- Mishra, A., Singh, P., Yadav, N. P., Ansari, J. A., and Vishvakarma, B. R. (2009). Compact shorted microstrip patch antenna for dual band operation. *Progress In Electromagnetics Research C*, 9:171 – 182.
- Nayeri, P., Lee, K.-F., Elsherbeni, A. Z., and Yang, F. (2011). Dual-band circularly polarized antennas using stacked patches with asymmetric U-slots. *Antennas and Wireless Propagation Letters, IEEE*, 10:492 – 495.
- Noh, H. S., Yun, J. S., Kim, J. M., and Ik Jeon, S. (2004). Microstrip patch array antenna with high gain and wideband for TxRx dual operation at Ku-band. *Antennas and Propagation Society International Symposium*, 3:2480 – 2483.
- Ozkaya, U. and Seyfi, L. (2015). Dimension optimization of microstrip patch antenna in X/Ku band via artificial neural network. *Procedia - Social and Behavioral Sciences*, 195:2520 – 2526.

- Parikh, H., Pandey, S. V., and Sahoo, M. (2012). Design of a modified E-shaped dual band patch antenna for Ku band application. In *Communication Systems and Network Technologies, International Conference on*, pages 49–52.
- Pavuluri, S. K., Wang, C. H., and Sangster, A. J. (2008). A high-performance aperture-coupled patch antenna supported by a micromachined polymer ring. *IEEE Antennas and Wireless Propagation Letters*, 7:283–286.
- Pozar, D. M. (1996). A review of aperture coupled microstrip antennas: History, operation, development, and applications. Available: <http://www.ecs.umass.edu/ece/pozar/aperture.pdf>.
- Pozar, D. M. and Schaubert, D. H. (1995). *Review Articles*, pages 1–56. Wiley-IEEE Press.
- Pozar, D. M. and Targonski, S. D. (1991). Improved coupling for aperture coupled microstrip antennas. *Electronics Letters*, 27:1129 – 1131.
- Rafii, V., Nourinia, J., Ghobadi, C., Pourahmadazar, J., and Virdee, B. S. (2013). Broadband circularly polarized slot antenna array using sequentially rotated technique for C-band applications. *Antennas and Wireless Propagation Letters, IEEE*, 12:128 – 131.
- Samsuzzaman, M., Islam, M. T., Misran, N., and Ali, M. A. M. (2013). Dual band X shape microstrip patch antenna for satellite applications. *Procedia Technology*, 11:1223 – 1228.
- Satya Dubey, S. P. and Modh, K. (2011). High gain multiple resonance Ku-band microstrip patch antenna. In *Applied Electromagnetics Conference, IEEE*, pages 1 – 3.
- Sharma, S. (2012). *Patch Antenna: Basics*. Lambert Academic Publishing.
- Singh, I. and Tripathi, V. S. (2011). Microstrip patch antenna and its applications: a survey. *International Journal of Computer and Information Technology*, 2:1595 – 1599.
- Swanson, D. G. and Hofer, W. J. R. (2003). *Microwave Circuit Modeling Using Electromagnetic Field Simulation*. Artech House.
- Waterhouse, R. B. (2003). *Microstrip Patch Antennas: A Designer’s Guide*. Springer Science + Business Media.
- Wu, Y.-F., Wu, C.-H., Lai, D.-Y., and Chen, F.-C. (2007). A reconfigurable quadri-polarization diversity aperture-coupled patch antenna. *IEEE Transactions on Antennas and Propagation*, 55:1009 – 1012.
- Yeh, C. and Shimabukuro, F. (2008). *The Essence of Dielectric Waveguides*. Springer.
- Zürcher, J.-F. and Gardiol, F. (1995). *Broadband Patch Antennas*. Artech House.



# Appendix A

## CD index

In the following directories on the attached CD you may find:

PAPERS *A selection of the material this thesis is based in. Some papers may be missing because of hard copies, etc.*

REPORT *This report including .tex files and figures.*

SIMULATION *The AWRDE project files used for design and simulations.*